ARINAN DE PIEMONTE DOURADO

FUZZY LOGIC AS A TOOL FOR UNCERTAINTY, ROBUSTNESS AND RELIABILITY ANALYSES OF MECHANICAL SYSTEMS

UNIVERSIDADE FEDERAL DE UBERLÂNDIA

FACULDADE DE ENGENHARIA MECÂNICA

2018

ARINAN DE PIEMONTE DOURADO

FUZZY LOGIC AS A TOOL FOR UNCERTAINTY, ROBUSTNESS AND RELIABILITY ANALYSES OF MECHANICAL SYSTEMS

Tese apresentada ao Programa de Pós-graduação em Engenharia Mecânica da Universidade Federal de Uberlândia, como parte dos requisitos para a obtenção do título de **DOUTOR EM ENGENHARIA MECÂNICA.**

Área de Concentração: Mecânica dos Sólidos e Vibrações.

Orientador: Prof. Dr. Valder Steffen Jr.

UBERLÂNDIA – MG

2018

Dados Internacionais de Catalogação na Publicação (CIP)
Sistema de Bibliotecas da UFU, MG, Brasil.

D739f
2018

Dourado, Arinan de Piemonte, 1987-
Fuzzy logic as a tool for uncertainty, robustness and reliability analyses of mechanical systems / Arinan de Piemonte Dourado. - 2018.
89 f. : il.

Orientador: Valder Steffen Junior.
Tese (Doutorado) - Universidade Federal de Uberlândia, Programa de Pós-Graduação em Engenharia Mecânica.
Disponível em: http://dx.doi.org/10.14393/ufu.te.2018.778
Inclui bibliografia.

1. Engenharia mecânica - Teses. 2. Lógica difusa - Teses. 3. Controle robusto - Teses. 4. Confiabilidade (Engenharia) - Teses. I. Steffen Junior, Valder. II. Universidade Federal de Uberlândia. Programa de Pós-Graduação em Engenharia Mecânica. III. Título.

CDU: 621

Maria Salete de Freitas Pinheiro – CRB6/1262

SERVIÇO PÚBLICO FEDERAL
MINISTÉRIO DA EDUCAÇÃO
UNIVERSIDADE FEDERAL DE UBERLÂNDIA
FACULDADE DE ENGENHARIA MECÂNICA
PROGRAMA DE PÓS-GRADUAÇÃO EM ENGENHARIA MECÂNICA

ALUNO: Arinan de Piemonte Dourado

NÚMERO DE MATRÍCULA: 11413EMC001

ÁREA DE CONCENTRAÇÃO: Mecânica dos Sólidos e Vibrações

LINHA DE PESQUISA: Dinâmica de Sistemas Mecânicos

PÓS-GRADUAÇÃO EM ENGENHARIA MECÂNICA: NÍVEL DOUTORADO

TÍTULO DA TESE:

"Fuzzy Logic as a Tool for Uncertainty, Robustness and Reliability Analyses of Mechanical Systems"

ORIENTADOR: Prof. Dr. Valder Steffen Júnior

A Tese foi **APROVADA** em reunião pública, realizada na Sala 313 - Bloco 1M, Campus Santa Mônica, em 12 de abril de 2018, às 14:00 horas, com a seguinte Banca Examinadora:

NOME		ASSINATURA
Prof. Dr. Valder Steffen Júnior	UFU	
Prof. Dr. Aldemir Ap. Cavalini Júnior	UFU	
Prof. Dr. Enio Pedone Bandarra Filho	UFU	
Prof. Dr. Leopoldo P. Rodrigues de Oliveira	EESC/USP	
Prof. Dr. Milton Dias Júnior	UNICAMP	

Uberlândia, 12 de abril de 2018

“I don’t want to believe; I want to know.”

Carl Sagan.

ACKNOWLEDGMENTS

I would like to express my sincere gratitude to my family, in special my mother for having provided to me the education basis that led me to all my accomplishments and for her encouragements to look for achievements that are more important.

I am grateful to have a true angel in my life, my wife Mirella, thank you for sharing my dreams and for helping me to make our dreams come true.

I thank also my colleges in the LMEst laboratory for the support you all assured to me during this journey, especially Prof. Dr. Aldemir Cavalini, whose contribution made this work possible. Thank you Prof. Dr. Leonardo Sanches for being a true friend along all these years.

I would also like to express my sincere thanks to my advisor Prof. Valder Steffen Jr, who I learned to admire not only professionally but also as a person. I will consider myself fulfilled if I can achieve half of your accomplishments.

A special thanks to the faculty and staff of FEMEC-UFU, and to my advisory committee members for their willingness on evaluating my thesis and contributing to its improvement.

Finally, my sincere thanks to the financial support provided by the Brazilian research agencies CNPq, CAPES and FAPEMIG, and to the support of the INCT-EIE. I am also thankful to the companies CERAN, BAESA, ENERCAN, and Foz do Chapecó for the financial support through the R&D project *Robust Modeling for the Diagnosis of Defects in Generating Units* (02476-3108/2016).

DOURADO, A. De P. **Fuzzy Logic as a Tool for Uncertainty, Robustness and Reliability Analyses of Mechanical Systems.** 2018. 89 pages. PhD Thesis, Universidade Federal de Uberlândia, Uberlândia.

Abstract

.

The main goal of this doctoral research work is to evaluate fuzzy logic as a tool for uncertainty, robustness and reliability analyses of mechanical systems. In this sense, fuzzy logic approaches are used on various design scenarios, such as the uncertainty analysis of rotating systems, robust balancing procedures, and reliability-based design problems. Firstly, the so-called α-level optimization technique is both numerical and experimentally evaluated in the context of uncertainty analysis of rotating systems. A numerical application considering a rotor test rig with uncertainties affecting shaft Young's modulus and bearing stiffness is used to evaluate and compare fuzzy uncertainty analysis with well stablished stochastic procedures. Then, this fuzzy logic uncertainty analysis is used to predict the extreme responses of a flexible rotor supported by hydrodynamic bearings with uncertainties affecting oil properties. Afterwards, fuzzy logic is evaluated as a tool for robust optimization by means of two novel fuzzy logic balancing approaches: *i*) a non-parametric approach formulated to enhance the so-called IC method balancing robustness, and *ii*) a parametric methodology formulated to increase the balancing robustness of model-based balancing technique. In the first approach fuzzy logic tools, particularly fuzzy logic transformation and defuzzification procedures, are used to define a preprocessing stage in which system vibration responses sets are evaluated in order to obtain a more representative unbalance condition. In the second approach, fuzzy logic optimization is used to define fuzzy logic objective functions in which uncertainties affecting the balancing responses are assessed. Finally, a novel fuzzy logic reliability-based design methodology is proposed, revising the traditional fuzzy logic approach in terms of the reliability index. The resulting reliability design methodology consists of a nested algorithm in which an inner optimization loop is used to obtain the uncertain variables limits and an outer optimization loop evaluates a predefined fuzzy reliability index within the previously obtained bounds. Obtained results confirm fuzzy logic as a prominent tool for uncertainty, robustness and reliability analyses.

Keywords: Fuzzy Logic, Uncertainty Analysis, Robustness and Reliability

DOURADO, A. De P. **Lógica Nebulosa como uma Ferramenta para Análise de Incerteza, Robustez e Confiabilidade de Sistemas Mecânicos.** 2018. 89 páginas. Tese de Doutorado, Universidade Federal de Uberlândia, Uberlândia.

Resumo

O principal objetivo desta tese de doutorado é avaliar o uso da lógica nebulosa como uma ferramenta para análise de incerteza, robustez e confiabilidade de sistemas mecânicos. Neste sentido, abordagens baseadas em lógica nebulosa são definidas e utilizadas para a análise de incertezas em máquinas rotativas, a formulação de procedimentos de balanceamento robusto e para formulação de problemas de projetos baseados em confiabilidade. Primeiramente, a técnica conhecida como otimização de níves α é avaliada tanto numérica como experimentalmente para a análise de incertezas de máquinas rotativas. Uma aplicação numérica considerando um rotor com incertezas que influenciam o módulo de Young do eixo e as rigidezes dos mancais é usada para avaliar e comparar a análise de incertezas *fuzzy* com procedimentos estocásticos já estabelecidos. Então, este procedimento de lógica nebulosa é utilizado para prever as respostas extremas de um rotor flexível suportado por mancais hidrodinâmicos com incertezas que influem sobre as propriedades do lubrificante. Posteriormente a lógica nebulosa é avaliada como uma ferramenta para otimização robusta por meio de dois novos procedimentos de balanceamento robusto, a saber: *i*) uma abordagem não-paramétrica formulada para elevar a robustez do procedimento de balanceamento conhecido como método dos coeficientes de influência, e *ii*) uma abordagem paramétrica formulada para fazer aumentar a robustez do método de balanceamento baseado em modelos matemáticos representativos. Por fim, uma nova metodologia de lógica nebulosa para projetos baseados em confiabilidade é proposta, revisando a abordagem de lógica nebulosa tradicional em termos da métrica de confiabilidade. O procedimento proposto consiste de um algoritmo aninhado, no qual um laço interno é utilizado para obter os limites dos parâmetros incertos enquanto um laço externo avalia uma métrica de confiabilidade *fuzzy* predefinida, considerando os intervalos obtidos no laço interno. Resultados obtidos indicam a lógica nabulosa como uma ferramenta proeminente para análises de incerteza, robustez e confiabilidade.

Palavras-Chave: Lógica Nebulosa, Análise de Incertezas, Robustez e Confiabilidade.

NOMENCLATURE

CHAPTER 2

SFEM	Stochastic Finite Element Method
PCE	Polynomial Chaos Expansion
FE	Finite Element
MCS	Monte Carlo Simulation
KL	Karhunen-Lòeve
$H(\boldsymbol{x}, \theta)$	one-dimensional random field in a Hilbert space
$\boldsymbol{x}$	spatial component of a random field
θ	random process
$C_{HH}(\boldsymbol{x}, \boldsymbol{x}')$	autocovariance function
σ	variance of a random field
ρ	correlation coefficient
Ω	a given geometry
λ_i	eigenvalues of the autocovariance function
φ_i	deterministic function
$\mu(x)$	mean value of a random field
$\xi_i(\theta)$	random variables
X	classical set
x	generic set elements
A	subset
μ_A	membership function
$\tilde{A}$	fuzzy set
E	Young's modulus
ρ	material density
υ	Poisson's coefficient
M	mass matrix
D	damping matrix

$\mathbf{D}_g$	gyroscopic matrix
$\mathbf{K}$	stiffness matrix
$\mathbf{K}_{st}$	stiffness matrix resulting from the transient motion
$\mathbf{W}$	weight of the rotating parts
$\mathbf{F}_u$	unbalance forces
$\mathbf{F}_m$	shaft supporting forces
$\mathbf{q}$	generalized displacement
γ	mass proportional damping coefficient
β	stiffness proportional damping coefficient
k_{ROT}	angular stiffness
FRF	frequency response function
FRF_i^{model}	FRFs generated by a FE model
FRF_i^{exp}	experimental FRFs
Ω	operational rotation speed of the rotor
$\mathbf{K}^{(e)}$	elementary stiffness matrix
$\mathbf{K}_S^{(e)}$	shaft elementary stiffness matrix
$\mathbf{K}_B^{(e)}$	bearings elementary stiffness matrix
I_s	shaft area moment of inertia
$L_{cor,x}$	correlation length
$\overline{K}_{s_r}^{(e)}$	random elementary stiffness matrices
k_o	mean value of the bearings stiffness coefficients
δ_k	dispersion level
SQP	Sequential Quadratic Programming
RMS	mean square convergence analysis
C	bearings radial clearance
μ_h	oil viscosity
T_{oil}	oil temperature
$\mathbf{Out}_{exp,i}$	experimental vibration response
$\mathbf{Out}_{model,i}$	FE model vibration response

CHAPTER 3

$\mathbf{U}^p$	Rotor unbalance distribution
$\mathbf{V}^j$	Vibration amplitudes
$\boldsymbol{\alpha}^{jp}$	Influence coefficients
$\mathbf{V}_0$	Vibration responses for the original unbalance condition
$\mathbf{U}_0$	Original unbalance distribution
m_t	Trial weight
W^1	Trial weight unbalance force
h	Eccentricity
unb	Unbalance condition fuzzy set
N_{pos}	Number of no rejections
N_{neg}	Number of rejections
H_0	Null hypothesis
α	Significance level of a hypothesis test
p-value	Statistic test metric
α_{min}	Minimum significance level
α_{max}	Maximum significance level
E	Young's modulus
ρ	material density
u	Poisson's coefficient
I_{DX}	Discs inertia moment in X direction
I_{DY}	Discs inertia moment in Y direction
I_{DZ}	Discs inertia moment in Z direction
k_{xx}	Self-alignment ball bearing stiffness coefficient in X direction
k_{zz}	Self-alignment ball bearing stiffness coefficient in Z direction
d_{xx}	Self-alignment ball bearing damping coefficient in X direction
d_{zz}	Self-alignment ball bearing damping coefficient in Z direction
F	Model-based balancing objective function
$U_i^{FEmodel}(x)$	FE model vibration responses in the model-based balancing
x	Vector of proposed correction weights in the model-based balancing

$U_i^{Original}$	Rotor original vibration responses in the model-based balancing
Pe	Pessimist objective function in robust model-based balancing
Op	Optimist objective function in robust model-based balancing
$\overline{p}$ and $\underline{p}$	Upper and lower limits of uncertain parameters
$U_i^{FEmodel}(x^*, p_n)$	FE model vibration response with deterministic correction weights and nominal configuration
$U_i^{FEmodel}(x, \overline{p})$	FE model vibration response at optimist configuration
$U_i^{FEmodel}(x, \underline{p})$	FE model vibration response at pessimist configuration

CHAPTER 4

$FLSF_j$	Fuzzy limit state function
R_j	Structural strength
S_j	Structural stress
$g_j(\mathbf{x})$	Inequality constraints
$\mathbf{x}$	Vector of design variables
$\eta_{j\alpha k}$	Traditional reliability index
η_j'	Revised reliability index
f_m	Failure metric
x_d	Design variables
x_r	Random variables
x_f	Fuzzy variables

FUZZY LOGIC AS A TOOL FOR UNCERTAINTY, ROBUSTNESS AND RELIABILITY ANALYSES OF MECHANICAL SYSTEMS

TABLE OF CONTENTS

CHAPTER 1: INTRODUCTION 3

CHAPTER 2: FUZZY UNCERTAINTY ANALYSIS 6

2.1. UNCERTAINTY ANALYSIS REVIEW 6
2.2. STOCHASTIC APPROACH 7
2.2.1 MONTE CARLO SIMULATION 7
2.2.2 STOCHASTIC FINITE ELEMENT METHOD 8
2.3. FUZZY LOGIC 10
2.3.1 FUZZY VARIABLES 11
2.3.2 FUZZY DYNAMIC ANALYSIS 12
2.4. NUMERICAL VALIDATION 13
2.4.1 ROTOR TEST RIG 13
2.4.2 UNCERTAINTY SCENARIOS 16
2.4.3 FREQUENCY DOMAIN ANALYSIS 20
2.4.4 TIME DOMAIN ANALYSIS 23
2.5 EXPERIMENTAL VALIDATION 29
2.5.1 ROTOR TEST RIG 29
2.5.2 UNCERTAINTY ANALYSIS 34

CHAPTER 3: ROBUST OPTIMIZATION BY MEANS OF FUZZY LOGIC 42

3.1 ROTOR BALANCING REVIEW 42
3.2 NON-PARAMETRIC EVALUATION 44
3.2.1 IC BALANCING METHOD 44
3.2.2 FUZZY LOGIC CONCEPTS 46
3.2.3 NUMERICAL APPLICATION 51
3.2.4 EXPERIMENTAL VALIDATION 56
3.3 PARAMETRIC EVALUATION 61
3.3.1 MODEL-BASED BALANCING METHOD 61
3.3.2 ROBUST MODEL-BASED BALANCING METHOD 63
3.3.3 NUMERICAL EVALUATION 65

CHAPTER 4: RELIABILITY DESIGN USING FUZZY LOGIC 69

4.1 Reliability-based Optimization Review 69
4.2 Fuzzy Set Theory Revisited 71
4.3 Traditional Fuzzy Reliability Analysis 72
4.4 Proposed Fuzzy Reliability Analysis 74
4.5 Numerical Evaluation 76
4.5.1 Nonlinear Limit State Function 76
4.5.2 Cantilever Beam Problem 77
4.5.3 Car-side Impact Problem 82

CHAPTER 5: FINAL REMARKS 86

REFERENCES 90

APPENDIX A: PUBLISHED AND SUBMITTED PAPERS 95

RESUMO EXPANDIDO EM PORTUGUÊS 97

CHAPTER I

INTRODUCTION

The increasing demand for higher industrial productivity as driven the development of more efficient mechanical systems, implying on increasing reliability and robustness and lowering operational costs. Consequently, the development of more representative mathematical models is crucial in the context of modern engineering.

Mechanical systems in general are subjected to the effects of inherent uncertainties that arise mainly due to operational fluctuations, manufacturing errors, damage, wear or merely due to the lack of knowledge regarding the system itself. These effects can be directly related to system performance, durability and reliability and usually are unaccounted for in design stages.

Commonly, in the design or analysis of mechanical systems deterministic models are derived from known physical phenomena in an attempt to represent the system behavior. These deterministic models are unable to account for system uncertainties and usually an uncertainty analysis is performed in order to obtain the system extreme responses, which is essential for the assessment of system robustness and reliability.

In this sense, the main goal of this PhD thesis can be defined as the evaluation of fuzzy logic, a simpler mathematical representation of system uncertainties, aiming at uncertainty, robustness and reliability analyses. Uncertainty analysis can be viewed as a mathematical process that aims to obtain system extreme responses when exposed to the effect of uncertainties. Robustness can be interpreted as the system sensitivity with respect to the influence of uncertainties; consequently, robust system responses are as less sensitive as possible to system fluctuations. Reliability emphasizes on the achievement of predefined constraints related to design stability and/or safety performance. Figure 1.1 illustrates the concept of robustness and reliability.

The fuzzy logic approach is an intuitive technique based on fuzzy sets (ZADEH, 1965) and on the possibility theory (ZADEH, 1968). In the fuzzy set theory, the inherent uncertainties are described as incomplete and/or inaccurate information, represented by means of weighted

intervals. Despite being relatively recent, fuzzy set theory is gaining more attention and successful applications have been reported in the literature (MÖLLER, GRAF and BEER, 2000; MÖLLER and BEER, 2004; OZBEN, HUSEYINOGLU and ARSLAN, 2014; DE ABREU *et al.*, 2015).

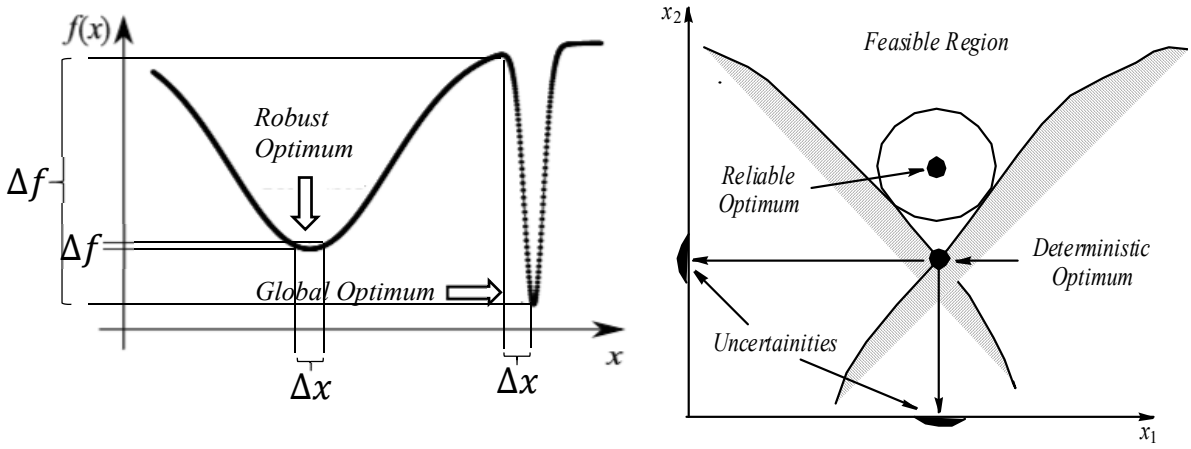

a) robustness b) reliability

Figure 1.1 Concept of robustness and reliability.

In the context of the research effort at the LMEst laboratory (UFU – Federal University of Uberlândia) on uncertainty analysis and robustness evaluation, the present contribution is a continuation of the following research projects as developed by:

- BUTKEWITSCH (2002): evaluated a robust optimization of safety vehicular components;
- KOROISHI *et al.* (2012): considered uncertainties effects on a flexible rotor by means of the Stochastic Finite Element Method (SFEM);
- LARA-MOLINA, KOROISHI and STEFFEN Jr (2015): evaluated uncertainty effectes on a flexible rotor considering fuzzy and random-fuzzy parameters;
- CAVALINI Jr *et al.* (2015): proposed a fuzzy approach to assess uncertainties effects in a flexible rotor supported by fluid film bearings;
- CARVALHO (2017): adopted a model based balancing appraoch to obtain robust balancing responses considering uncertainties through Monte Carlo simulations.

Consequently, the present contribution aims to evaluate the fuzzy logic approach as tool for uncertainty, robustness and reliability analyses. In this sense, a fuzzy uncertainty analysis methodology is evaluated both numerically and experimentally for a flexible rotor, wherein the proposed methodology performance is compared with well-established uncertainty

analysis techniques. In the sequence, two distinct approaches based on fuzzy set theory and fuzzy uncertainty analysis are proposed and evaluated for the robust balancing of rotating machines. Finally, a fuzzy reliability-based design methodology is formulated and evaluated for the reliability-based design of mechanical systems.

The outline of the remainder of this contribution is as follows:

- Chapter 2: Presents the proposed fuzzy uncertainty analysis methodology and the results of the numerical and experimental validation of the proposed approach. A brief discussion of the obtained results is also addressed.
- Chapter 3: Introduces the proposed fuzzy robust balancing approaches. Both methodologies are presented; numerical and experimental results are obtained and discussed.
- Chapter 4: Focuses on the proposed fuzzy reliability-based design approach, addressing its formulation and numerical results obtained.
- Chapter 5: Brings some final remarks regarding the results and a brief discussion of possible future research steps on this topic.

CHAPTER II

FUZZY UNCERTAINTY ANALYSIS

In this chapter, the so-called α-level optimization procedure for fuzzy uncertainty analysis is presented and discussed. First, the performance of the proposed methodology is numerically compared with well-established uncertainty analysis approaches, whereas the dynamic responses of a horizontal rotor test rig are evaluated under the influence of uncertain rotor shaft Young's modulus and uncertain bearing stiffness. Then, the proposed fuzzy uncertainty analysis methodology is experimentally validated for a flexible rotor containing three rigid discs and supported by two cylindrical fluid film bearings.

The chapter begins by addressing the key issues related to uncertainty analysis and the proposed fuzzy approach. After, the numerical validation of the proposed methodology is presented. Then, the experimental validation of the fuzzy approach is demonstrated. Finally, a brief discussion of the obtained results is presented.

2.1. Uncertainty Analysis Review

There are different techniques that can be used to modeling uncertainties in mechanical systems. The stochastic approach exhibits a longer history of applications on mechanical systems, while the fuzzy logic technique is recently gaining more attention.

The stochastic methodology is based on the probability theory. GHANEM and SPANOS (1991) contextualize the stochastic approach within the scope of structural dynamics through the Stochastic Finite Element Method (SFEM) and the so-called Polynomial Chaos Expansion (PCE) technique. The fuzzy logic approach is an intuitive technique based both on fuzzy sets and on the possibility theory. KOSKO (1990) brings a review about the main issues on fuzziness and probability.

Concerning rotor dynamics associated problems, RÉMOND, FAVERJON and SINOU (2011) assessed the flexible rotor dynamics subject to uncertain parameters by SFEM and

PCE technique. KOROISHI *et al.* (2012) applied the SFEM approach to a flexible rotor with uncertain parameters modeled as homogeneous Gaussian random fields discretized by

the Karhunen-Lòeve series expansion (KL series expansion). SEGUÍ, FAVERJON and JACQUET-RICHARDET (2013) investigated the effects of uncertainties affecting the material properties of blades in a multistage bladed disc system by using the PCE technique. More recent rotor dynamic applications of the stochastic approach can be found in (SEPAHVAND, NABIH and MARBURG, 2015; SINOU and JACQUELIN, 2015; SINOU, DIDIER and FAVERJON, 2015).

Following the fuzzy approach, RAO and QIU (2011) presented a methodology for the fuzzy analyses of nonlinear rotor-bearing systems along with numerical results that were presented to demonstrate the computational feasibility of the proposed approach. LARA-MOLINA, KOROISHI and STEFFEN JR. (2015) analyzed the dynamics of flexible rotors under uncertain parameters modeled as fuzzy and fuzzy random variables. CAVALINI JR *et al.* (2015) evaluated the dynamic behavior of a flexible rotor with three rigid discs, supported by two fluid film bearings. The uncertainties were considered as affecting the oil viscosity and the radial clearance of both bearings that support the machine.

Both the stochastic and fuzzy logic approaches were applied to the analysis of uncertainties affecting the steady state characteristics and the overall dynamic behavior of rotating machines. In this chapter, a systematic study dedicated to compare both methodologies is presented aiming to assess their suitability regarding rotor dynamics applications.

2.2. Stochastic Approach

In the stochastic approach, the purpose is to evaluate the randomness and the variability of the uncertain parameters of the model. Thereby, the uncertainties are modeled either as random variables or as random fields. Among the various stochastic techniques that aim at accomplishing this goal, the SFEM and the Monte Carlo Simulation (MCS; i.e., as stochastic solver) are extensively used (KUNDU *et al.*, 2014; JENSEN and PAPADIMITRIOU, 2015; SEPAHVAND, 2016).

2.2.1 Monte Carlo Simulation

MCS belongs to a class of methods that can be viewed as exhaustive search techniques. The idea is to infer the statistical behavior of the model response without previous knowledge about the statistical behavior of the uncertain quantities. In this case, the uncertain quantities are considered as random fields and a large number of samples are evaluated (i.e., simple realizations of the considered field). The samples are tested by using the deterministic

model of the analyzed mechanical system, generating the uncertain quantity response (which implies a high computational cost). Therefore, the statistical characteristics of the outputs (i.e., the model responses) can be estimated and the variability of the model can be inferred. Figure 2.1 presents a schematic representation of the main features associated with MCS. More details concerning this approach can be found in (BINDER, 1979; NEWMAN and BARKEMA, 2001).

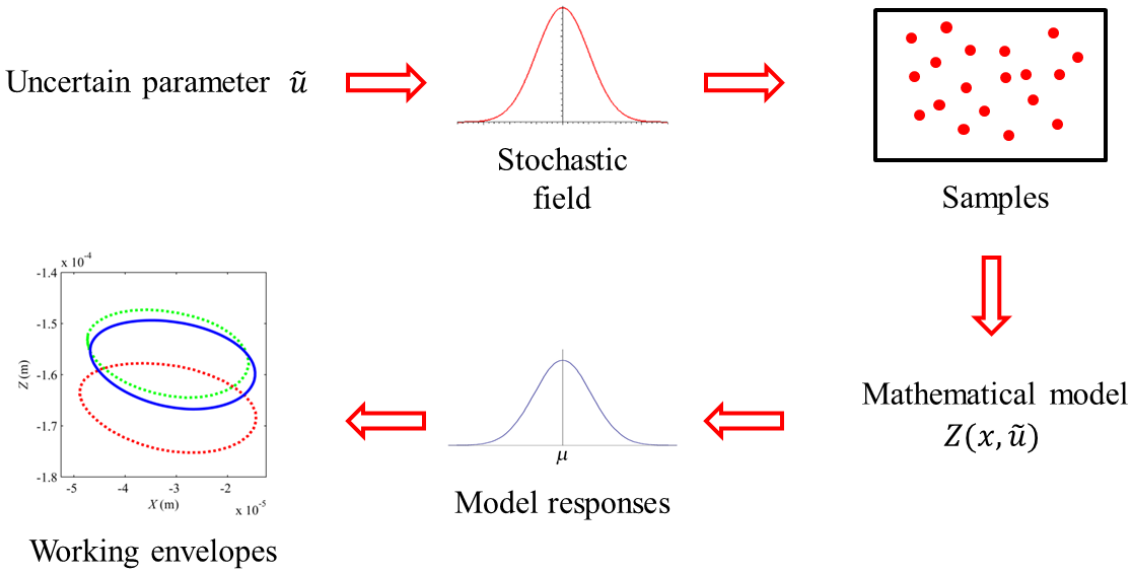

Figure 2.1 - Schematic representation of the main features associated with MCS.

It is worth mentioning that the convergence of the MCS is practically guaranteed in different applications, making this stochastic solver extensively used for the cases in which the statistical characteristic of the mechanical system is not available (HUDSON and TILLEY, 2014; BAO and WANG, 2015; CHEN and SCHUH, 2015; CADINI and GIOLETTA, 2016).

2.2.2 Stochastic Finite Element Method

The SFEM can be considered as an extension of the FE method. In the classical FE method, the geometry of the mechanical system is discretized according to a number of finite elements that form the spatial mesh of the model. The deterministic responses are approximated by the nodal displacements, which are obtained from the solution of coupled differential equations.

If the parameters of the mechanical system are uncertain (modeled as random fields), the model should be represented by stochastic differential equations. Adopting the same spatial discretization used in the classical FE method, an incomplete representation of the random field is obtained. Therefore, a series expansion technique is used to discretize the random dimension efficiently. In this sense, the KL series expansion (GHANEM and SPANOS, 1991) or various orthogonal series (ZHANG and ELLINGWOOD, 1994) can be applied.

The KL series expansion is based on the application of the spectral theorem for compact normal operators in conjunction with Mercer's theorem, which connects the spectral representation of a Hilbert-Schmidt integral operator to the corresponding Hilbert-Schmidt kernel. LOÈVE (1977) and GHANEM and SPANOS (1991) provide an interesting discussion of the mathematical basis involving KL series expansion. The key aspects of KL series expansion related to uncertainty analysis are presented next.

The KL series expansion of a random field is based on the spectral decomposition of its auto covariance function. It is a continuous representation of the random field expressed by the superposition of orthogonal random variables, which are weighted by deterministic spatial functions (GHANEM and SPANOS, 1991).

The auto covariance function of a one-dimensional random field $H(\boldsymbol{x}, \theta)$, where $\boldsymbol{x}$ denotes the spatial dependence of the field and θ represents a random process, can be defined as shown in Eq. (2.1).

$$C_{HH}(\boldsymbol{x}, \boldsymbol{x}') = \sigma(\boldsymbol{x})\sigma(\boldsymbol{x}')\rho(\boldsymbol{x}, \boldsymbol{x}') \tag{2.1}$$

in which σ denotes the variance of the field and ρ is the correlation coefficient.

The set of deterministic functions for which any event of the field is expanded with respect to a given geometry Ω is defined by the eigenvalue problem presented in Eq. (2.2).

$$\forall\, i = 1, \ldots \int_{\Omega} C_{HH}(\boldsymbol{x}, \boldsymbol{x}')\, \varphi_i(\boldsymbol{x}') d\Omega_{\boldsymbol{x}'} = \lambda_i \varphi_i(\boldsymbol{x}) \tag{2.2}$$

where λ_i are the eigenvalues of the auto covariance function $C_{HH}(\boldsymbol{x}, \boldsymbol{x}')$ and $\{\varphi_i\}$ is a deterministic function.

Due to the mathematical properties of the deterministic function $\{\varphi_i\}$ (i.e., the eigenfunctions of the autocovariance function $C_{HH}(\boldsymbol{x}, \boldsymbol{x}')$) that are the solution of Eq. (2.2), any event of the random field can be expanded as shown by Eq. (2.3).

$$H(\boldsymbol{x},\theta) = \mu(\boldsymbol{x}) + \sum_{i=1}^{\infty} \sqrt{\lambda_i}\, \xi_i(\theta)\varphi_i(x) \tag{2.3}$$

where $\mu(x)$ is the mean value of the field, λ_i are the eigenvalues of the auto covariance function $C_{HH}(\boldsymbol{x},\boldsymbol{x}')$, and $\xi_i(\theta)$ are random variables.

The intrinsic eigenvalue problem associated with the series expansion can be analytically solved only for a few auto covariance functions and geometries. Detailed solutions for triangular and exponential covariance functions and one-dimensional homogeneous random fields are shown in GHANEM and SPANOS (1991) for $\Omega = [-a, a]$. The eigenvalue problem has to be solved numerically regarding different cases.

In the KL series expansion of a Gaussian process, the random variables $\xi_i(\theta)$ are independent standard normal random variables. This property is useful in practical applications, especially for the SFEM. Moreover, the convergence of the series representation given by Eq. (2.3) is guaranteed in the cases for which a Gaussian process is considered (LOÈVE, 1977).

Both series expansions procedures (i.e., KL and orthogonal series) aim at determining the random variables that are related to the stochastic differential equations that represent the mechanical system. The KL and orthogonal series decompositions are not able to solve these equations. In order to obtain the solution of the differential equations, a stochastic solver is used (e.g., MCS). The solver should infer the variability of the system through the evaluation of the random variables.

2.3. Fuzzy Logic

ZADEH (1965) first introduced the fuzzy logic theory with the purpose of formalizing the notion of graded membership, as represented by the so-called membership function. The fuzzy sets are understood as the counterpart of the Boolean notion of regular sets, in a sense that in a fuzzy set an element can belong, not belong, or partially belong to the set.

As presented by DUBOIS and PRADE (1997) the membership function of a fuzzy set can basically be seen from three different perspectives: a degree of similarity, in which the membership function quantifies how similar an element of the set is compared to a prototype element; a degree of preference, where the membership function quantifies the preference or the feasibility of an element of the set; or a degree of uncertainty, in which the membership function is the degree of possibility that a determined parameter *u* has the value of an specific

element *x* of the set. The notion of degree of uncertainty is the base of the possibility theory (ZADEH, 1968) and the main tool for fuzzy uncertainty analysis.

Based on the concept of degree of uncertainty and through the fuzzy set theory, uncertainties can be modeled as fuzzy variables for the cases in which the statistical process that describes the random variables is unknown. The uncertain parameters are modeled as fuzzy numbers, where the actual value of the parameter is unknown, but limited to an interval weighted by a membership function. At this point, it is important to highlight that the membership function is a possibility distribution, not a probability distribution as required in the stochastic theory. Possibility is the measure of whether an event can happen, while probability is a measure of whether an event will happen. Therefore, the possibility distribution of a given uncertain parameter *u* quantifies the possible values that this parameter can assume. A probability distribution quantifies the chances that the uncertain parameter *u* has to assume a certain value *x*.

2.3.1 Fuzzy Variables

Let *X* be a universal classical set of objects whose generic elements are denoted by *x*. The subset *A* ($A \in X$) is defined by the classical membership function $\mu_A: X \rightarrow \{0,1\}$, shown in Figure 2.2, in which $\tilde{A}$ represents the fuzzy set and x_l and x_r are the lower and upper bounds of the fuzzy set support, respectively. Furthermore, a fuzzy set $\tilde{A}$ is defined by means of the membership function $\mu_A: X \rightarrow [0,1]$, being [0,1] a continuous interval. The membership function indicates the degree of compatibility between the element *x* and the fuzzy set $\tilde{A}$. The closer the value of $\mu_A(x)$ is to 1, more *x* belongs to $\tilde{A}$.

A fuzzy set is completely defined by (where $0 \leq \mu_A \leq 1$):

$$\tilde{A} = \left\{ \left(x, \mu_A(x) \right) \middle| x \in X \right\} \tag{2.4}$$

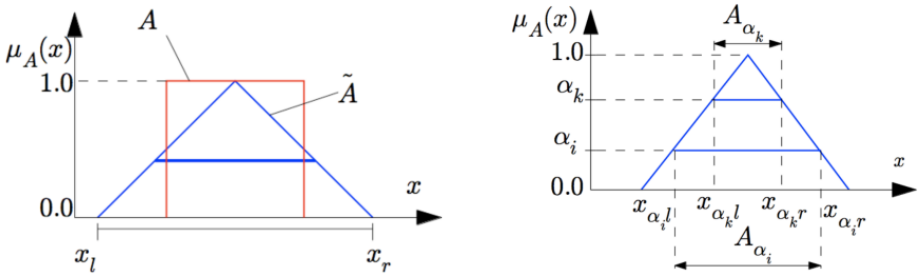

a) Fuzzy set. **b) The *α*-levels.**

Figure 2.2 - Fuzzy set and α-level representation

The fuzzy set $\tilde{A}$ can be represented by means of subsets that are denominated *α*-levels (see Figure 2.2), which correspond to real and continuous intervals.

2.3.2 Fuzzy Dynamic Analysis

The fuzzy dynamic analysis is an appropriate method to map a fuzzy vector of parameters onto output fuzzy functions by using the deterministic model of the mechanical system. In structural analysis, the combination of uncertainties modeled as fuzzy variables with the deterministic model based on the finite element method is denominated fuzzy finite element method. The fuzzy dynamic analysis includes two stages, based on the *α*-level optimization (MÖLLER, GRAF and BEER, 2000), as shown in Figure 2.3. In the first stage, for computational purposes, the input vector that corresponds to the fuzzy parameter is discretized by means of the *α*-level representation (see Figure 2.2). Thus, each element of the fuzzy parameter vector is considered as an interval. The second stage is related to solving an optimization problem. This optimization problem consists in finding the maximum or minimum value of the output at each *α*-level.

The fuzzy analysis of a transient time-domain system demands the solution of a large number of optimization problems regarding all *α*-levels of interest for each considered time step. Each upper and lower bounds of the system analysis at a given time instant is obtained from an optimization algorithm (VANDERPLAATS, 2007). The output value of the transient analysis at the evaluated time-step constitutes the objective function. The inputs to this function are the uncertain parameters described previously as fuzzy, or fuzzy random variables.

The fuzzy dynamic analysis based on the *α*-level optimization method is an eficient methodology for uncentainty analysis. However, the effectiveness of the method is highlly related to the performance of the optimization technique.

Depending on the features of the related optimization problems (i.e., multimodal objective functions), only global optimization algorithms can be used, such as the Differential Evolution algorithm (STORN and PRICE, 1995). The use of global optimization algorithms imposes high computational cost to some engineering applications.

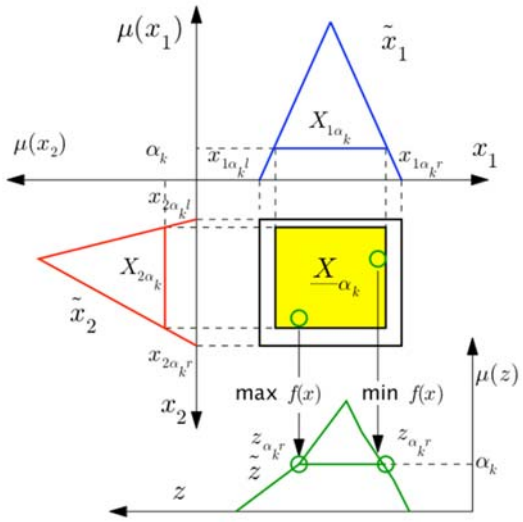

Figure 2.3 - The α-Level optimization

2.4. Numerical Validation

The numerical analysis considered the influence of uncertainties in the Young's modulus of the shaft of a rotor test rig and in the stiffness of the bearings of the rotating machine, on the dynamic response of the system. A straightforward numerical method was applied to simulate the dynamic responses of a representative Finite Element model (FE model) of the flexible rotor with two rigid discs and two self-alignment ball bearings. It is worth mentioning that the FE model was derived by using the approach previously presented by (CAVALINI JR *et al.*, 2016).

2.4.1 Rotor Test Rig

Figure 2.4a shows the rotor test rig used as a reference in the numerical validation process of the proposed fuzzy uncertainty analysis, which was mathematically represented by a model with 33 finite elements (FE model; Figure 2.4b).

The considered rotating machine is composed of a flexible steel shaft with 860 mm length and 17 mm of diameter (E = 205 GPa, ρ = 7850 kg/m^3, υ = 0.29), two rigid discs D_1 (node #13; 2,637 kg; according to the FE model) and D_2 (node #23; 2,649 kg), both of steel and with 150 mm of diameter and 20 mm of thickness (ρ = 7850 kg/m^3), and two self-alignment ball bearings (B_1 and B_2, located at the nodes #4 and #31, respectively). Displacement sensors are orthogonally mounted on the nodes #8 (S_{8X} and S_{8Z}) and #28 (S_{28X} and S_{28Z}) to collect the shaft vibration. The system is driven by an electric DC motor.

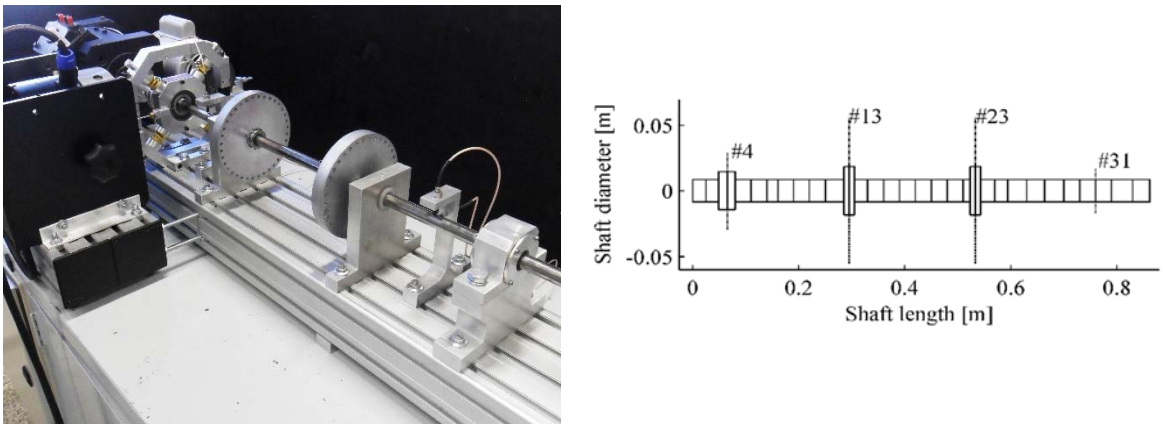

a) Test rig **b) FE model**

Figure 2.4 - Experimental test rig (a) and its corresponding FE model (b)

Equation 2.5 presents the equation of motion that governs the dynamic behavior of the flexible rotor supported by roller bearings (LALANNE and FERRARIS, 1998).

$$\mathbf{M}\ddot{\mathbf{q}} + \left[\mathbf{D} + \Omega\mathbf{D}_g\right]\dot{\mathbf{q}} + \left[\mathbf{K} + \dot{\Omega}\mathbf{K}_{st}\right]\mathbf{q} = \mathbf{W} + \mathbf{F}_u + \mathbf{F}_m \tag{2.5}$$

where **M** is the mass matrix, **D** is the damping matrix, $\mathbf{D}_g$ is the gyroscopic matrix, **K** is the stiffness matrix, and $\mathbf{K}_{st}$ is the stiffness matrix resulting from the transient motion. All these matrices are related to the rotating parts of the system, such as couplings, discs, and shaft. **W** stands for the weight of the rotating parts, $\mathbf{F}_u$ represents the unbalance forces, $\mathbf{F}_m$ is the vector of the shaft supporting forces produced by the ball bearings (incorporated as stiffness and damping coefficients in the matrix **K**), and **q** is the vector of generalized displacement.

Due to the size of the matrices involved in the equation of motion, the pseudo-modal method is used to reduce the dimension of the FE model and provided the solution, as proposed by LALANNE and FERRARIS (1998). In this work, the first twelve vibration modes of the rotor were used to generate the displacement responses.

A model updating procedure was used in order to obtain a representative FE model (Figure 2.4 - Experimental b). In this sense, a heuristic optimization technique (Differential Evolution, see (STORN and PRICE, 1995)) was used to determine the unknown parameters of the model, namely the stiffness and damping coefficients of the bearings, the proportional damping added to **D** (coefficients γ and β; $\mathbf{D}_p = \gamma\mathbf{M} + \beta\mathbf{K}$), and the angular stiffness k_{ROT} due to the coupling between the electric motor and the shaft (added around the orthogonal

directions *X - horizontal* and *Z - vertical* of the node #1). Further information regarding the model updating procedure adopted in this work can be found in CAVALINI JR *et al.* (2016).

The entire frequency domain process (i.e., comparison between simulated and experimental frequency response functions; FRF) was performed 10 times, considering 100 individuals in the initial population of the optimizer. The objective function adopted is presented in Eq. (2.6). For this case only the regions close to the peaks associated with the natural frequencies were taken into account.

$$F = \sum_{i=1}^{n} \frac{\left\| \mathrm{FRF}_i^{model}(x) - \mathrm{FRF}_i^{exp} \right\|}{\left\| \mathrm{FRF}_i^{exp} \right\|} \tag{2.6}$$

where *n* is the number of FRFs used in the minimization procedure, $\mathrm{FRF}_i^{model}(x)$ is the FRFs generated by the FE model, x is the vector containing the proposed unknown parameters, and FRF_i^{exp} is the experimental FRFs measured on the test rig.

The experimental FRF were measured for the test rig at rest by applying impact forces along the *X* and *Z* directions of both discs, separately. The response signals were measured by two proximity probes positioned along the same directions of the impact forces, resulting 8 FRFs. The measurements were performed by the analyzer Agilent® (model 35670A) in a range of 0 to 200 Hz and a frequency resolution of 0.25 Hz.

Table 2.1 summarizes the parameters determined in the end of the minimization process associated with the smallest fitness value (i.e., value of the objective function; Eq (6)). Figure 2.5 compares simulated and experimental FRFs, and the associated phase diagram, considering the parameters shown in Table 2.1. Note that the FRF generated from the FE model is satisfactorily close to the one obtained directly from the test rig.

Table 2.1 Parameters determined by the model updating procedure

Parameters	Value	Parameters	Value	Parameters	Value
k_X / B_1	8.551 *x* 10^5	k_X / B_2	5.202 *x* 10^7	γ	2.730
k_Z / B_1	1.198 *x* 10^6	k_Z / B_2	7.023 *x* 10^8	β	4.85 *x* 10^{-6}
d_X / B_1	7.452	d_X / B_2	25.587	k_{ROT}	770.442
d_Z / B_1	33.679	d_Z / B_2	91.033		

*k: stiffness [N/m]; d: damping [Ns/m].

Figure 2.6 compares the experimental orbit measured at the measure plane S_8 (full acquisition time of 4 s in steps of 0.002 s, approximately) with the one determined by the

updated FE model. The operational rotation speed of the rotor Ω was fixed to 1200 rev/min and an unbalance of 487.5 g.mm / 0^0 applied to the disc D_1 was considered. Note that the responses are close, as for the FRF previously shown, thus validating the updating procedure performed.

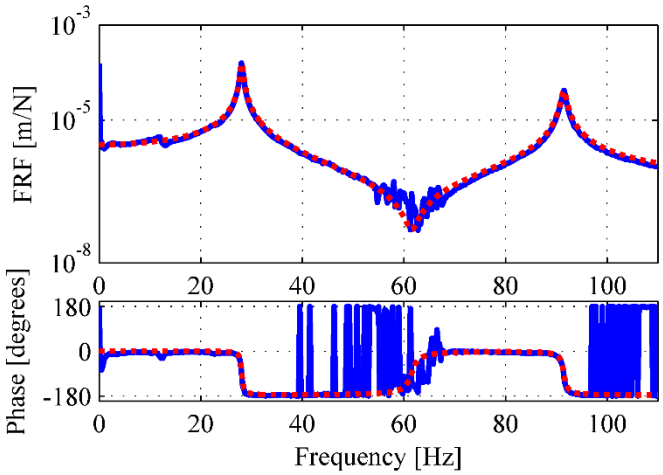

Figure 2.5 Simulated (- - -) and experimental (—) FRFs, and associated phases, obtained from impact forces on D_1 (X direction and S_{8X}).

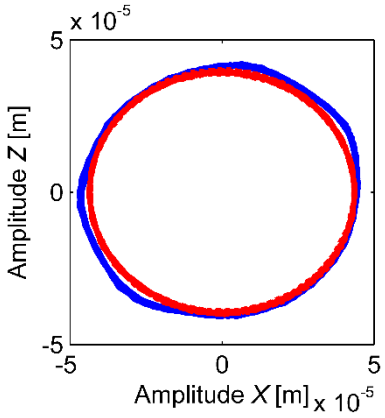

Figure 2.6 Simulated (—) and experimental (—) orbits for the rotor under consideration.

2.4.2 Uncertainty Scenarios

Aiming at evaluating the performance of the techniques previously described, two uncertain scenarios concerning the rotating machine presented by Figure 2.4 were considered. The first scenario is confined to the analysis of the rotor FRFs, considering uncertainties affecting the Young's modulus of the shaft. This material property is determined with reasonable accuracy by using standard material testing procedures, leading to small uncertain

values. It is worth mentioning that even these small variations can affect the dynamic behavior of the rotor system, influencing its performance, life, and reliability. The second uncertain scenario is dedicated to the analysis of the orbits and unbalance responses (run-up tests) of the rotor, introducing variations on the stiffness coefficients k_X and k_Z of the bearing B_1 (see Figure 2.4 and Table 2.1).

Three different methodologies were used to model the uncertain parameters of the rotating system (i.e., the Young's modulus and the stiffness coefficients). Regarding the stochastic theory, two different methodologies were tested. In the first approach, the variability of the system was estimated through MCS associated with the Latin Hypercube sampling technique (see VIANA *et al.*, 2007). No discretization procedure was used to discretize the random variables of the system; the deterministic FE model was used to evaluate the generated samples. From now on, this methodology will be referred to as MCS approach along the text, in a direct reference to the stochastic solver used to infer the variability of the system. The second approach is based on the SFEM associated with KL series expansion, considering an exponential autocovariance function. In this case, the random variables are discretized through a series expansion technique and evaluated by using the SFEM model. MCS combined with Latin Hypercube is used to solve the associated stochastic problem. This methodology will be referred to as KL method.

Note that the main diference between the two stochastic methodologies is associated with the discretization of the random variables. No discretization is considered in the first approach (i.e., MCS approach); while for the second methodology (i.e., KL method), a random discretization is performed to completely represent the random variables.

It is important to point out that the uncertain parameters were modeled as Gaussian random fields in both approaches. Gaussian random fields were adopted since it is expected that the realizations of the considered uncertain parameters are concentrated and symmetrically dispersed around their nominal values, approximately thus a 3σ model of Gaussian fields. Besides, another interesting feature of Gaussian fields is its guarantee convergence in the KL series expansion (LOÈVE, 1977), as previously mentioned. Also, in this contribution the interest in the uncertainty analysis is in the rotor working envelopes, so if other random fields, for instance, uniform fields, were selected, if the dispersion (3σ) were the same, is expected that obtained results to be identical, since the extreme realizations of the random field were note altered.

In order to apply the KL decomposition, the stochastic model of the rotating machine (Figure 2.4b) is formulated. Therefore, the deterministic FE model was parameterized aiming at factoring-out the uncertain parameters of the FE elementary matrices. Equation (2.7) presents the parametrization performed on the stiffness matrix $\mathbf{K}^{(e)}$ (elementary matrix

associated with **K** in Eq. (2.5)). Only the stiffness matrix of the rotating machine was parametrized, since the considered uncertain parameters are associated only to **K**.

$$\mathbf{K}^{(e)} = \mathbf{K}_S^{(e)} + \mathbf{K}_B^{(e)} \tag{2.7a}$$

$$\mathbf{K}_S^{(e)} = EI_S\overline{K}_S^{(e)} \tag{2.7b}$$

$$\mathbf{K}_B^{(e)} = \boldsymbol{f}(k_X, k_Z) \tag{2.7c}$$

where $\mathbf{K}_S^{(e)}$ is the elementary stiffness matrix of the shaft (following the Timoshenko beam theory), and $\mathbf{K}_B^{(e)}$ is the elementary stiffness matrix associated with the bearings. In this formulation the shaft and bearings stiffness are considered to be in series resulting in the resulting elementary matrix $\mathbf{K}^{(e)}$. Also, I_s represent the area moment of inertia of the shaft and *E* is the Young's modulus of the shaft. Further, $\mathbf{K}_B^{(e)}$ is considered to be a function $\boldsymbol{f}$ of k_X and k_Z. The parameters k_X and k_Z designate the stiffness coefficients of the bearings along the *X* and *Z* directions, respectively (see the deterministic parameters in Table 2.1).

As presented in Eq. (2.3), the KL series decomposition of a random field requires the knowledge of the eigenvalues λ_i and eigenfunctions φ_i of the random field associated with the autocovariance function. Considering a one-dimensional Gaussian field, GHANEM and SPANOS (1991) have shown that the eigen problem associated with the exponential covariance function presented in Eq. (2.8) has an analytical solution in the domain $\Omega_x = (x_1, x_2)$.

$$C_{HH}(x_1, x_2) = exp\left(-|x_1 - x_2|/L_{cor,x}\right) \tag{2.8}$$

where $(x_1, x_2) \in [0, L]$ and $L_{cor,x}$ indicates the correlation length, characterizing the decreasing behavior of the covariance with respect to the distance between the observation points along the *y* direction.

Considering the property of the covariance function, the eigenvalues and eigenfunctions are given as a function of the roots $\omega_r (r \geq 1)$ of two transcendental equations through a procedure that can be summarized as follows:

- For *r* odd, with $r \geq 1$:

$$\lambda_r = \frac{2L_{cor,x}}{L_{cor,x}^2\omega_r^2+1},\ \varphi_r(x) = \alpha_r cos(\omega_r, x) \tag{2.9}$$

where $\alpha_r = 1/\sqrt{L/2 + sin(\omega_r L)/2L}$ and ω_r is the solution of the transcendental equation presented in Eq. (2.10).

$$1 + L_{cor,x}\omega_r \tan(\omega_r L) = 0 \tag{2.10}$$

defined in the domain $\left[(r-1)\frac{\pi}{L}, \left(r - \frac{1}{2}\right)\frac{\pi}{L}\right]$.

- For *r* even, with $r \geq 1$:

$$\lambda_r = \frac{2L_{cor,x}}{L_{cor,x}^2\omega_r^2 + 1},\ \varphi_r(x) = \alpha_r sin(\omega_r, x) \tag{2.11}$$

where $\alpha_r = 1/\sqrt{L/2 - sin(\omega_r L)/2L}$ and ω_r is the solution of the transcendental equation presented in Eq. (2.12).

$$L_{cor,x}\omega_r + \tan(\omega_r L) = 0 \tag{2.12}$$

defined in the domain $\left[\left(r - \frac{1}{2}\right)\frac{\pi}{L}, r\frac{\pi}{L}\right]$.

From the solution of the eigenproblem shown previously, the elementary random matrices of the shaft can be computed by using Eq. (2.13).

$$\mathbf{K}_S^{(e)}(\theta) = \mathbf{K}_S^{(e)} + \sum_{r=1}^{n} \overline{K}_{S_r}^{(e)}\, \xi_r(\theta) \tag{2.13}$$

where θ is the random process and the random matrices $\overline{K}_{S_r}^{(e)}$ are calculated by using Eq. (2.14).

$$\overline{K}_{S_r}^{(e)}(\theta) = \int_0^L \sqrt{\lambda_r}\, \varphi_r(x) \boldsymbol{B}^T(x) \overline{\boldsymbol{E}} \boldsymbol{B}(x) dx \tag{2.14}$$

where $\overline{\boldsymbol{E}}$ is the matrix of material properties in which the parameters E_S and I_S were factored-out.

The elementary matrices of the bearings are obtained by applying a dyadic structural transformation rather than an integration scheme as in the case of the shaft. The corresponding uncertainties are introduced by using $k(\theta) = k_o + k_o \delta_k \xi(\theta)$, where k_o designates the mean value of the stiffness coefficients of the bearings with the corresponding dispersion level δ_k.

Further information regarding the parametrization procedure can be found in KOROISHI *et al.* (2012).

From the stochastic finite element matrices and by performing the standard FE matrix assembling procedure, the frequency domain and the time domain responses of the rotating machine can be obtained. The stochastic model of the flexible rotor has to be solved by a stochastic solver. As mentioned, in this contribution the stochastic model was solved through MCS combined with the Latin Hypercube technique.

Finally, the third methodology used to model the uncertain parameters of the rotating system (i.e., the Young's modulus and the stiffness coefficients) is based on the fuzzy logic approach. In this case, the uncertain parameters are modeled as fuzzy triangular numbers (i.e., fuzzy variables) and mapped through the α-level optimization method. The Sequential Quadratic Programming algorithm (SQP; see (VANDERPLAATS, 2007)) was used to perform the required minimizations and maximizations (see Figure 2.3). The respective optimization problems are monomodal, thus allowing the direct optimization procedure to find global optimal solutions.

2.4.3 Frequency Domain Analysis

This analysis is confined to the frequency domain, as being characterized by the envelopes of the FRFs of the rotor responses. In this case, the influences of the uncertainties affecting the Young's modulus of the shaft on the dynamic behavior of the system are evaluated.

Regarding the stochastic procedures (i.e., MCS approach and KL method), the inherent uncertainty was modeled as a Gaussian random field with nominal value E = 205 GPa with a deviation of ±5% (3σ model, i.e. E±15%). The convergence of the response variability was verified regarding the number of terms retained in the truncated KL expansion series (n_{KL}) and the number of samples used for MCS (n_S). In order to determine n_{KL} and n_S, the mean square convergence analysis (RMS) with respect to the independent realizations θ of the FRF was obtained according to Eq. (2.15).

$$RMS = \sqrt{\frac{1}{n_S}\sum_{i=1}^{n_S}|H_i(\theta) - H_i|^2} \tag{2.15}$$

in which H_i represents the response obtained by the deterministic model and $H_i(\theta)$ is the response determined from a specific realization θ.

Figure 2.7 presents the convergence analysis performed for the MCS approach and for the KL method (Figure 2.7a and Figure 2.7b, respectively). The number of terms retained in the series was verified, in which the convergence was achieved for $n_s \geq 250$ and $n_{KL} \geq 40$.

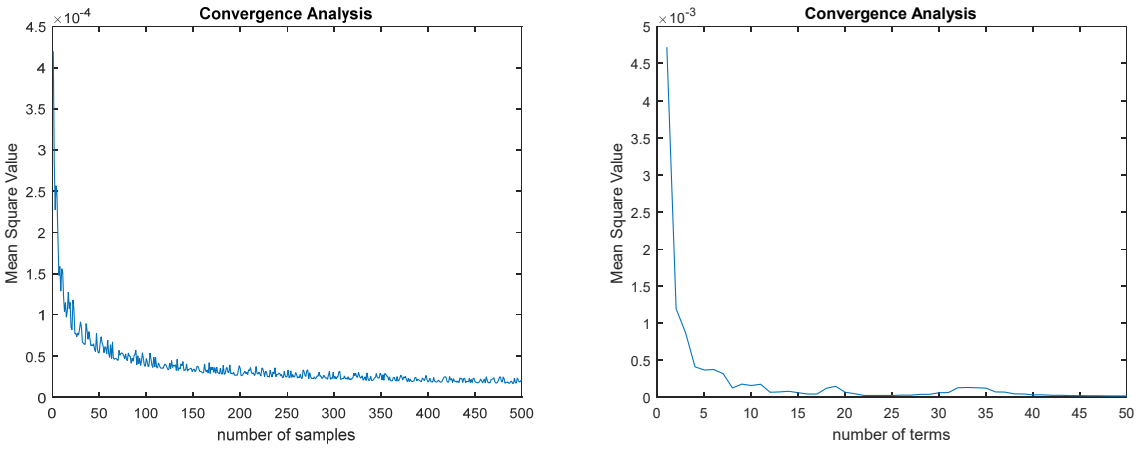

a) n_S **b)** n_{KL}

Figure 2.7 Convergence verification for the frequency domain analysis.

Regarding the fuzzy approach, the uncertain parameter was modeled as a fuzzy triangular number with the same nominal value and deviation adopted for the stochastic procedures (i.e., $\tilde{E} = 205 \pm 15\%$ GPa). For the fuzzy uncertainty analysis, the objective function related to the *α*-level optimization procedure was the norm of the H_i vector; i.e., the lower bound corresponds to the $\tilde{E}$ value that minimizes the system response and the upper bound is related to the $\tilde{E}$ value that maximizes the system response.

The uncertainty analysis in the context of rotating machines can be performed aiming at different goals. In the case of both robust design and robust control design, the objective of uncertainty analysis is to obtain the minimum and maximum responses of the rotor (i.e., the working envelopes). In the present contribution, the fuzzy logic approach was confined to the uncertainty level $\alpha = 0$ of the model. Clearly, the stochastic analysis was formulated to obtain the minimum and maximum responses of the rotating machine.

Figure 2.8 shows the comparison between the uncertain envelopes of the rotor FRFs obtained by the stochastic and fuzzy methodologies. In this case, the FRFs were obtained by considering the force applied along the *X* direction of the disc D_1 and the measures obtained from the sensor S_{8X} (see Figure 2.5). Note that the results obtained by the different approaches are similar. Table 2.2 summarizes the results shown in Figure 2.8, in which the

referred upper and lower limits (and the related values of Young's Modulus) indicates the FRFs (H) working envelopes bounds.

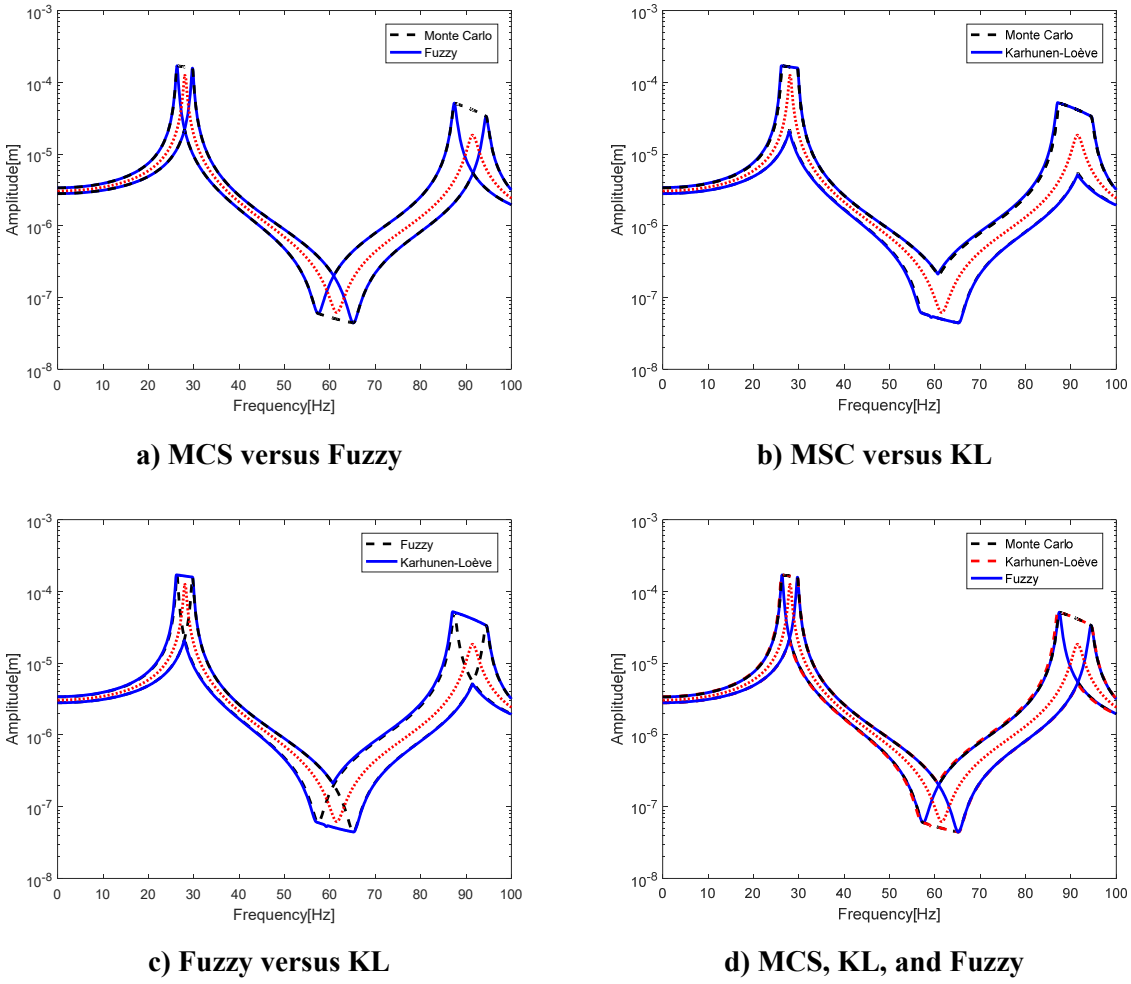

Figure 2.8 FRFs determined for different methods of uncertainty analysis (.... deterministic FRF; see Figure 2.5).

Table 2.2 Results for the frequency domain analysis.

Method	Lower Limit		Upper Limit	
	$\underline{E}$ (GPa)*	$\|\underline{H}\|$	$\overline{E}$ (GPa)**	$\|\overline{H}\|$
MCS	235.52	$6.4\ x\ 10^{-4}$	174.31	$7.04\ x\ 10^{-4}$
KL	235.63	$6.4\ x\ 10^{-4}$	174.37	$7.06\ x\ 10^{-4}$
Fuzzy	235.75	$6.4\ x\ 10^{-4}$	174.25	$7.04\ x\ 10^{-4}$

* $\underline{E}$ indicates the Young's modulus value that generates the minimum response.

**$\overline{E}$ represents the Young's modulus value that generates the maximum response.

Regarding the associated computational cost, the fuzzy logic approach required 14 evaluations of the FE model, while the stochastic methods required 250 evaluations of the deterministic model (number of samples).

2.4.4 Time Domain Analysis

The time domain analyses (i.e., rotor orbits and run-up test) were performed considering the uncertainties affecting the stiffness coefficients k_X and k_Z of the bearing B_1 (see Table 2.2). For the stochastic methods, the uncertain parameters were modeled as Gaussian random fields with nominal values of k_X = 8.551x10^5 N/m and k_Z = 1.198x10^6 N/m (see Table 2.1) with a deviation of ±10% (3σ model).

Regarding the rotor orbits, the operational rotation speed of the rotor Ω was fixed to 1200 rev/min and an unbalance of 487.5 g.mm / 0^0 was applied to the disc D_1 (see Figure 2.6). A simulation time of 10 seconds with steps of 0.001 seconds was adopted.

The convergence of the response variability was also verified in terms of the number of samples n_S for the MCS approach and the number of terms n_{KL} in the KL expansion. Analogous to the frequency domain analysis, the RMS value with respect to the independent realizations θ of the orbits was performed - Eq. (15) - considering that H_i represents the orbits computed by the deterministic model and $H_i(\theta)$ represents the orbits computed for the realization θ. Figure 2.9 presents the convergence analysis performed for both the MCS approach and KL method (Figure 2.9a and Figure 2.9b, respectively). Convergence was achieved for $n_s \geq 500$ and $n_{KL} \geq 100$.

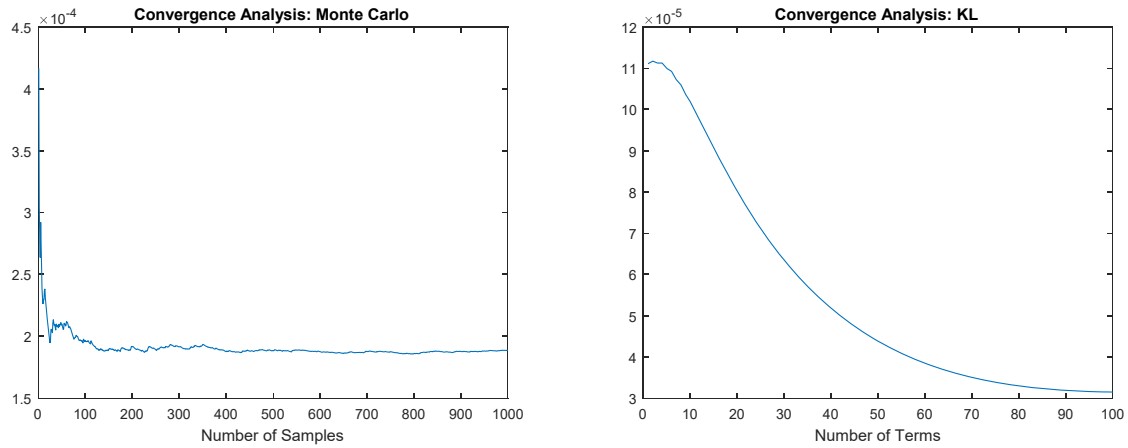

a) n_S **b) n_{KL}**

Figure 2.9 Convergence verification for the time domain analysis associated with the orbits of the rotor.

Regarding the fuzzy approach, the uncertain parameter was modeled as belonging to a fuzzy triangular function with the same nominal value and deviation adopted for the stochastic procedures (i.e., k_X = 8.551x10^5 N/m and k_Z = 1.198x10^6 N/m with a deviation of ±30%). The objective function related to the α-level optimization procedure was the norm of the displacement vector.

Figure 2.10 shows the comparison between the uncertain envelopes of the rotor orbits obtained by using the stochastic and fuzzy methodologies. Note that the results determined by these two approaches are similar. However, MCS approach leads to a bigger stiffness coefficient k_Z. Therefore, small vibration amplitudes can be observed along the Z direction as compared with the results obtained by the KL method and the fuzzy approach. Table 2.3 summarizes the results shown in Figure 2.10 in which the referred upper and lower limits (and the related values of stiffness coefficients) indicates working envelopes bounds of the of the orbits (z). The fuzzy logic approach required 26 evaluations of the FE model and the stochastic methods required 500 evaluations of the deterministic model.

Regarding the run-up test, the operational rotation speed Ω of the rotor was considered as varying linearly from 0 to 3000 rev/min (simulation time of 10 seconds; steps of 0.001 seconds). An unbalance of 487.5 g.mm / 0^0 was applied to the disc D_1.

The convergence of the response variability was also verified in terms of the number of samples n_S for the MCS approach and the number of terms n_{KL} for the KL expansion (see Figure 2.11). Similarly, to the analyses performed for the rotor orbits, the convergence of the RMS value was obtained for $n_s \geq 500$ and $n_{KL} \geq 100$.

Figure 2.12 presents the comparison between the envelopes of the rotor responses (run-up test from 0 to 3000 rev/min in 10 seconds) determined along the X direction of the disc D_1. Note that the amplitudes associated with the lower limit were similar to the ones obtained by using the fuzzy and MCS approaches. A similar behavior could not be verified by using the KL method. However, different values of amplitudes were observed in all of the remaining unbalance responses. Table 2.4 summarizes the results shown in Figure 2.12.

Similar to the orbits analysis, in the run-up test the fuzzy logic approach required 26 evaluations of the FE model while the stochastic methods required 500 evaluations of the deterministic model.

The main objective of the present contribution was to evaluate the suitability of three different methodologies for uncertainty analysis in the context of rotating systems.

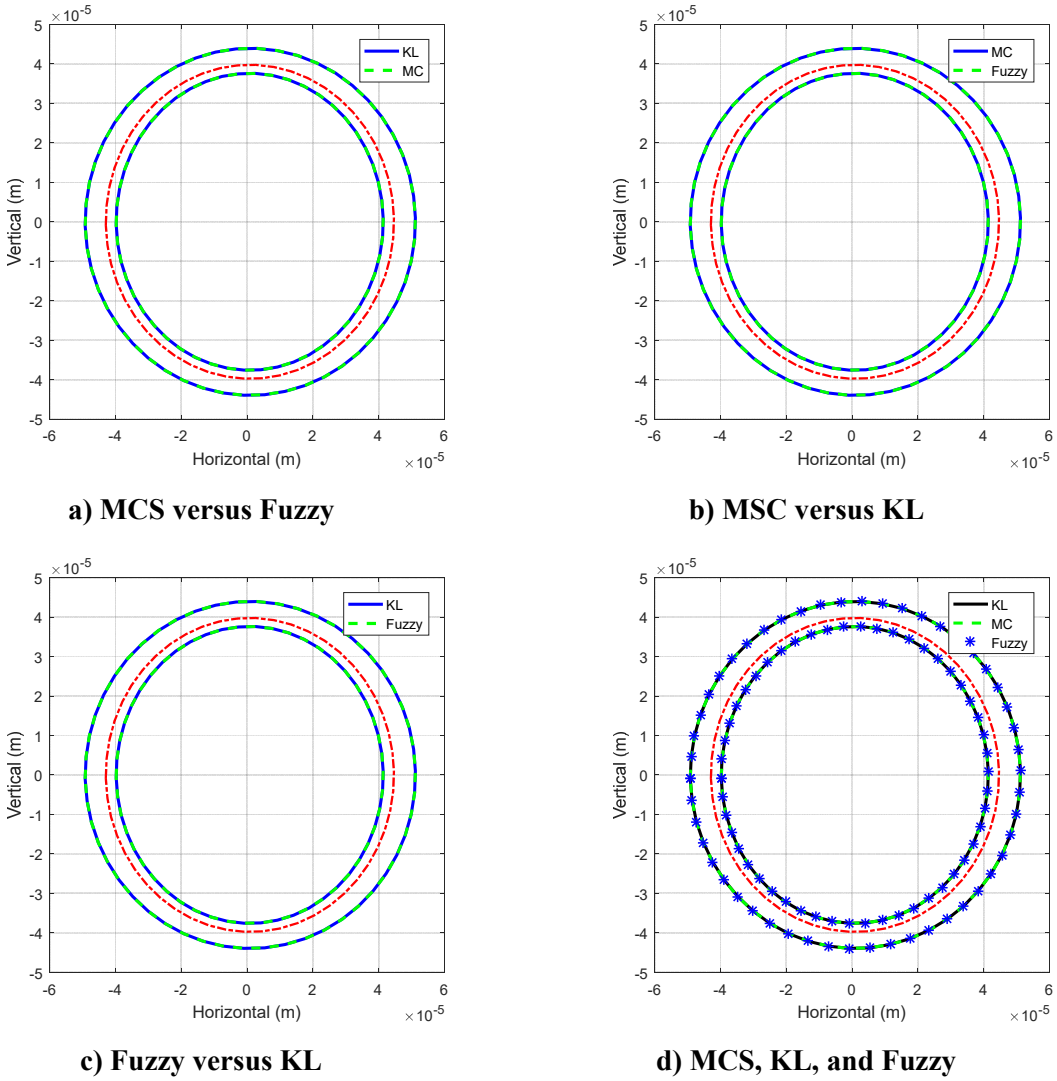

Figure 2.10 Orbits determined for the different uncertainty methods (-.-.- deterministic response; see Figure 2.6).

Table 2.3 Results for the time domain analysis associated with the rotor orbits.

Method	Lower Limit			Upper Limit		
	$\underline{k}_X$(N/m)	$\underline{k}_Z$(N/m)	$\underline{z}$	$\overline{k}_X$(N/m)	$\overline{k}_Z$(N/m)	$\overline{z}$
MCS	$1.112x10^6$	$1.557x10^6$	0.0038	$5.991x10^5$	$8.39x10^5$	0.0044
KL	$1.112x10^6$	$1.556x10^6$	0.0038	$5.991x10^5$	$8.39x10^5$	0.0044
Fuzzy	$1.112x10^6$	$1.557x10^6$	0.0038	$5.986x10^5$	$8.384x10^5$	0.0044

* $\underline{k}$ indicates the stiffness coefficients that generates the minimum response $\underline{z}$.

**$\overline{k}$ represents the stiffness coefficients that generates the maximum response $\overline{z}$.

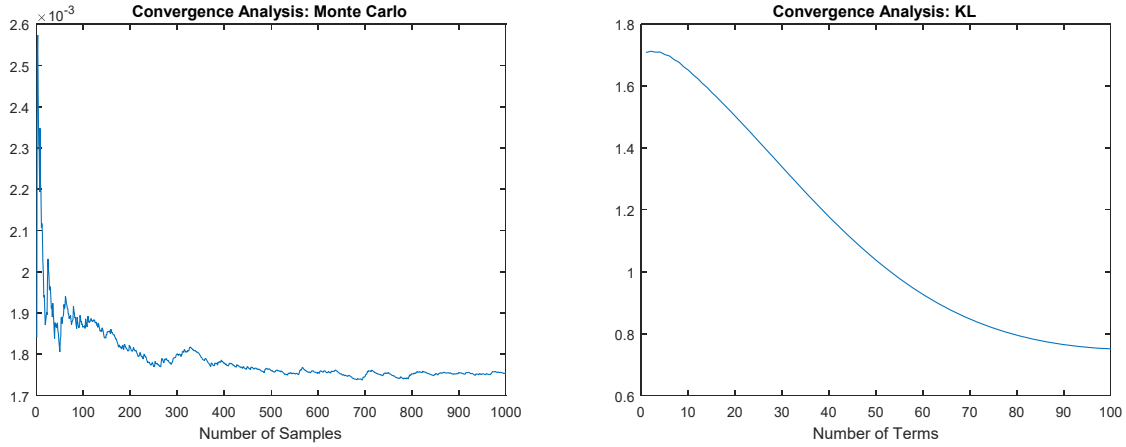

a) n_S **b)** n_{KL}

Figure 2.11 Convergence verification for the time domain analysis associated with the linear run-up test.

Table 2.4 Results for the time domain analysis associated with the run-up test.

Method	Lower Limit			Upper Limit		
	$\underline{k}_X$(N/m)	$\underline{k}_Z$(N/m)	$\underline{z}$	$\overline{k}_X$(N/m)	$\overline{k}_Z$(N/m)	$\overline{z}$
MCS	$1.109x10^6$	$1.101x10^6$	0.0291	$5.987x10^5$	$9.968x10^5$	0.0351
KL	$1.089x10^6$	$1.063x10^6$	0.0293	$6.104x10^5$	$1.526x10^6$	0.0347
Fuzzy	$1.091x10^6$	$1.083x10^6$	0.0291	$6.596x10^5$	$1.196x10^6$	0.0349

* $\underline{k}$ indicates the stiffness coefficients that generates the minimum response $\underline{z}$.

**$\overline{k}$ represents the stiffness coefficients that generates the maximum response $\overline{z}$.

Through numerical simulations, the stochastic and fuzzy approaches were compared in terms of uncertain envelopes generated by the analysis of the dynamic behavior of a flexible rotor. For this aim, uncertainties were introduced in the Young's modulus of the shaft and the stiffness coefficients of the bearing.

The evaluated methodologies presented similar results regarding the FRFs of the rotating machine, suggesting that the proposed methods lead to equivalent results. However, this equivalence was not verified in the time domain analysis.

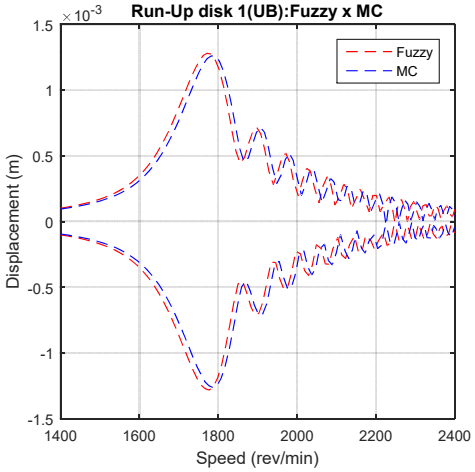

a) Upper limit – MCS versus Fuzzy

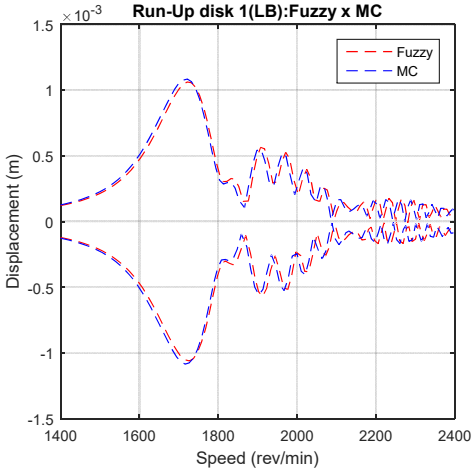

b) Lower limit – MCS versus Fuzzy

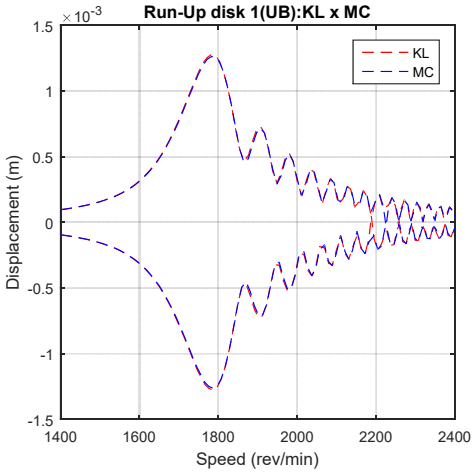

c) Upper limit – MSC versus KL

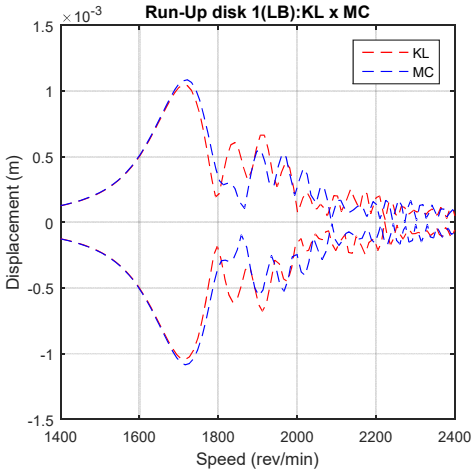

d) Lower limit – MSC versus KL

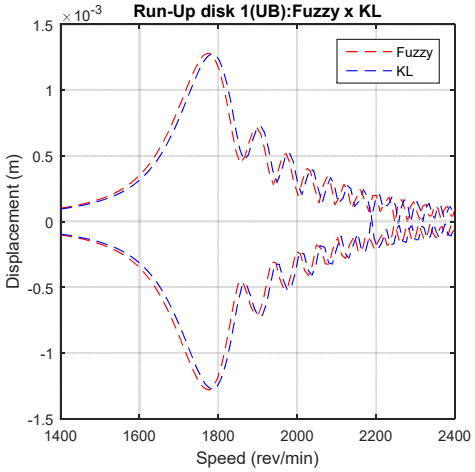

e) Upper limit – Fuzzy versus KL

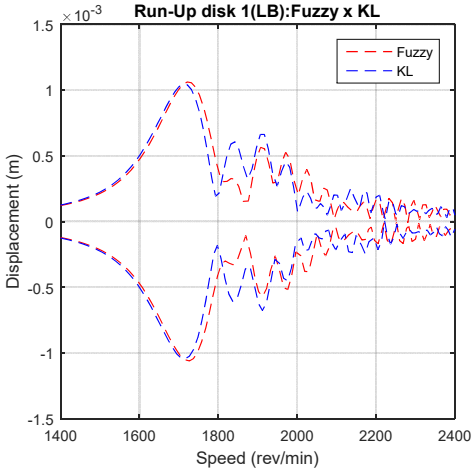

f) Lower limit – Fuzzy versus KL

Figure 2.12 Run-up responses determined for the different uncertainty approaches.

The uncertainty methodologies presented different behavior with respect to the run-up simulations. Regarding the better scenario (i.e., minimum response – lower bound of the envelope), the KL method presented the less critical response (smallest vibration amplitude). The MCS approach obtained the most critical response (largest vibration amplitude), while the fuzzy approach converged to an amplitude value which lies between the responses provided by the stochastic methods.

The responses obtained by using the fuzzy approach are associated to a global optimization solution. Therefore, it is suggested that the KL method underestimates the vibration amplitude of the rotor while the MCS overestimates the vibration response. Further analyses are necessary to confirm this conclusion. Regarding the worst scenario (i.e., maximum response – upper bound of the envelope), the KL method and the MCS converged to similar responses. The fuzzy approach obtained the most critical response (largest vibration amplitude), suggesting that the stochastic approaches underestimate the system response.

The uncertainty analysis procedure is considered as a previous step that contributes to the decision making related to procedures such as robust design, robust control, predictive maintenance and risk management. The under and overestimation of one of the bounds lead to some difficulties for these procedures. Therefore, further analysis should be performed to evaluate the behavior of the system response as determined through stochastic methods.

Regarding the computational costs, the fuzzy approach required no more than 30 evaluations of the deterministic FE model to obtain the system responses. The stochastic methods required up to 500 evaluations of the deterministic FE model to determine the same responses. In this contribution, this relative high number of evaluations required by the stochastic methods did not lead to prohibitive computational time, a feature that may not be true in the case of complex applications, such as industrial applications.

Another important feature to take into consideration is the mathematical complexity of the uncertainty approaches. The KL series expansion method has a relative mathematical complexity, requiring the solution of an integral eigenvalue problem. The MCS and the fuzzy approaches presented a simpler and straightforward mathematical modeling. Nevertheless, the SFEM associated with series expansion (KL method) presents a practically guaranteed convergence (LOÈVE, 1977). The mathematical simplicity of the MCS and fuzzy methods is counterweighted by the computational cost that the corresponding algorithms may require.

In the context of the rotordynamic applications presented in this analysis, it may be concluded that the most adequate methodology used for uncertainty analysis in rotating systems depends on the problem considered. However, the author consider that the fuzzy logic approach appears as the most indicated methodology due to its mathematical simplicity, convergence characteristics, and the fact that no previous knowlegde of the uncertain values

variability is required or has to be adopted. Finally, the fuzzy method performance is related to the performance of the optimization algorithm and the features of the associated optimization problems.

2.5 Experimental Validation

For safety reasons the uncertainty scenarios considered in the numerical validation (fluctuations regarding shaft and bearing stiffness) of the proposed fuzzy uncertainty analysis could not be experimentally implemented. Thus, new uncertainty scenarios were formulated considering now a flexible with three rigid discs supported by two fluid film bearings. Uncertainties affecting the bearings parameters, namely oil viscosity and radial clearance were considered in the experimental analysis. In the remaining of this subtopic the new rotor test rig and its related FE model are presented along with the considered uncertainty scenarios and obtained results.

2.5.1 Rotor Test Rig

The proposed uncertainty analysis was applied to a horizontal rotating machine modeled by using 35 Timoshenko beam elements, which is shown in Figure 2.13. The rotor system is composed by a flexible steel shaft with 840 *mm* length and 19.05 *mm* diameter (E = 1.9 x 10^{11} Pa, ρ = 8030 kg/m^3, and u = 0.3), three rigid discs D_1 (node #16; 0.658 kg), D_2 (node #20; 5.013 kg), and D_3 (node #25; 0.658 kg), and two cylindrical hydrodynamic bearings (B_1 and B_2, located at the nodes #9 and #35, respectively), each one with 19.05 *mm* diameter and 12.8 *mm* length. The rotating parts take into account a proportional damping added to the matrix **D** (Eq. (1); $\mathbf{D}_p = \gamma\,\mathbf{M} + \beta\,\mathbf{K}$) with coefficients γ = 5 and β = 5 x 10^{-6}. Following the model proposed by LALANNE and FERRARIS (1998), it is assumed that the disc D_2 increases the stiffness of the shaft at the disc location (elements #19 and #20; see Figure 2.13b). Special care was dedicated to the model of the disc D_2 to comply with the stiffness increase due to coupling of the disc to the shaft.

According to MEGGIOLARO and ALMEIDA (1997), the hypothesis of short sleeve bearing is based on the relationship $L_h/2R \leq 0.5$. However, in this case $L_h/2R$ = 12.8/19.05 = 0.672. The displacement responses obtained from the nonlinear short bearing theory presented in this work were compared with the linear long bearing theory in a previous work (CAVALINI JR. *et al.*, 2015). The verified similarity between the linear and nonlinear responses combined with the large computational cost associated with the linear theory regarding the

optimization task involved in this application; RIUL, STEFFEN JR and RIBEIRO (1992), justify the consideration of the short nonlinear bearing theory.

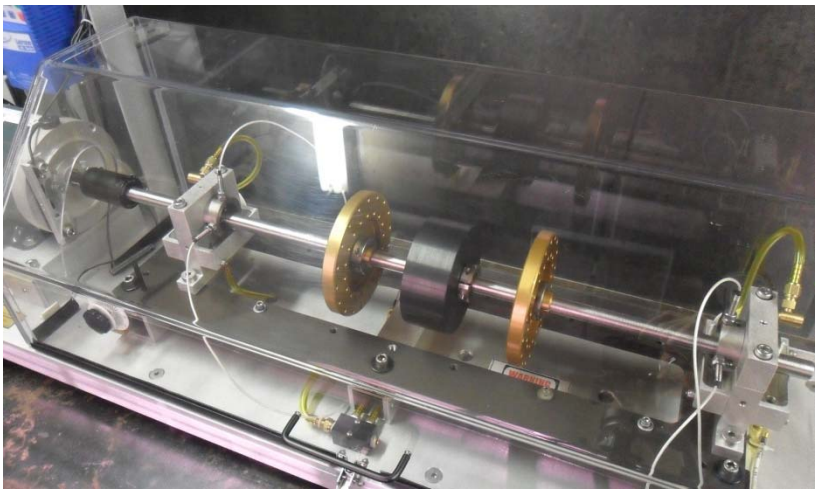

a) Rotating machine.

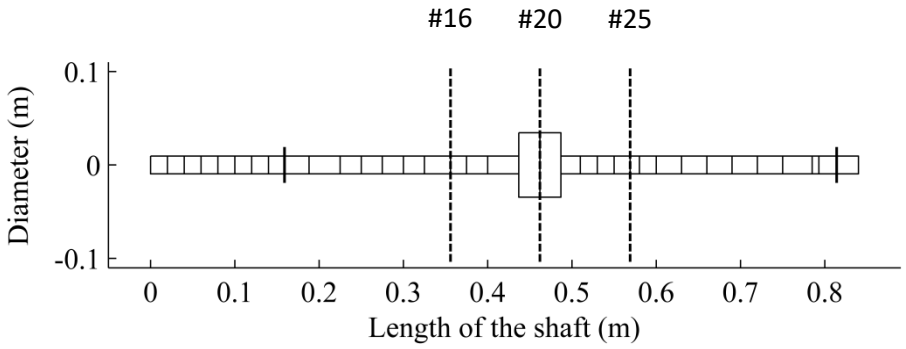

b) FE model.

Figure 2.13 Flexible rotor used on the experimental analysis.

Experimental frequency response functions (FRFs) were measured on the rotor at stand still for the free-free end condition by applying impact forces along the horizontal direction (i.e., *X* direction) at the nodes #4, #11, #18, #27 and #34, separately. The response signals were measured by three accelerometers installed along the same direction of the impact forces at the nodes #4, #11, and #34, resulting fifteen FRFs. The measurements were performed by a signal analyzer, *Agilent*® (model 35670A), in a range from 10 to 300 *Hz* and steps of 0.5 *Hz*. Figure 2.14 compares the four simulated and experimental FRFs by considering the parameters of the rotating machine presented above. Note that the FRFs generated from the FE model are satisfactorily close to the ones obtained directly from the test rig.

Concerning now the assembled test rig (i.e., rotor under operating condition), displacement responses are collected in the vicinity of the bearings locations (measuring planes S_1 and S_2; nodes #10 and #33, respectively) along the horizontal and vertical directions (X and Z, respectively).

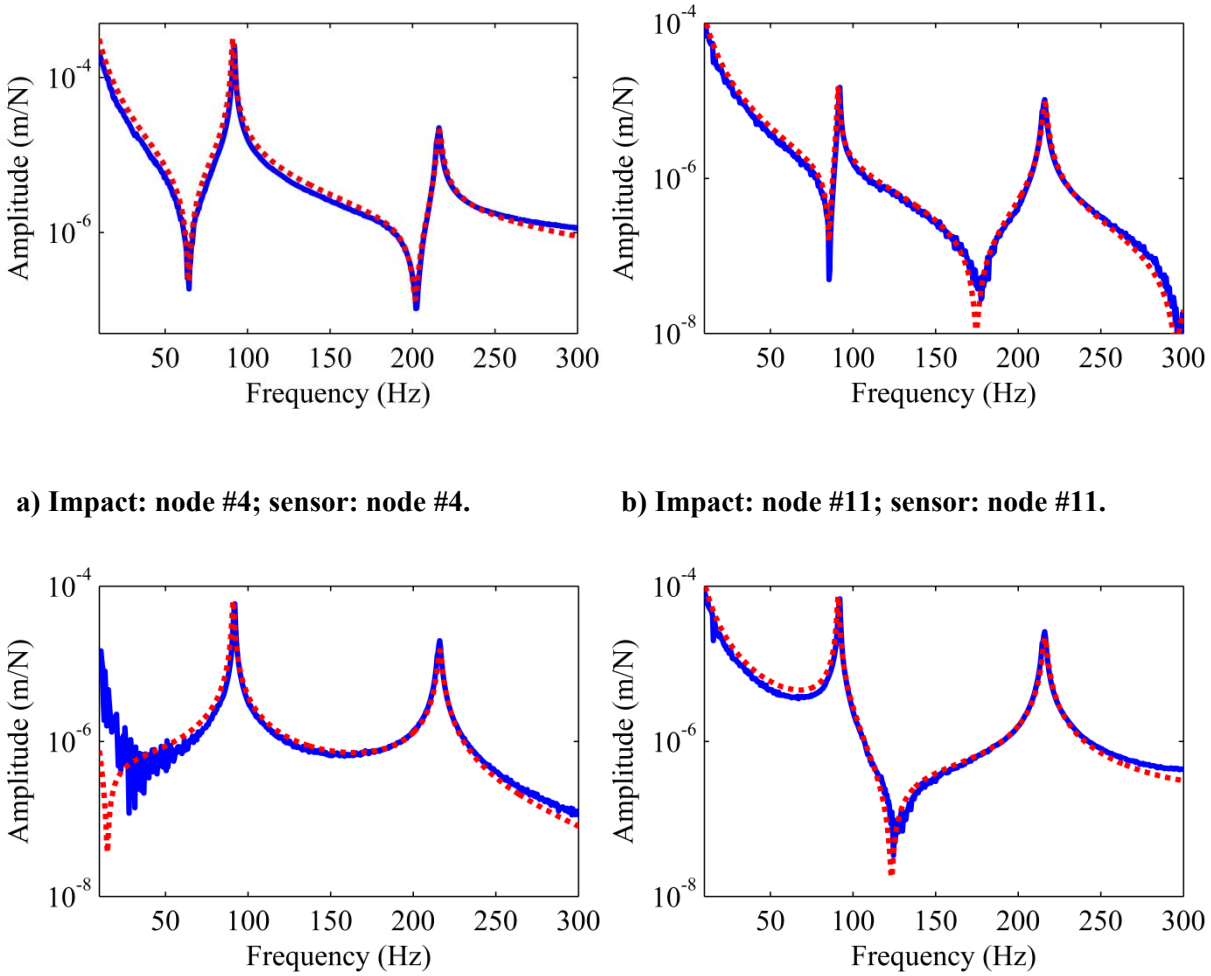

a) Impact: node #4; sensor: node #4.

b) Impact: node #11; sensor: node #11.

c) Impact: node #18; sensor: node #34.

d) Impact: node #34; sensor: node #34.

Figure 2.14 Simulated (- - -) and experimental (----) FRFs

Figure 2.15 illustrates the displacements obtained from the measuring plane S_2 (close to the bearing B_2) with the rotor performing a linear run-down condition (2500 to 0 *rpm* in 10 *secs*; numerical simulation). It can be observed that the first critical speed of the rotating machine is, approximately, 1600 *rpm*. In order to obtain the displacements shown in Figure 2.15, the radial clearance of the bearings B_1 and B_2 were taken as $C = 76.2\ \mu m$. The oil viscosity was considered equal to 0.0449 *Pa.s* (MINERAL OIL ISO 13 at 22.5°*C*) and calculated as a function of the temperature (HAMROCK, SCHMID and JACOBSON, 2004), as shows the Eq.

(2.16). Additionally, the simulations were performed considering the system vibrating around its equilibrium position.

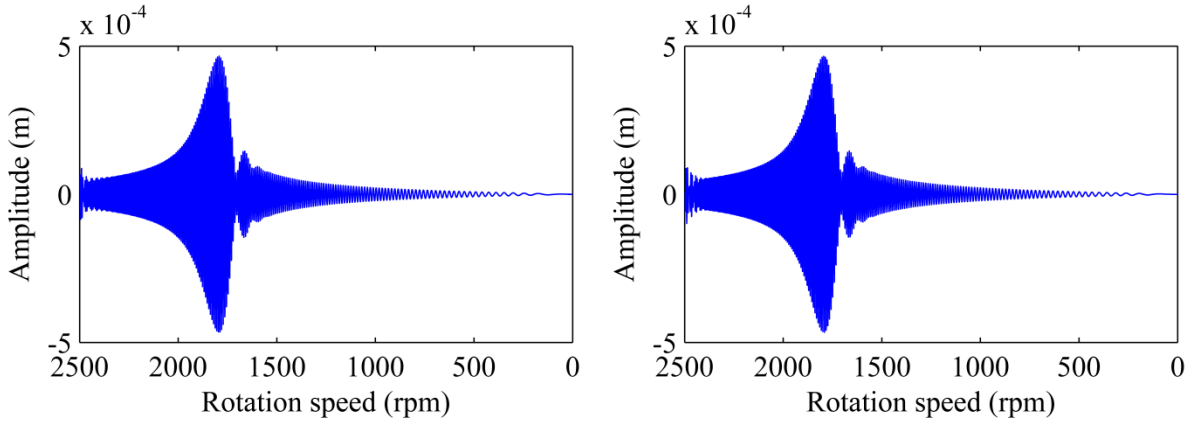

a) Horizontal vibration (*X* direction). **b) Vertical vibration (*Z* direction).**

Figure 2.15 Simulated linear run-down responses obtained on the plane S2 (node #33)

$$\mu_h = 10^{\left[k_1(1+0.007407T_{oil})^{k_2}+4.2\right]} \tag{2.16}$$

where T_{oil} is the oil temperature (°*C*). The coefficients k_1 = 3.3914 and k_2 = -1.1232 were determined from the measured oil viscosity.

A model updating procedure was carried out to quantify the unbalance condition and the effect caused by the coupling between the electric motor and the shaft on the dynamic behavior of the test rig. In this sense, the Differential Evolution optimization technique (STORN and PRICE, 1995) was used to determine the unknown parameters of the model. In this way, the linear and angular stiffness of the coupling (k_{linear} and $k_{angular}$ added around the orthogonal directions *X* and *Z* at the node #2) and the equivalent masses/phases that should be inserted on each disc to obtain the real unbalanced condition of the test rig were determined. The entire identification process was based on time domain dynamic responses (i.e., comparison between simulated and experimental displacement responses) was performed 10 times, considering 40 individuals in the initial population of the optimizer. The objective function to be minimized is given by Eq. (2.17).

$$O_f = \sum_{i=1}^{n} \frac{\left\| \max\left(\mathbf{Out}_{exp,i}\right) - \max\left(\mathbf{Out}_{model,i}\right) \right\|}{\left\| \max\left(\mathbf{Out}_{exp,i}\right) \right\|} \tag{2.17}$$

where $\mathbf{Out}_{exp,i}$ is the experimental vibration response measured directly on the test rig and $\mathbf{Out}_{model,i}$ is the associated response determined by the FE model. In this case, n is the number of displacement responses considered in the minimization process.

It is well known that the unbalanced masses/phases and the stiffness of the coupling do not change with the rotation speed of the rotor. Therefore, the minimization process was performed considering the rotor operating at two different rotating speeds: 1100 and 1200 *rpm*, separately. Consequently, the experimental displacement responses were measured on the planes S_1 and S_2 with the rotor operating at the same rotation speeds (full acquisition time of 0.4 *sec*. in steps of 0.0005 *sec*., approximately; measurements performed by the analyzer *Agilent*® model 35670A).

Table 2.5 summarizes the parameters determined in the end of the minimization process associated with the smallest value of the objective function (Eq. (2.17)) and the lower and upper limits imposed to the optimization process. Figure 2.16 compares the simulated (the last 0.4 *sec*. of the simulation) and experimental displacement responses of the rotor obtained on the plane S_1 for the rotor operating at both considered rotation speeds. Note that the time responses generated from the FE model are not close enough to the ones obtained directly from the test rig, which can be associated with the inherent uncertainties affecting the bearings.

Table 2.5 Parameters determined by the model updating procedure

Parameters		*Lower limit*	*Upper limit*	*Optimized values*
Disc D_1	*Unbalance* (*kg.m*)	0	1.0×10^{-3}	8.3583×10^{-4}
	Phase (*degrees*)	-180	180	-23.1591
Disc D_2	*Unbalance* (*kg.m*)	0	1.0×10^{-3}	7.6299×10^{-4}
	Phase (*degrees*)	-180	180	154.7898
Disc D_3	*Unbalance* (*kg.m*)	0	1.0×10^{-3}	9.7153×10^{-4}
	Phase (*degrees*)	-180	180	142.8335
Coupling	k_{linear} (*N/m*)	0	1.0×10^{2}	70.8333
	$k_{angular}$ (*N.rad/m*)	0	1.0×10^{2}	9.6127

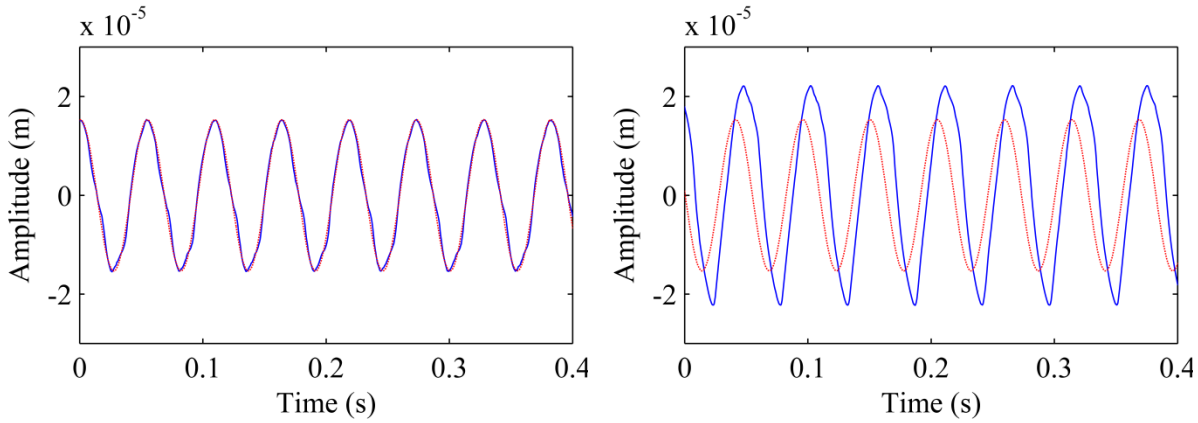

a) Rotation speed: 1100 *rpm*; *X* direction. **b) Rotation speed: 1100 *rpm*; *Z* direction.**

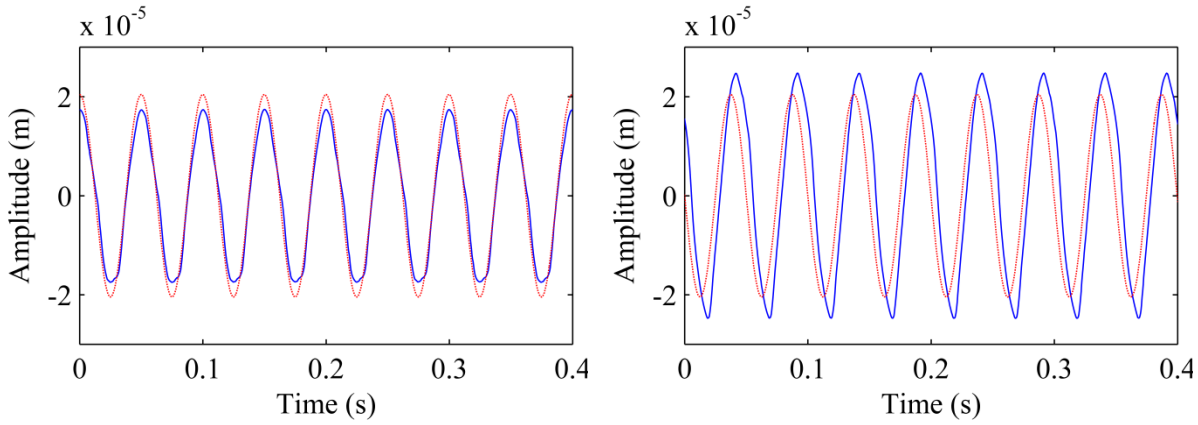

c) Rotation speed: 1200 *rpm*; *X* direction. **d) Rotation speed: 1200 *rpm*; *Z* direction.**

Figure 2.16 Simulated (- - -) and experimental (----) displacement responses obtained on the plane S_1.

It is worth mentioning that the simulated responses that were determined along the *X* direction (Figure 2.16a and Figure 2.16c) matched the ones associated with the experimental measurements. To obtain this result it was necessary to adjust the time shift between the two responses (simulated and experimental).

2.5.2 Uncertainty Analysis

Generally, the results determined by FE models of flexible rotors supported by fluid film bearings present small differences as compared with the experimental ones. This behavior can be attributed to the variation of the oil film temperature along the bearing, which is disregarded in the nonlinear model considered in this work. Additionally, the mentioned discrepancies are associated with machining problems affecting directly the deterministic

radial clearance of the bearings (leading to non-cylindrical bearings). Different malfunctions can lead to discrepancies between numerical and experimental vibration responses in rotating machines. As an example, the cavitation is a common problem observed in oil film bearings (ZAPOMEL and FERFECKI, 2011).

Figure 2.17 shows the fluid film bearings used in the rotor test rig presented in Figure 2.13a. In this case, diameter measures were taken along the sections *A*, *B*, *C*, and *D*, considering four different measuring points (i.e., *1*, *2*, *3*, and *4*). Table 2.6 and Table 2.7 presents the measures performed on the bearings located at the left and right-hand sides of the rotor, respectively. The left-hand side bearing is the one located close to the electric motor of the test rig (Figure 2.13a).

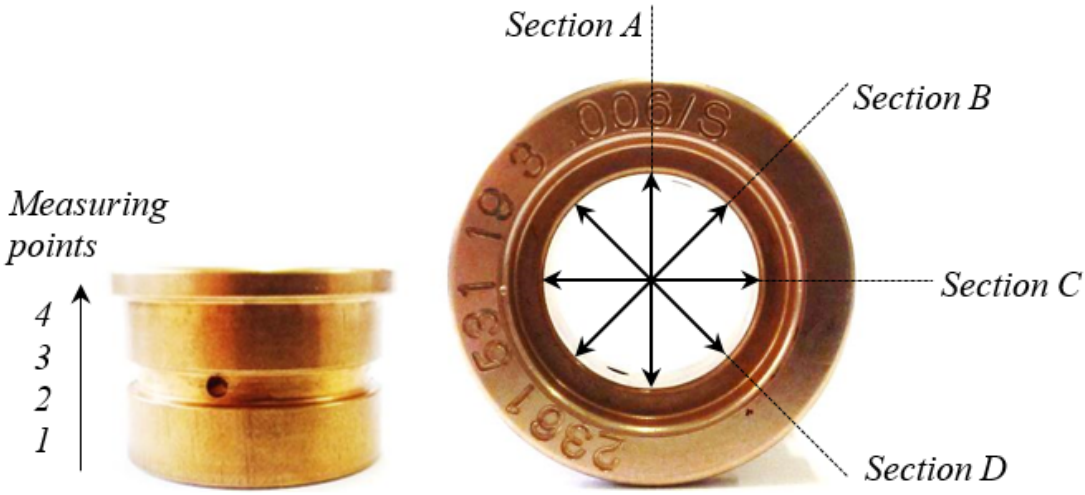

Figure 2.17 Measuring points and measuring sections on the bearings.

Table 2.6 Diameter measures performed on the bearing near the coupled.

	Measuring points				
Sections	*1*	*2*	*3*	*4*	***Mean value (mm)*
A (*mm*)	19.199	19.191	19.180	19.167	19.184
B (*mm*)	19.196	19.192	19.179	19.168	19.184
C (*mm*)	19.199	19.193	19.178	19.169	19.185
D (*mm*)	19.199	19.192	19.179	19.171	19.185
**Mean value (mm)*	19.198	19.192	19.179	19.169	**19.185**

**Mean value considering a given measuring point. **Mean value considering a given section.*

Table 2.7 Diameter measures performed on the right-hand side bearing.

	Measuring points				
Sections	*1*	*2*	*3*	*4*	***Mean value* (*mm*)
A (*mm*)	19.222	19.194	19.180	19.168	19.191
B (*mm*)	19.225	19.194	19.177	19.168	19.191
C (*mm*)	19.225	19.196	19.180	19.167	19.192
D (*mm*)	19.224	19.194	19.179	19.167	19.191
**Mean value* (*mm*)	19.224	19.195	19.179	19.168	**19.191**

**Mean values considering a given measuring point. **Mean values considering a given section.*

The diameter of the shaft was also measured at the position of the bearings, resulting a mean value of 19.01 *mm* (the deterministic diameter is equal to 19.05 *mm*, as given by the manufacturer). It can be observed that the left hand side bearing presented mean values (***Mean value* – Table 2.6) of radial clearance as $C_{SectionA} = C_{SectionB} = 87$ *μm* and $C_{SectionC} = C_{SectionD} = 87.5$ *μm* (variations of 14.17% and 14.83%, respectively, related to the deterministic value of the radial clearance; i.e., $C = 76.2$ *μm*). Regarding the opposite bearing, the following mean values (***Mean value* – Table 2.7) were found: $C_{SectionA} = C_{SectionB} = C_{SectionD} = 90.5$ *μm* and $C_{SectionC} = 91$ *μm* (variations of 18.77% and 19.42%, respectively, related to the deterministic value of the radial clearance). Therefore, the bearings seem to be non-cylindrical (see all the diameters measured along the measuring points and measuring sections in Table 2.6 and Table 2.7). However, the radial clearance is considered as being constant in the nonlinear model proposed by CAPONE (1986). Consequently, uncertainty analysis is necessary to predict the dynamic behavior of the rotating machine. It is worth mentioning that both journal bearings are not perfectly cylindrical. Note in Table 2.6 and Table 2.7 that a non-perfect cylindrical shape is obtained by measuring the diameters along different measuring sections and measuring points. Additionally, the diameter measures reveal a quasi-conic shape for both bearings.

Table 2.8 shows the uncertainty scenarios considered in this contribution, namely the introduction of uncertainties in the radial clearance of both bearings (scenario 01), the influence of uncertainties in the oil viscosity (scenario 02), and the influence of both uncertain parameters on the dynamic behavior of the rotating machine (uncertainties in the radial clearance and in the oil viscosity; scenario 03). The analysis were performed considering the rotor operating at two rotating speeds: 1100 and 1200 *rpm*, separately. The uncertain parameters were modeled by using fuzzy triangular numbers as shown above. The uncertainty intervals associated with the radial clearances (i.e., ± 32.0%) were defined from the maximum variation obtained from

the measures performed at the bearings. The intervals associated with the oil film temperature were defined by following the variation adopted for the radial clearances (i.e., ± 32.0%). It is worth mentioning that the literature suggests large variations in the oil film temperature along the bearing (DANIEL and CAVALCA, 2013; HEINRICHSON, 2006).

Table 2.8 Uncertainty scenarios considered in the present contribution.

Scenarios	*Deterministic parameters*	*Uncertainty intervals* (± 32%)
Scenario 01	$C = 76.2\ \mu m$	$51.82\ \mu m \leq C \leq 100.58\ \mu m$
Scenario 02	$T_{oil} = 22.5^{o}C$	$15.3^{o}C \leq T_{oil} \leq 29.7^{o}C$
Scenario 03	$C = 76.2\ \mu m$	$51.82\ \mu m \leq C \leq 100.58\ \mu m$
	$T_{oil} = 22.5^{o}C$	$15.3^{o}C \leq T_{oil} \leq 29.7^{o}C$

In order to solve the optimization problem associated with the described fuzzy analysis, the SQP algorithm was used (VANDERPLAATS, 2007). The norm of the vibration response obtained along the *X* direction of the measuring plane S_2 (node #33) was written to represent the objective function of the minimization and maximization problems inherent to the fuzzy analysis.

Figure 2.18a shows the orbits determined in the measuring plane S_1 by the updated FE model (i.e., obtained from the deterministic parameters; see Table 2.8), the lower and upper limits ($\alpha = 0$) for the uncertainty scenario 01 (i.e., variations in the radial clearances), and the associated experimental orbit. In this case, the rotor is operating at 1100 *rpm*. The results obtained from the measuring plane S_2 is presented in Figure 2.18b., Figure 2.18c and Figure 2.18d present the corresponding orbits for the rotor operating at 1200 *rpm*. Note that the displacements determined by applying the uncertainty scenario 01 in the FE model can predict satisfactorily the dynamic behavior of the rotor shown in Figure 2.13.

In CAVALINI JR *et al.* 2015), it was demonstrated that the uncertainties in the radial clearances are able to modify the location of the orbits center. This is an expected result, since the hydrodynamic force is directly affected by the radial clearance and oil viscosity. However, the same phenomena cannot be observed in the numerical simulations presented in this work since the system is vibrating around its equilibrium position.

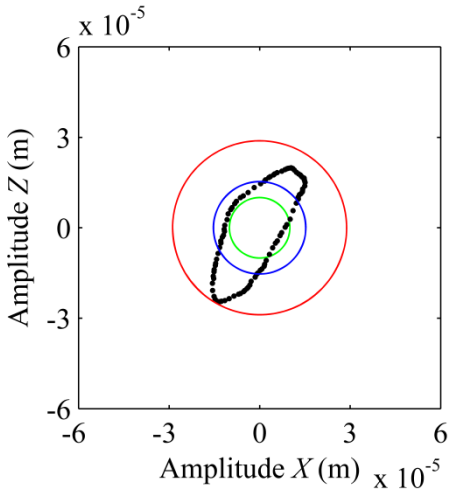

a) Rotation speed: 1100 *rpm*; Plane S_1.

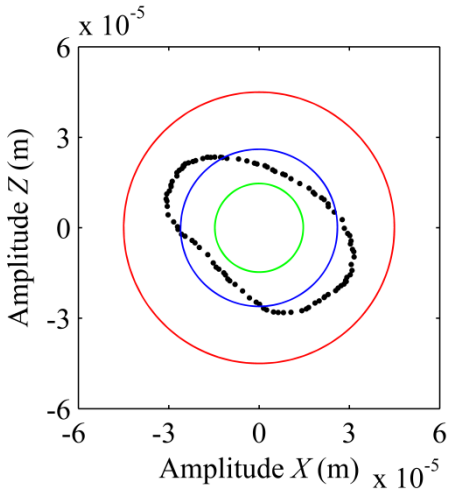

b) Rotation speed: 1100 *rpm*; Plane S_2.

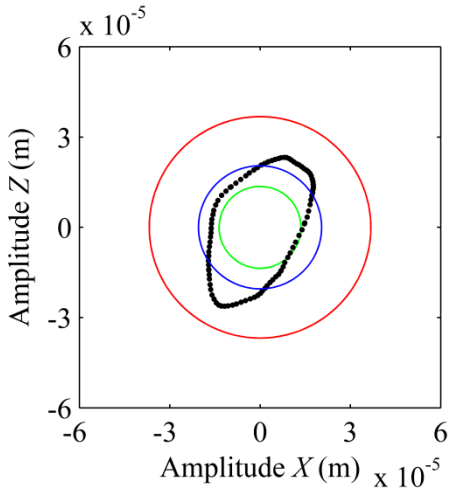

c) Rotation speed: 1200 *rpm*; Plane S_1.

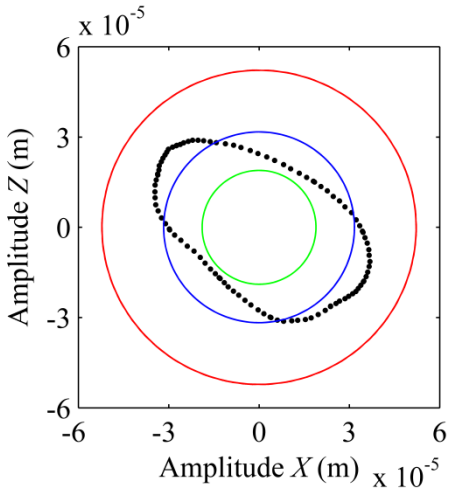

d) Rotation speed: 1200 *rpm*; Plane S_2.

Figure 2.18 Envelope of the orbits considering the uncertainty scenario 01 (---- lower limit / α = 0; ---- upper limit / α = 0; ---- nominal; •••• experimental)

Figure 2.19 shows the orbits determined in the measuring planes S_1 and S_2 by the updated FE model (i.e., obtained from the deterministic parameters; see Table 2.8), the lower and upper limits (α = 0) for the uncertainty scenario 02 (i.e., variations in the oil film temperature), and the associated experimental orbits. In this case, the rotor is operating at 1100 and 1200 *rpm*, separately. Note that smaller changes are observed in the results when uncertainties are introduced in the oil viscosity. Additionally, the displacements determined by applying the uncertainty scenario 02 in the FE model is not able to predict the dynamic behavior of the system. Remember that the intervals associated with the oil film temperature were defined by following the variation adopted for the radial clearances (i.e., ± 32.0%).

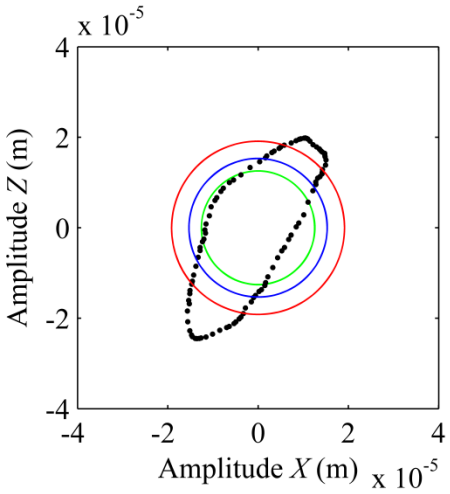

a) Rotation speed: 1100 *rpm*; Plane S_1.

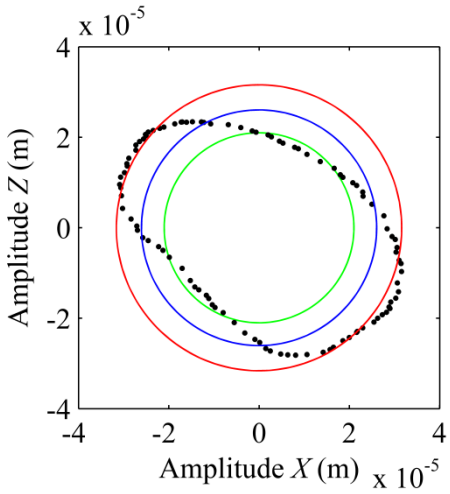

b) Rotation speed: 1100 *rpm*; Plane S_2.

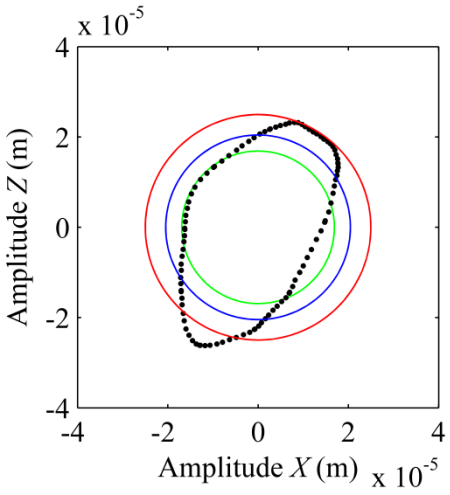

c) Rotation speed: 1200 *rpm*; Plane S_1.

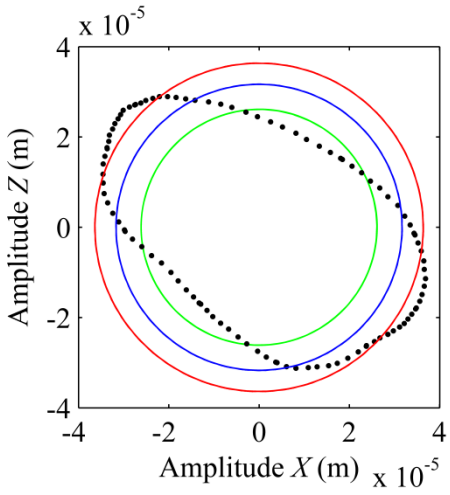

d) Rotation speed: 1200 *rpm*; Plane S_2.

Figure 2.19 Envelope of the orbits considering the uncertainty scenario 02 (---- lower limit / α = 0; ---- upper limit / α = 0; ---- nominal; •••• experimental

The results shown in Figure 2.19 suggest that a combination of both considered uncertain parameters (i.e., the radial clearance and the oil film temperature) are affecting the dynamic behavior of the rotating machine, which is expected in industrial rotating machines suported by journal bearings. Therefore, Fig. 2.20 shows the theoretical orbits determined at the measuring planes S_1 and S_2 by the updated FE model, the lower and upper limits ($\alpha = 0$) for the uncertainty scenario 03 (i.e., variations in the radial clearance and oil film temperature, simultaneously; see Table 2.8). The associated experimental orbits measured in the rotor test rig are presented for comparison purposes (the rotor is operating at 1200 *rpm*). Note that the displacements determined by applying the uncertainty scenario 03 in the FE model can predict

satisfactorily the dynamic behavior of the rotor as shown in Figure 2.13. Additionally, the difference between the vibration responses associated with the lower and upper limits ($\alpha = 0$) in Fig. 2.20 are greater than the ones obtained for the uncertain scenario 01 (compare Figure 2.18 and Fig. 2.20 for $\Omega = 1200$ *rpm*). Therefore, the combination of both uncertain parameters leads to an addition effect on the vibration response of the rotor system. The amplitude of the vibration response associated with the upper limit increased as compared with the results shown in Figure 2.18. Differently, the amplitude of the responses associated with the lower limit is now decreased.

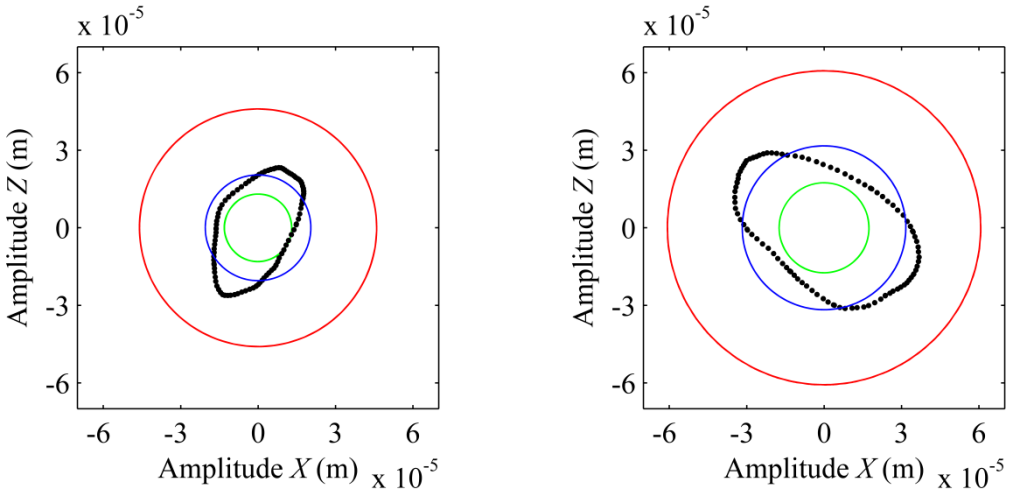

a) Rotation speed: 1200 *rpm*; Plane S_1. **b) Rotation speed: 1200 *rpm*; Plane S_2.**

Figure 2.20 Envelope of the orbits considering the uncertainty scenario 03 (---- lower limit / α = 0; ---- upper limit / α = 0; ---- nominal; •••• experimental)

In this section the fuzzy logic approach was used to evaluate the dynamic responses of a flexible rotor supported by oil film bearings. Three uncertainty cases were analyzed: *i*) uncertainties in the oil viscosity, *ii*) uncertainties in the radial clearance applied to both bearings that support the machine, and *iii*) the influence of both uncertain parameters on the dynamic behavior of the rotating machine. The fuzzy analysis is an advantageous approach since it is able to predict the real upper and lower limits of the uncertainty envelope. The numerical applications and experimental tests led to similar results. The small differences observed are attributed to the variation of the oil film temperature along the bearing (normally disregarded in the models) and to machining problems affecting the radial clearance. It was observed that the left-hand side bearing presented variations of approximately 14.5% considering the various measuring sections, as related to the deterministic value of the radial clearance. Similarly, the opposite bearing presented variations of approximately 19%. The diameter measurements

presented in Table 2.6 and Table 2.7 revealed that the bearings used in the test rig have a non-cylindrical shape.

Finally, in this chapter the use of fuzzy logic applied to the uncertainty analysis of rotating systems, by means of the so-called α-level optimization procedure was evaluated. The proposed methodology was numerically validated presenting responses (in terms of uncertainty envelopes) similar to well-established stochastic approaches with the advantage of reduced computational cost and simpler mathematical formulation. The proposed methodology was also experimentally evaluated obtaining satisfactory results in the uncertainty analysis of a flexible rotor. Therefore, the obtained results demonstrate that the proposed fuzzy uncertainty analysis methodology is well suited for the uncertainty analysis of rotating systems.

CHAPTER III

ROBUST OPTIMIZATION BY MEANS OF FUZZY LOGIC

In this chapter, two distinct fuzzy robustness optimization approaches are presented and evaluated in terms of rotor balancing applications. First, a non-parametric approach is proposed in an attempt to enhance an existing balancing technique robustness. This methodology is based on the concept of fuzzy sets and defuzzification, which are revisited in this chapter. The proposed approach is evaluated both numerically and experimentally. Then, a parametric robustness optimization methodology is proposed and evaluated numerically aiming at increasing balancing robustness of the so-called model-based balancing approach. This approach strongly relies in concepts of fuzzy optimization.

Throughout the chapter, the key aspects related to both methodologies are addressed and the obtained results for each approach are evaluated. Finally, a brief discussion regarding obtained results is presented.

3.1 Rotor Balancing Review

Balancing is a systematic procedure for adjusting the radial mass distribution of a rotor to approximate its barycenter to the geometric centerline, thus reducing the vibration amplitude and lateral forces applied to the bearings and surrounding structures due to unbalancing (EISENMANN and EISENMANN JR, 1998). Different signal-based solutions have been proposed to minimize the damage effects of unbalance, such as the modal balancing, four-runs without phase, combined techniques, and the so-called influence coefficients method (IC method) (STEFFEN JR and LACERDA, 1996; WOWK, 1998; ISHIDA and YAMAMOTO, 2012).

Although widely used in industry, the signal-based techniques present some adverse aspects that encourage researchers to propose new balancing approaches. Existing methods demonstrated to be time-consuming, since trial weights are positioned at specific locations along the rotor to determine the sensitivity of the vibration responses to unbalance variations. The correction weights and their corresponding angular positions are obtained so that the vibration amplitudes of the rotor system are minimized. Additionally, classical signal-based balancing methodologies consider that the relationship between the unbalance excitation and

the resulting vibration is linear. However, if some nonlinearity exists in the structure, the obtained results are not satisfactory (CAVALINI JR *et al.*, 2012).

KANG *et al.* (2008) evaluated the accuracy of an improved IC method that minimizes the condition number of the influence coefficients. The authors observed an inverse relation between the condition number and the balancing efficiency. The obtained results demonstrate that the balancing performance can be improved by proper selection of sensors and balancing planes locations. The sensitivity of the signal-based techniques with respect to the locations of sensors and balancing planes was considered as adverse condition.

An important practical problem of the IC balancing is associated with the availability of balancing planes to accept correction weights obtained by optimization. UNTAROIU, ALLAIRE and FOILES (2008) focused on practical constraints related to balancing in industrial applications. Regarding restrictions associated with the positions of correction weights, the authors proposed a constrained optimization approach based on the IC method.

Aiming at overcoming some limitations faced by the signal-based techniques, a model based balancing approach was presented by SALDARRIAGA *et al.* (2010). This technique does not require linear relationship between unbalance and vibration responses; besides, trial weights are not required. The unbalance is identified by solving a typical inverse problem through a pseudo-random optimization method, such as Genetic Algorithms, Simulated Annealing, Particle Swarm Optimization, Ant Colony, Differential Evolution, etc. The method presented by SALDARRIAGA *et al.* (2010) showed to be well adapted for industrial applications only if a representative mathematical model of the rotating machine is available (even for the uncertain parameters affecting the system).

According to LI, LIN and ALLAIRE (2008), the effect of uncertain parameters on balancing techniques have been ignored over the years except for a few authors, who claim that vibration responses can vary with the uncertainties. However, it is worth mentioning that the industry is aware of uncertainties affecting the balancing results and have developed in-house procedures to overcome this problem for specific products. Measurement errors (i.e., disturbance and noise), unbalance variation (e.g., change of unbalance due to thermal bow and variation of the oil film temperature in journal bearings), and geometric restrictions associated with the introduction of correction masses in the machine, are sources of uncertainties. Consequently, the success of signal-based balancing techniques depends on both the accuracy of vibration measurements and the knowledge on the uncertainties affecting the rotor vibration responses.

In this context, LI, LIN and ALLAIRE (2008) proposed a robust balancing approach devoted to high speed rotating machines. The methodology was formulated based on a convex optimization problem, combining the advantages of the IC method and the modal balancing

approach. The influence coefficients, unbalanced rotor vibration, and correction masses were modeled as random parameters (i.e., uncertain variables). Both uniform and normal probability distributions were considered in Monte Carlo simulations (MC simulations).

3.2 Non-Parametric Evaluation

In this section, a revised IC balancing methodology based on fuzzy logic approach is evaluated in terms of overall balancing robustness. In the proposed approach, rotor vibration responses measured over a long period are submitted to a fuzzy transformation procedure, adapted from POTA, ESPOSITO and DE PIETRO (2013), wherein rotor unbalance fuzzy sets are generated. Rotor unbalance condition (i.e., vibration amplitudes and associated angular positions) is obtained through a defuzzification process, which is introduced in the IC method for balancing purposes. Therefore, system uncertainties manifested in the measurement data set are assessed by means of a fuzzy logic approach at a proposed preprocessing stage. The effectiveness of the methodology is demonstrated both numerically and experimentally. A test rig composed by a horizontal flexible shaft, two rigid discs, and supported by rolling and oil film bearings is used. The rotation speed of the rotor system and the temperature of the lubricant oil (oil film bearing) are considered as uncertain parameters. The goal of this approach is to obtain vibration amplitudes that are less sensitive to operational fluctuations of the rotating machine.

3.2.1 IC Balancing Method

The IC method is widely used in industry to balance flexible rotors, leading to satisfactory and reliable results. Once the balancing planes, measuring planes, and trial weights are defined, the additional information required by the IC method is the vibration amplitudes and corresponding phase angles associated to the unbalanced system. As mentioned, the vibration responses are considered as uncertain information in the proposed robust balancing approach.

Few definitions are important to understand the mathematical formulation of the IC method. Trial weights are masses fixed to proper planes defined to apply a known unbalance force in the rotating machine. Measuring planes are locations suitable to the installation of vibration sensors. Correction weights are masses fixed at certain angular positions so that the vibration amplitude is reduced to a satisfactory level. The correction masses and corresponding angular positions are determined by the IC method. Balancing planes are planes in which the correction weights are installed (WOWK, 1998).

Equation (3.1) presents the relationship between the original rotor unbalance distribution $\mathbf{U}^p$, the associated vibration amplitudes $\mathbf{V}^j$, and the so-called influence coefficients $\boldsymbol{\alpha}^{jp}$. The influence coefficients are complex values (i.e., amplitude and phase angle information) that relate the resulting vibration amplitudes measured at the position *j* due the unbalance force generated by the mass fixed at the position *p*.

$$\mathbf{V}^{j}_{vx1} = \boldsymbol{\alpha}^{jp}_{vxn}\mathbf{U}^{p}_{nx1} \tag{3.1}$$

where *v* is the number of measurement points (*j* = 1, …, *v*) and *n* is the number of balancing planes (*p* = 1, …, *n*). In this case, the residual unbalance presented in the rotor is neglected.

For a given rotation speed Ω, Eq. (3.1) can be rewritten as follows:

$$\mathbf{V}_0 = \begin{Bmatrix} V_0^1 \\ V_0^2 \\ \vdots \\ V_0^v \end{Bmatrix} = \begin{bmatrix} \alpha^{11} & \alpha^{12} & \cdots & \alpha^{1n} \\ \alpha^{21} & \alpha^{22} & \cdots & \alpha^{2n} \\ \vdots & \vdots & \ddots & \vdots \\ \alpha^{v1} & \alpha^{v2} & \cdots & \alpha^{vn} \end{bmatrix} \begin{Bmatrix} U_0^1 \\ U_0^2 \\ \vdots \\ U_0^n \end{Bmatrix} = \boldsymbol{\alpha}\mathbf{U}_0 \tag{3.2}$$

in which $\mathbf{V}_0$ is the vector of vibration responses associated with the original unbalance distribution $\mathbf{U}_0$ of the rotor.

The influence coefficients matrix $\boldsymbol{\alpha}$ is determined by using a trial weight m_t attached first in the balancing plane *p* = 1. The angular position of m_t is taken as a reference value for the correction weights. This trial weight introduces an additional unbalance force in the rotor given by $W^1 = m_t h$, where *h* is the eccentricity of the trial weight. For the same rotation speed Ω, the new unbalance condition of the rotor is shown in Eq. (3.3).

$$\mathbf{V}_1 = \begin{Bmatrix} V_1^1 \\ V_1^2 \\ \vdots \\ V_1^v \end{Bmatrix} = \begin{bmatrix} \alpha^{11} & \alpha^{12} & \cdots & \alpha^{1n} \\ \alpha^{21} & \alpha^{22} & \cdots & \alpha^{2n} \\ \vdots & \vdots & \ddots & \vdots \\ \alpha^{v1} & \alpha^{v2} & \cdots & \alpha^{vn} \end{bmatrix} \begin{Bmatrix} U_0^1 + W^1 \\ U_0^2 \\ \vdots \\ U_0^n \end{Bmatrix} = \boldsymbol{\alpha}\mathbf{U}_1 \tag{3.3}$$

where $\mathbf{V}_1$ is the vector of vibration responses associated with the new unbalance distribution $\mathbf{U}_1$.

Disregarding the trial weights from the total mass of the rotating machine, the matrix $\boldsymbol{\alpha}$ can be considered constant in Eq. (3.2) and Eq. (3.3). Therefore, Eq. (3.4) is obtained by subtracting Eq. (3.3) from Eq. (3.2), as follows:

$$\mathbf{V}_1 - \mathbf{V}_0 = \begin{Bmatrix} V_1^1 - V_0^1 \\ V_1^2 - V_0^1 \\ \vdots \\ V_1^v - V_0^v \end{Bmatrix} = \boldsymbol{\alpha} \begin{Bmatrix} W^1 \\ 0 \\ \vdots \\ 0 \end{Bmatrix} \tag{3.4}$$

The trial weight is then removed from the balancing plane p = 1 and the process is repeated for the remaining balancing planes. Therefore, **α** can be fully determined. The generalization of the IC method is given by Eq. (3.5), in which α, V, and W are complex quantities.

$$\alpha^{jp} = \frac{V_1^j - V_0^j}{W^p} \tag{3.5}$$

The correction masses m_c are obtained by inverting **α** and multiplying the resulting equation by the initial vibration response $\mathbf{V}_0$ (see Eq. (3.2)). If the number of balancing planes is equal to the number of vibration sensors (i.e., $n = v$ in Eq. (3.1)), **α** is inverted directly. Otherwise, the pseudo-inverse technique should be used. Different rotation speeds Ω can be used simultaneously in the IC method, providing a broad band balancing efficiency. Additional information on the IC method can be found in (EHRICH, 1992; EISENMANN and EISENMANN JR, 1998; WOWK, 1998; MUSZYNSKA, 2005; BENTLY and HATCH, 2002).

In the proposed approach, the uncertainty analysis is performed as a preprocessing stage. Measurement data sets are used to define an unbalance condition that takes into account the effects of operational fluctuations on the rotor vibration responses. This means that the basic mathematical formulation of the IC method is not modified. The uncertain information is associated only with the rotor vibration responses.

3.2.2 Fuzzy Logic Concepts

Epistemic uncertainties (i.e., uncertainties that are not random in nature) are commonly identified in balancing applications. For instance, what are the interval of vibration amplitudes and their corresponding phase angles that defines a balanced or unbalanced rotor? This question is more related to the lack of knowledge about the operating conditions of the rotor system (e.g., rotation speed, oil film temperature in the journal bearings, thermal bow, etc.) than to the randomness of the associated phenomenon (e.g., disturbance and noise affecting the vibration measures, etc.).

As previously mentioned, possibility is considered as the measure of whether an event can happen. Differently, probability is defined as a measure of whether an event will happen.

Thus, the possibility distribution of a given parameter *u* (i.e., parameter *u fuzzy set*) quantifies possible values that this parameter can assume, while a probability distribution quantifies the odds that the parameter *u* has to assume a certain value *x*. In the proposed methodology, the rotor unbalance condition is treated as an uncertain information. Fuzzy sets are derived from measured vibration responses (i.e., vibration amplitudes and corresponding phase angles) representing the unbalance conditions that the rotating machine can assume, instead of concerning which is the current response of the system.

Considered uncertainties are computationally modeled as fuzzy numbers through the fuzzy set theory, where the actual value of the parameter is unknown but limited by an interval weighted by a membership function. Following the interpretation of *degree of uncertainty*, the membership function of a fuzzy set is the continuous interval [0, 1] that weights the degree of pertinence of the element *x* with respect to the fuzzy set $\tilde{A}$. Thus, the values of $\tilde{A}(x)$ close to 1 indicate a high compatibility of the element *x* with the set $\tilde{A}$.

In this contribution, the fuzzy set is regarded as a possibility distribution and is used to model the rotor unbalance condition. Treating the unbalance condition as a fuzzy set, i.e., $unb=\{(u,\mu_{unb}(u^*))|u^* \in U\}$, where *u* is a measured data and μ is the membership function of the unbalance fuzzy set, the resulting fuzzy numbers are weighted intervals that indicate the condition of the rotor. In this way, $\mu_{unb} = 0$ indicates a balanced condition, $\mu_{unb} = 1$ indicates an unbalanced condition, and $0 < \mu_{unb} < 1$ indicates a condition that could either be balanced or unbalanced.

The key aspect of the fuzzy approach for uncertainty analysis is the definition of the so-called membership function. A membership function can assume different shapes, which can affect the results of the uncertainty analysis. Usually, in a fuzzy decision system, the user imposes the shape of the membership function. The triangular or pseudo-triangular are the most used shapes. However, in this paper, the knowledge contained in the rotor vibration responses measured over a long period is incorporated into a fuzzy set. In this case, the method presented by POTA, ESPOSITO and DE PIETRO (2013) was adapted to extract fuzzy interpretation from the statistical data for inference purposes.

The transformation scheme is based on the application of the statistical test of hypothesis (i.e., Fisherian test). The method enables the construction of normal fuzzy sets, which can be adapted to have pseudo-triangular, pseudo-trapezoidal, or pseudo-CDF shapes (i.e., cumulative distribution function). From the measured vibration responses (large set of statistical samples), the membership function is obtained by using Eq. (3.6).

$$\mu_{\tilde{A}}(x) = \frac{N_{pos}}{N_{pos} + N_{neg}} \tag{3.6}$$

where N_{pos} represents the number of no rejections of the hypothesis test (i.e., acceptance of the null hypothesis) and N_{neg} is the number of rejections. Equation (3.6) is applied to all the measured vibration responses.

Consider the construction of the membership function $\mu_{unb}(U)$, where U represents a set of vibration responses measured along the rotor. A hypothesis test is applied to determine the fraction of U that belongs to the set *unb*. The no rejection of the null hypothesis reveals the fraction of U that belongs to the unbalance set, while the rejection of the null hypothesis reveals the fraction of U that does not belong to the set *unb*. The membership function is determined first by obtaining the probability density function of U (i.e., PDF(U)). Then, for a given vibration response u^* of the set U, the null hypothesis $H_0 \equiv$ "u^* belongs to *unb*" can be interpreted as the hypothesis $H_0 \equiv$ "u^* is an occurrence of a random variable for which the probability density function is PDF(U)". The acceptance or rejection of the null hypothesis is made by comparing the *p-value* of the statistic test with the decision rule α (i.e., the significance level of the hypothesis test).

Assuming, for instance, a set of vibration responses U uniformly distributed on the interval [15, 30] μm with PDF(U) unknown, what can be inferred if u^*= 26 μm? Considering a statistic test *p-value* = 0.2 and the decision rule of α = 0.1, u^*= 26 μm corresponds to not rejecting the null hypothesis (*p-value* >α). Adopting the same set of vibration responses U, the test can be performed for all measured vibration responses (e.g. 100 samples) by varying the decision rule value in the interval [α_{min}, α_{max}]. Suppose, for instance that 15 tests return requiring that H_0 has to be rejected, since they have been processed considering the decision rule α> 0.2. Consequently, 85 tests did not reject the null hypothesis and $\mu_{unb}(u^*)$ = 0.85 (i.e., 85/(85+15) = 0.85; see Eq. (3.6)). This value of membership function indicates a high compability of the measured value 26 μm with the set of unbalance response *unb*.

The values adopted for the interval of α may change the shape of the membership function of the corresponding fuzzy set. Consequently, pseudo-triangular, pseudo-trapezoidal, or pseudo-CDF shapes can be obtained based on the decision rule interval [α_{min}, α_{max}]. More details about the fuzzy transformation procedure is found in POTA, ESPOSITO and DE PIETRO (2013). A pseudo-code for the fuzzy transformation approach is shown in Figure 3.1.

The fuzzy transformation procedure is able to construct a fuzzy set based on the vibration responses of the rotor system. Considering that the balancing procedure is a decision-making approach, the fuzzy information must be aggregated into a single value (i.e., a *crisp* value) that represents the uncertain information. The aggregation process of a fuzzy set is known as defuzzification in which all the information contained in a fuzzy set is aggregated into a real value (for further information regarding defuzzification, see (MÖLLER

and BEER, 2004 and TAKAGI and SUGENO, 1985). Thus, a fuzzy logic defuzzification tool is required by the proposed methodology.

Data: $PDF_u(U)$, U_{min}, U_{max} **Result:** $\mu_{unb}(U)$
choose α_{min}, α_{max}, $PDF_\alpha(\alpha)$ and $t \in$ {right tail, left tail, two tails}
for $u \leftarrow U_{min}$ to U_{max} **do**
    CF ← 0; $\xi \leftarrow U_{min}$
    while ($\xi < u$) **do**
        CF ← CF + $PDF_u(\xi)$. $d\xi$; $\xi \leftarrow \xi + d\xi$
    End
    if (t = right tail) **then**
        p-value ← (1 – CF)
    else if (t = left tail) **then**
        p-value ← CF
    Else
        If (CF < 0.5) **then**
            p-value ← 2 . CF
        Else
            p-value ← 2 . (1 – CF)
        End
    End
    mu ← 0; $\alpha \leftarrow \alpha_{min}$
    while ($\alpha < p$-value) **do**
        mu ← mu + $PDF_\alpha(\alpha)$. $d\alpha$; $\alpha \leftarrow \alpha + d\alpha$
    End
    $\mu_{unb}(u)$ ← mu
end

Figure 3.1 - Pseudo-code of the fuzzy transformation procedure (adapted from POTA, ESPOSITO and DE PIETRO, 2013).

Different defuzzification techniques are available in the literature, such as the *Centroid*, *Bisector*, smallest of maximum (*SOM*), mean of maximum (*MOM*), and the largest of maximum (*LOM*) (TAKAGI and SUGENO, 1985). The *Centroid* method determines the value that represents the uncertain information as being the area center (i.e., gravity center) of the

membership function. Similarly, the *Bisector* method calculates the bisector of the fuzzy set to obtain the value that represents the uncertain information. The selected value by *SOM* is the smallest component of the fuzzy set associated with $\mu_{unb}(u^*) = 1.0$. The largest component that results in $\mu_{unb}(u^*) = 1.0$ is chosen as being the value in the *LOM*.

The *MOM* approach determines the value that represents the uncertain information corresponding to the mean of the components that are associated with $\mu_{unb}(u^*) = 1.0$. Figure 3.2 illustrates the mentioned defuzzification techniques considering hypothetical rotor vibration responses represented by a pseudo-trapezoidal membership function. Note that the *Bisector*, *MOM*, and *Centroid* methods return intermediate defuzzified values arranged from the left to the right, respectively. The *SOM* and *LOM* approaches determined the left and right limit values, respectively (see $\mu_{unb}(u^*) = 1.0$ in Figure 3.2).

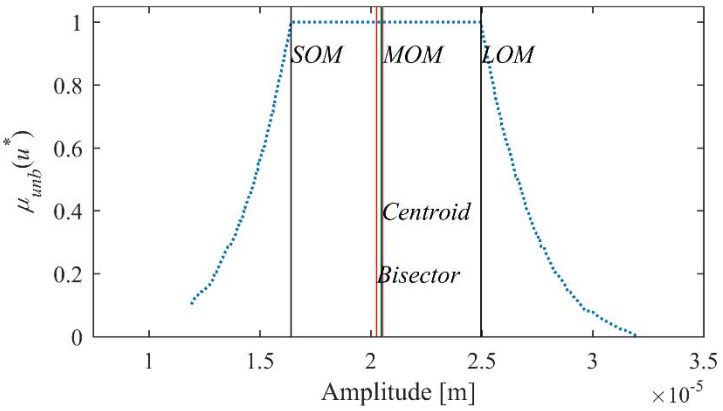

Figure 3.2 - Defuzzification techniques represented by a pseudo-trapezoidal membership function.

In the context of fuzzy logic, fuzzy transformation, and defuzzification approach, the proposed balancing methodology can be summarized as follows: *i*) the fuzzy transformation is used to determine fuzzy sets associated with the measured vibration amplitudes and corresponding phase angles; *ii*) a defuzzification technique is applied in each fuzzy set resulting in equivalent vibration amplitudes and phase angles; *iii*) these values are introduced in the IC method to determine correction weights and corresponding angular positions that minimizes the sensitivity of the rotor vibration responses to the uncertain parameters associated to the measured vibration data. Figure 3.3 presents a summarized flowchart of the proposed methodology.

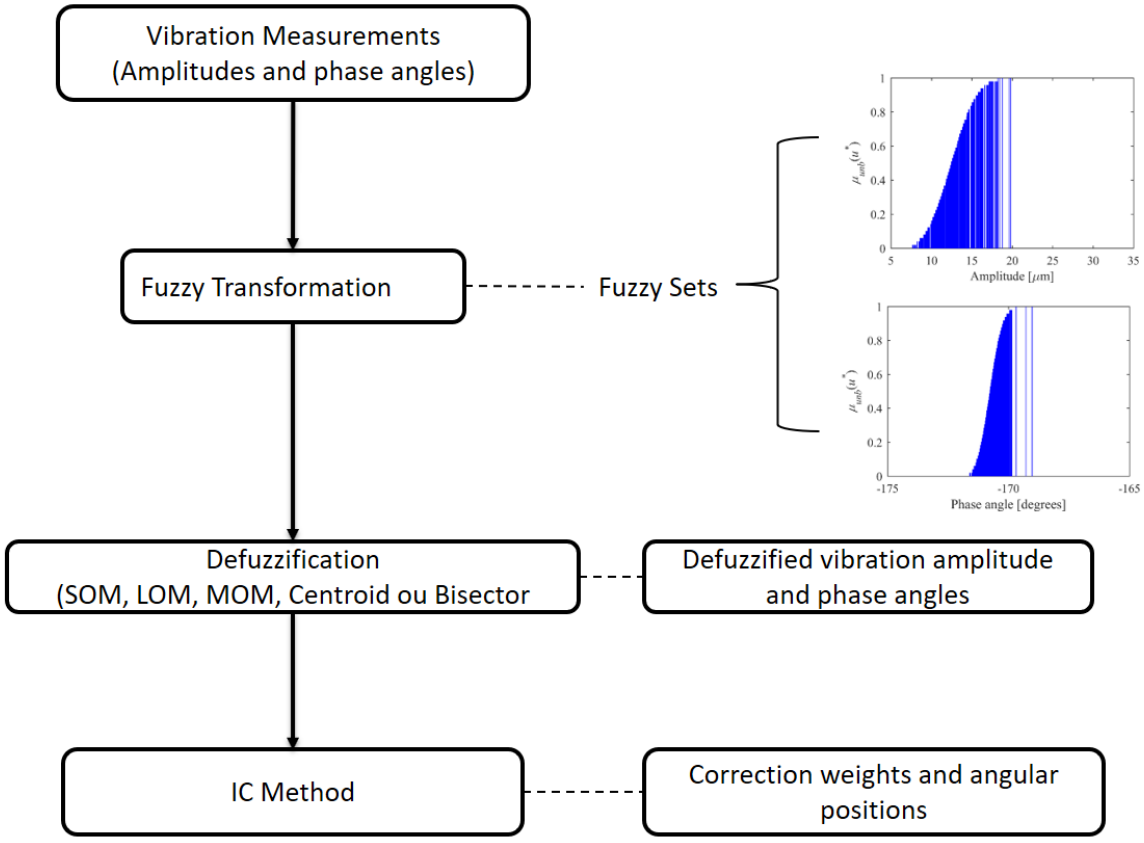

Figure 3.3 - Flowchart of the proposed revised IC method.

3.2.3 Numerical Application

Figure 3.4a shows the rotor test rig used for the validation of the proposed robust non-parametric balancing procedure, which is represented by a model with 24 finite elements formulated according to the Timoshenko beam theory (FE model; Figure 3.4b). The rotor is composed by a flexible steel shaft with 836 mm length and 19 mm diameter (E = 192 GPa, ρ = 7930 kg/m^3, u = 0.29), two aluminum rigid discs D_1 (node #8; 0.676 kg; I_{DX} = I_{DZ} = 1.028 x 10^{-3} kgm^2; I_{DY} = 2.028 x 10^{-3} kgm^2) and D_2 (node#18; 0.676 kg; I_{DX} = I_{DZ} = 1.028 x 10^{-3} kgm^2; I_{DY} = 2.028 x 10^{-3} kgm^2), and two bearings B_1 and B_2 located at the nodes #3 and #24, respectively. B_1 is a self-alignment ball bearing represented by the following stiffness k and damping d coefficients: k_{xx} = 1x10^8 N/m, k_{zz} = 1x10^9 N/m, d_{xx} = 100 Ns/m, and d_{zz} = 200 Ns/m. B_2 is a cylindrical oil film bearing with 12.8 mm length, 19 mm diameter, and 75 μm radial clearance. The stiffness and damping coefficients of the bearing B_1 were estimated by considering a previous model updating procedure similar to the one presented in section 2.4 of the previous chapter (see CAVALINI JR *et al.*, 2016). The oil viscosity was calculated as a

function of the temperature - according to the same procedure discussed in section 2.5 of chapter two (see Eq. 2.16). The rotating parts of the FE model presented in Figure 3.4b take into account a proportional damping added to the matrix **D** ($\mathbf{D}_p = \gamma\mathbf{M} + \beta\mathbf{K}$) with coefficients γ = 2.327 Ns/kg.m and $\beta = 3.97 \times 10^{-6}$ s.

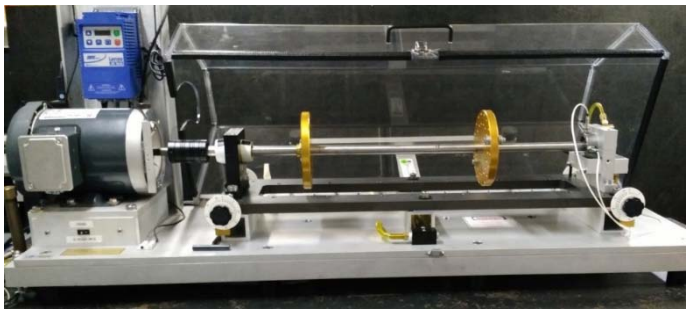

(a)

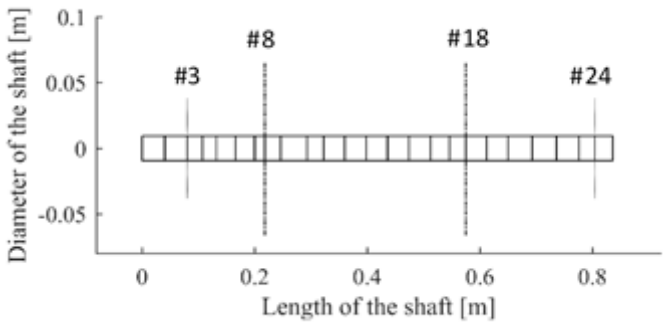

(b)

Figure 3.4 – Rotor used in the numerical simulation: a) Test rig; b) FE model.

The set of vibration responses used in the proposed balancing approach was generated through Monte Carlo (MC) simulations, considering the oil film temperature (T_{oil}), the rotation speed (Ω), and the unbalance condition of the rotor system as uncertain variables. The oil film temperature was allowed to vary in the range 20.71°C to 25.3°C, while the rotation speed was limited in the interval 1080 rev/min to 1320 rev/min (mean values of 23 °C and 1200 rev/min). In this case, a mean unbalance value of $1.5x10^{-4}$ kgm / 180° was introduced in each disc of the rotor. Thus, the unbalance condition was allowed to vary in the range $1.35x10^{-4}$ kgm to $1.65x10^{-4}$ kgm. The variation of the associated angular positions was limited in the interval 162º to 198°. It is worth mentioning that the random variables were modeled as Gaussian random fields, in which the convergence of the MC simulations was achieved considering 400 samples. Obviously, different parameters could have been considered as uncertain information. In this numerical evaluation, the proposed balancing procedure was applied

considering the discs as corresponding to the balancing and measuring planes (horizontal vibration responses; see Figure 3.4b).

Figure 3.5 presents the membership functions obtained by using the fuzzy transformation procedure. Pseudo-CDF (or half bell) fuzzy sets were generated to represent the vibration amplitudes and their corresponding phase angles associated with the 400 configurations generated by the MC simulation (i.e., the vertical lines are associated with the samples). In this case, α_{max} = 0.99 (maximum decision rule value), α_{min} = 0 (minimum decision rule value), and the left tail hypothesis test were used (see Figure 3.1). Thus, 99% of the rotor vibration responses in the resulting fuzzy sets are treated as uncertain information, while 1% are interpreted as either a balanced or unbalanced rotor condition ($\mu_{unb}(u^*) = 0$ or $\mu_{unb}(u^*) = 1$, respectively). It is worth mentioning that different limits for the decision rule and hypothesis tests can be used to improve the performance of the proposed method.

For this particular analysis, both the *Centroid* and *Bisector* defuzzification methods lead to similar results (see Figure 3.2). Consequently, only the *Bisector* method was evaluated. Additionally, the *SOM*, *LOM*, and *MOM* approaches present similar values due to the reduced number of elements associated with $\mu_{unb}(u^*) = 1.0$ (see Figure 3.5). Thus, only the *SOM* (modeling the first unbalanced rotor vibration response) and *LOM* (representing the worst measured vibration response) techniques were applied in the fuzzy sets of Figure 3.5. The resulting fuzzy information was used as the initial unbalance condition for the IC method.

Table 3.1 presents the fuzzy unbalance condition, the obtained correction weights, and the corresponding angular positions. The results obtained by the deterministic IC method are also presented for comparison purposes. In this case, T_{oil} = 23°C, Ω = 1200 rev/min, and an unbalance of $1.5x10^{-4}$ kgm / 180° was applied to each disc of the rotor (i.e., nominal operating condition). The applied trial weight was $2.37x10^{-4}$ kgm / 180° (m_c = 3.9 g). Note that the correction weights obtained by the proposed methodology are smaller than the values determined by using the deterministic IC method, except for the *Bisector* technique considering the disc D_2.

The correction weights presented in Table 3.1 were applied in the FE model considering the 400 samples generated by MC simulations. Figures 3.6a, 3.6b, and 3.6c show the vibration amplitudes of the rotating machine balanced through the proposed robust IC method, which were obtained by applying the *Bisector*, *SOM*, and *LOM* defuzzification approaches, respectively (vibration responses measured along the horizontal direction of disc D_1). Fig. 3.6d shows the vibration amplitudes of the balanced rotor by using the deterministic IC method. The vibration responses of the unbalanced rotor are also presented for comparison purposes. As expected, the deterministic and robust balancing methodologies were able to attenuate the

rotor vibration amplitudes. Similar results were obtained by considering the vibration responses obtained along the horizontal direction of the disc D_2.

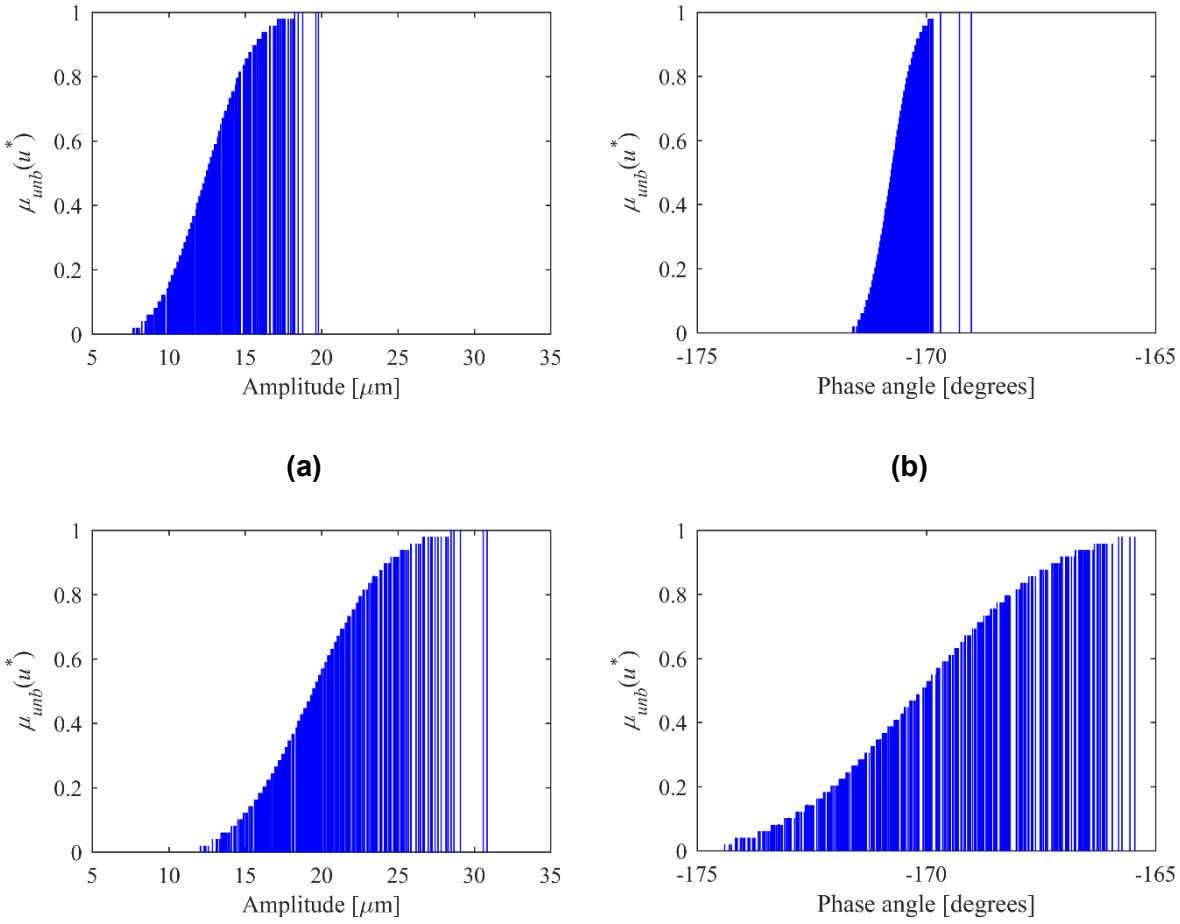

Figure 3.5 - Membership functions obtained by the considered transformation approach: a) vibration amplitude of D_1; b) phase angle of D_1; c) vibration amplitude of D_2; d) phase angle of D_2.

Table 3.1 Numerical application of the robust and deterministic balancing approaches.

	Unbalance [μm / degrees]		*Correction weight [g]*		*Angular position [degrees]*	
	Disc D_1	*Disc D_2*	*Disc D_1*	*Disc D_2*	*Disc D_1*	*Disc D_2*
Bisector	*13.85/-70.6*	*21.57/-68.4*	*2.38*	2.28	-1.278	16.783
SOM	18.24/-169	28.48/-65.4	2.25	2.23	-2.486	13.383
LOM	*19.81/-69.7*	*30.82/-65.8*	*2.21*	2.21	-2.872	12.876
Deterministic	14.34/-167	22.33/-66.5	2.45	2.25	-3.216	17.161

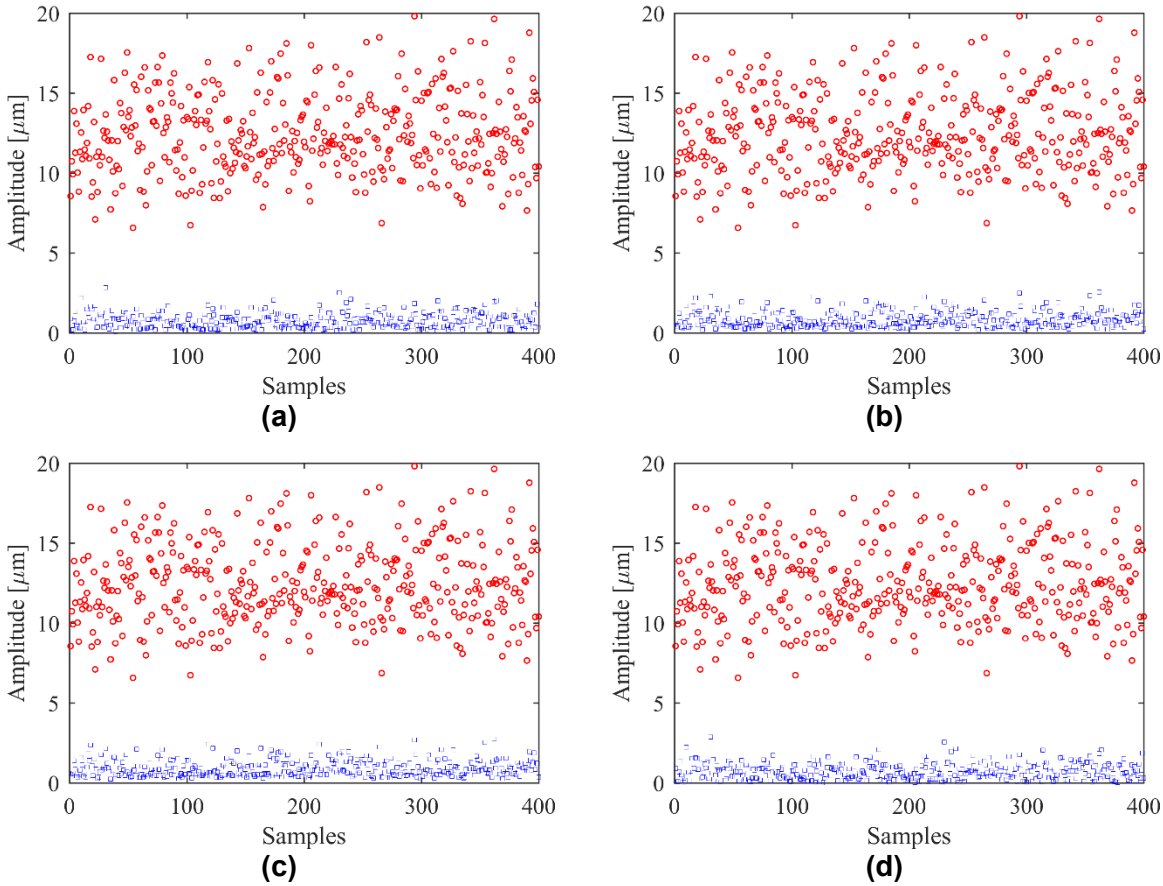

Figure 3.6 – Vibration responses obtained at the disc D1 considering the robust and deterministic IC methods (○ unbalanced; □ balanced): a)Bisector; b)SOM; c)LOM; d) Deterministic.

Table 3.2 presents the minimum and maximum vibration amplitudes obtained at the discs D_1 and D_2 considering the 400 simulations performed in the balanced rotating machine. In this case, the results obtained considering the *Bisector*, *SOM*, *LOM* (robust IC methods), and deterministic IC method are compared (results associated with Figure 3.6). Note that the deterministic IC method presented maximum vibration amplitudes of 2.87 μm and 4.65 μm (related to the discs D_1 and D_2, respectively) and variations of 2.87μm and 4.54 μm. The *SOM* based technique results in maximum vibration amplitudes of 2.55 μm and 4.28 μm, respectively, and variations of 2.35 μm and 4.21 μm, respectively. Additionally, smaller vibration amplitudes were reached by the *LOM* and *Bisector* approaches (compare the mentioned approaches with the deterministic maximum amplitudes in Table 3.2). Thus, the robust IC method demonstrated to be less sensitive to the uncertain configurations of the rotor.

It is worth mentioning that the result obtained by the SOM technique seems to be better adapted to the robust balancing approach. Additionally, the deterministic IC method leads to

the minimum vibration amplitudes when the nominal configuration of the rotor was considered (i.e., T_{oil} = 23ºC, Ω = 1200 rev/min, and an unbalance of 2.5x10^{-4} kgm / 0°applied to each disc).

Table 3.2 Vibration amplitudes obtained at the discs D_1 and D_2 considering the balanced rotating machine.

	Disc D_1				*Disc D_2*			
	Bisector	*SOM*	*LOM*	*Det**	*Bisector*	*SOM*	*LOM*	*Det**
Maximum[*μm*]	2.82	2.55	2.75	2.87	4.58	4.28	4.18	4.65
Minimum[*μm*]	0.09	0.2	0.25	0	0.01	0.07	0.04	0.11
Variation [*μm*]	2.73	2.35	2.5	2.87	4.57	4.21	4.14	4.54

** Det = deterministic IC method.*

3.2.4 Experimental Validation

The proposed balancing technique was applied to the rotor test rig shown in Figure 3.4a. In this case, the disc D_2 was considered as the balancing plane and the vertical vibration responses of the system were measured close to the bearing B_2 (i.e., oil film bearing; see Figure 3.7). Therefore, according to the machine configuration, the IC method was applied experimentally considering a single balancing plane and a single measuring plane.

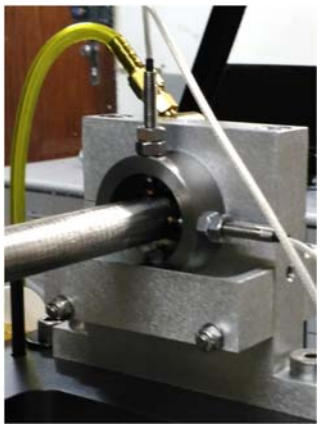

Figure 3.7 - Proximity sensors located close to the oil film bearing.

The set of vibration responses was generated by considering the oil film temperature (T_{oil}) and rotation speed (Ω) as uncertain variables. During 24 hours of experimental tests, T_{oil} was allowed to vary from 22 °C to 29 °C and Ω was limited in the interval 500 rev/min to 700 rev/min (changes in steps of 50 rev/min). The range of rotating speeds used in the experimental application was reduced as compared with the speeds used in the numerical

analyses. High vibration amplitudes were obtained with the system operating between 1080-1320 rev/min. Consequently, 560 experimental samples were acquired.

Figure 0.8 presents the membership functions obtained by using the fuzzy transformation procedure. Pseudo-CDF fuzzy sets were generated to represent the vibration amplitudes and their corresponding phase angles associated with the 560 rotor configurations. Similar to the numerical analysis, α_{max} = 0.99 (maximum decision rule value), α_{min} =0 (minimum decision rule value), and the *left tail* hypothesis test were used. Thus, 99% of the rotor vibration responses in the resulting fuzzy sets are treated as uncertain information, while 1% are interpreted as either a balanced or unbalanced rotor condition ($\mu_{unb}(u^*) = 0$ or $\mu_{unb}(u^*) = 1$, respectively). In this case, due to the similar results presented in Table 3.2, only the *SOM* approach was used to aggregate the fuzzy information into a single unbalance response. The shapes of the fuzzy sets were selected based on the numerical results.

Table 3.3 presents the fuzzy unbalance condition, the obtained correction weights, and the corresponding angular positions. The results obtained by the deterministic IC method are presented for comparison purposes.

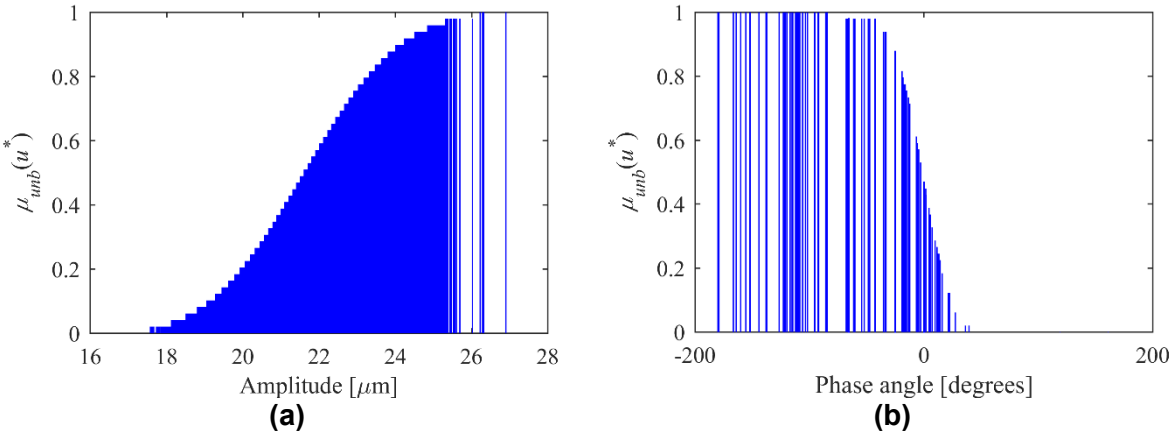

Figure 0.8 - Experimental membership functions obtained by the considered transformation approach: a) vibration amplitude; b) phase angle.

The applied trial weight was m_c = 4.3 g. Note that once more the correction weight obtained by the deterministic approach is bigger than the value determined through the proposed method. The correction weights presented in Table 3.3 were applied to the rotor test rig. Then, 560 *new samples* (i.e., 560 new vibration measurements) for each methodology (i.e. deterministic IC method and robust IC method) were acquired during 24 hours of experimental tests considering the same uncertain intervals (i.e., 22 °C ≤ T_{oil} ≤ 29 °C and 500 rev/min ≤ Ω ≤ 700 rev/min).

Table 3.3 Experimental application of the robust and deterministic balancing approaches.

	Unbalance [*μm / degrees*]	*Correction weight* [*g*]	*Angular position* [*degrees*]
SOM	26.16/-83.2	21.78	-140.0
Deterministic	27.61/-79.9	29.07	-160.0

Figure 3.9 shows both the vibration amplitudes of the balanced rotor by using the proposed robust IC method and the deterministic approach (vibration responses measured along the horizontal and vertical directions). The vibration responses of the unbalanced rotor are also presented for comparison purposes. As expected, the deterministic and robust balancing methodologies were able to attenuate the vibration amplitudes of the rotor. It is worth mentioning that the vibration amplitudes of the unbalanced and balanced conditions associated with a given sample may not correspond to the same rotor configuration (i.e., T_{oil} and Ω).

Table 3.4 presents the minimum and maximum experimental vibration amplitudes obtained for the balanced rotating machine. In this case, the robust and deterministic IC methods are compared (results associated with Figure 3.9). Note that the deterministic IC method presented variations of 2.9 *μ*m and 3.2 *μ*m (with respect to the horizontal and vertical directions, respectively), while the robust approach results in a variation of 2.2 *μ*m in both directions. However, higher maximum vibration amplitudes were obtained by the proposed approach (see Table 3.4). Nonetheless, the goal of the proposed approach is not to reduce the maximum overall vibration amplitude of the rotating system but rather to reduce the system sensitivity to the uncertain scenarios. As observed in the numerical analysis, the experimental results demonstrate that the proposed approach is less sensitive to operational fluctuations than the deterministic IC method (see the variation results in Table 3.4).

Aiming at assessing the proposed methodology effectiveness, an experimental test was performed, as follows. The rotor system was driven out of its considered uncertain information boundaries. Figure 3.10 shows both the robust and deterministic balancing results obtained by extrapolating the rotor operational speed range while considering constant oil temperature (23 ± 0.5 °C). In this particular test, the oil temperature was treated as a deterministic value for the sake of simplicity. The maximum vibration amplitudes measured for each rotating speed are being presented. The robust IC method correction weight was obtained considering the system rotation speed Ω limited in the interval 500 - 700 rev/min. In this test case, Ω was allowed to reach 1000 rev/min (i.e., 300 rev/min higher than the value used in the robust approach). Note that near 900 rev/min the maximum vibration amplitude obtained by using the robust balancing approach is smaller than the vibration amplitude measured considering the deterministic IC method. Therefore, these results suggest that the

robust IC method is able to provide smaller vibration amplitudes for the cases in which the rotor system is exposed to operating conditions in the neighborhoods of the range considered in the uncertainty analysis. Additionally, it can be observed that the robust balancing leads to a smaller variation of the vibration amplitude according to the evaluated speed range. The vibration amplitude along the horizontal direction changed from, approximately, 14 μm to 40 μm. In the vertical direction, the vibration amplitude changes from 10 μm to 32 μm. Regarding the deterministic balancing, the vibration amplitudes changed from, approximately, 8 μm to 42 μm and 6 μm to 35 μm along the horizontal and vertical directions, respectively.

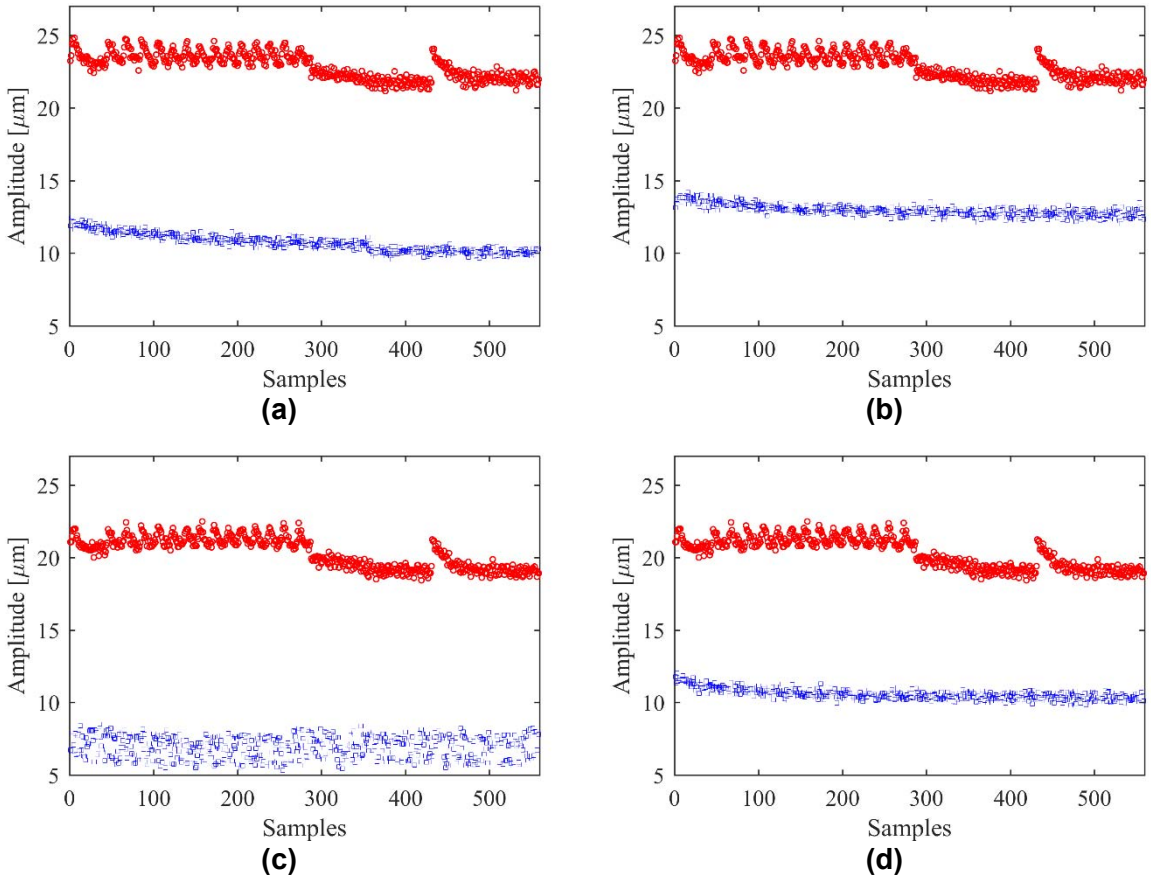

Figure 3.9 – Experimental vibration responses obtained by using the robust and deterministic IC methods (○ unbalanced; □ balanced): a) horizontal/deterministic; b) horizontal/robust; c) vertical/deterministic; d) vertical/robust.

Table 3.4 Vibration amplitudes of the balanced rotor obtained during the experimental tests.

	Horizontal direction		*Vertical direction*	
	Robust	*Deterministic*	*Robust*	*Deterministic*
Maximum[μm]	14.2	12.5	12	8.5
Minimum[μm]	12	9.6	9.8	5.3
Variation [μm]	2.2	2.9	2.2	3.2

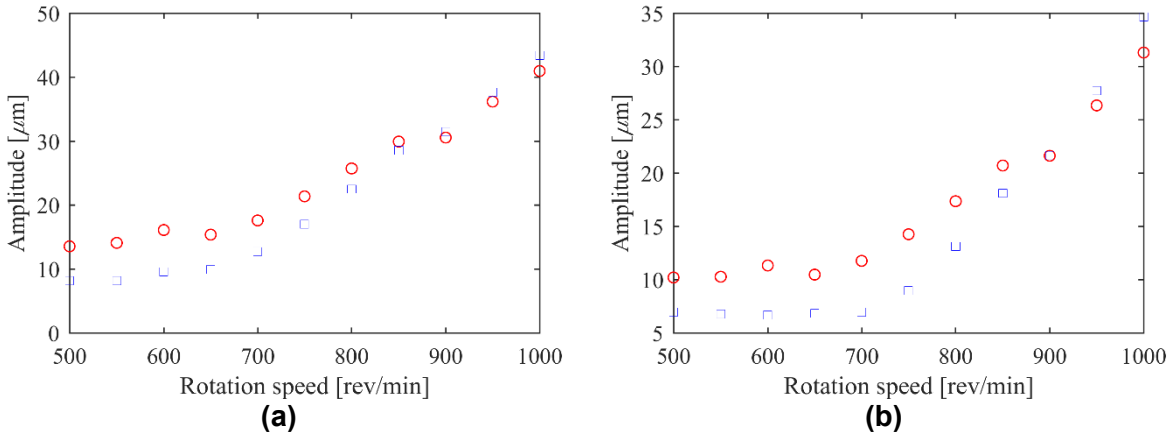

Figure 3.10 – Extrapolation of the rotation speeds considering the robust and deterministic IC method (□ deterministic; ○ robust): a) horizontal direction; b) vertical direction.

In this section, a robust non-parametric balancing approach was presented based on the well-known IC method. A preprocessing stage is added to the process. Vibration responses measured over a given period are assessed by means of fuzzy uncertainty analysis, wherein a fuzzy transformation is used to derive unbalance fuzzy sets of the measured data. Consequently, a representative unbalance condition of the rotating machine is determined through a defuzzification process. The unbalance condition that is determined through the uncertainty analysis of the measured data is then used in the algorithm of the IC method in order to obtain robust balancing responses.

The performance of the proposed methodology was evaluated both numerically and experimentally, so that uncertainties affecting oil temperature and the rotation speed of the rotor were taken into account. The robust IC method was able to find robust solutions for all test cases analyzed. In the numerical analysis, the influence of the defuzzification techniques on the balancing performance was evaluated. The numerical results indicated that the pseudo-CDF shape associated with the *SOM* defuzzification technique was more suitable to obtain a satisfactory performance of the robust IC method.

Regarding the experimental tests, the proposed methodology leads to better balancing results as compared with the deterministic approach, in terms of robustness. The proposed approach was able to reduce system sensitivity to uncertainties; however, higher maximum vibration amplitudes was observed. The robust IC method provided better results for the cases in which the system was exposed to conditions that were out of the uncertainty analysis range. It is worth mentioning that the robust IC method resulted in a correction weight 25% lighter than the value obtained by the deterministic approach.

As mentioned, the goal of the proposed methodology is to reduce the sensitivity of the system to operational fluctuations, rather than reducing the maximum observed vibration amplitude. In this sense, the presented results indicate that the proposed robust IC method leads to less sensitive balancing responses as compared with the standard IC method. Is important to point out that this robustness increasement was achieved through the simple addition of a preprocessing stage in which fuzzy logic tools are used to define a more representative rotor unbalance condition.

The results obtained indicate that the proposed methodology is sufficiently robust to handle changes on the rotor operational conditions, as long as these fluctuations are manifested in the measurement data set used to formulate the rotor fuzzy sets.

3.3 Parametric Evaluation

In this section a robust model-based balancing approach is evaluated. This alternative technique first identifies the model of the machine, and then the unbalance is determined by solving a typical inverse problem through an optimization method taking into account the inherent uncertainties that affect the balancing performance. The robust balancing methodology is based on a multi-objective fuzzy optimization procedure, in which the uncertainties are treated as fuzzy variables. The balancing response robustness is evaluated by means of an additional objective function that minimizes a predefined robustness metric. The numerical investigation is applied to a rotor composed by a horizontal flexible shaft, two rigid discs, and two ball bearings, the same rotor of Section 2.4 of Chapter 2.

3.3.1 Model-based Balancing Method

Figure 3.11 shows a flowchart to illustrate the balancing methodology as proposed by SALDARRIAGA *et al.* (2010). The model based balancing method begins by inserting a set of randomly generated masses and phase angles in each balancing plane of the representative FE model. In this case, the simulated time-domain responses are obtained for each generated unbalance forces. The vibration responses are determined at the same positions along the shaft in which the responses were acquired on the rotor in an unknown unbalance condition (original rotor). Such measures are compared by using the objective function *F* presented in Eq. (3.7). If the best result of this function corresponds to a minimum value, the unbalance affecting the rotor is identified. This means that obtained weights with its respective angular positions are capable of reproducing the unbalance response of the original rotor. If the function does not find a value close to zero, the optimization method will propose new

unbalance values and the process will continue iteratively until the target is found. In order to obtain the balancing conditions of the rotor, it is necessary to add 180^0 to the previously found phase angles, keeping however the same masses obtained, which are now the correction weights.

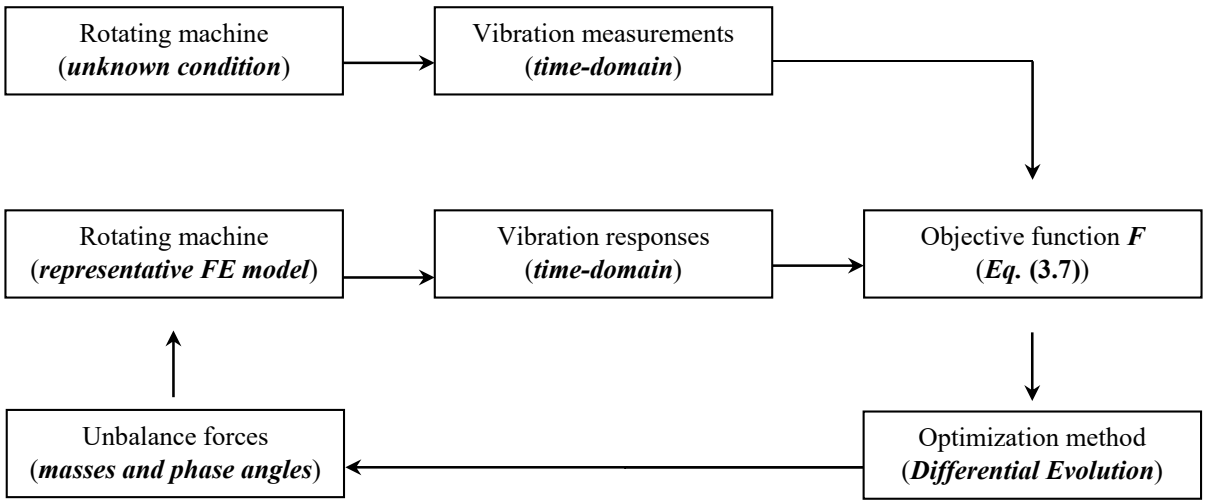

Figure 3.11 - Model-based balancing methodology flowchart.

$$F = \sum_{i=1}^{n} \frac{\left\| U_i^{FEmodel}(x) - U_i^{Original} \right\|}{\left\| U_i^{Original} \right\|} \tag{3.7}$$

where n is the number of sensors used in the procedure, $U_i^{FEmodel}(x)$ is the vibration response obtained by using the FE model, x is the vector containing the proposed correction weights and associated phase angles by the optimization method, and $U_i^{Original}$ is the vibration response measured on the original rotor.

The uncertainties considered on the applications presented in this section are introduced directly on the FE model parameters, thus defining a parametric uncertainty analysis. The proposed robust balancing methodology is characterized by uncertainties affecting, for example, the stiffness and damping of the bearings (i.e., due to fixation problem), the dimensions of the discs and shaft (i.e., due to wear), and so on. Therefore, it is expected that a superior balancing performance be obtained when the correction weights and associated phase angles determined by using the robust methodology are used. Possible variations on the geometric and physic properties of the rotating machine can be considered during the balancing process, which explain the expected superior performance.

3.3.2 Robust Model-based Balancing Method

The goal of the proposed methodology is to increase the robustness of the model based balancing technique. In this sense, fuzzy optimization is used to assess balancing robustness. Fuzzy optimization is a tool based on fuzzy uncertainty analysis. As previously discussed (see Section 2.3) based on the possibility theory (ZADEH, 1968), a fuzzy set can be understood as the union of the pessimist and optimist values (i.e. lower and upper values, respectively) of an uncertain parameter with each level of possibility (i.e., levels of the membership function) been possible realizations of the uncertain parameter. In the fuzzy set theory, the uncertainties are described as fuzzy inputs and the mathematical model is represented as a fuzzy function that maps those inputs. The so-called α-level optimization (MÖLLER, GRAF and BEER, 2000, also see Section 2.3) is a method used for mapping fuzzy inputs, in which, the fuzzy inputs are discretized by means of α-cuts creating a *crisp* subspace that is the search space of an optimization problem. The optimization process is carried out in order to find the minimum and maximum values of the model output for each α-level (i.e., lower and upper limits of the correspondent α-level, respectively; see Figure 2.2 and Figure 2.3).

At the end of the fuzzy uncertainty analysis of a system, the set of values of the uncertain information that maximizes the model response (the optimist values) and the set of values that minimizes the model response (the pessimist values) are known. Therefore, two uncertain scenarios can be considered: (i) a scenario in which the uncertain values assume its pessimist values; and (ii) a scenario where the uncertain values are at its optimist values. Thus, is expected that a robust solution will represent a better solution when both scenarios are considered. Considering the proposed robust balancing methodology, the pessimist scenario and the optimist scenarios are defined, respectively, by Eq. (3.8) and Eq. (3.9).

$$Pe\left(x,\underline{p}\right)=\sum_{i=1}^{n}\left(\frac{\left\|U_i^{FEmodel}(x,\underline{p})-U_i^{FEmodel}(x^*,p_n)\right\|}{\left\|U_i^{FEmodel}(x^*,p_n)\right\|}\right) \tag{3.8}$$

$$Op(x,\overline{p})=\sum_{i=1}^{n}\left(\frac{\left\|U_i^{FEmodel}(x,\overline{p})-U_i^{FEmodel}(x^*,p_n)\right\|}{\left\|U_i^{FEmodel}(x^*,p_n)\right\|}\right) \tag{3.9}$$

where Pe and Op are the objective functions associated with the pessimist and optimist evaluations, respectively. The upper and lower limits of the uncertain information are represented by $\overline{p}$ and $\underline{p}$, respectively. $U_i^{FEmodel}(x,\underline{p})$ stands for the vibration response determined from the FE model considering the lower limit values of the uncertain parameters.

Consequently, $U_i^{FEmodel}(x,\overline{p})$ stands for the vibration response determined from the FE model considering the upper limit values of the uncertain parameters. In this case, the value $U_i^{FEmodel}(x^*,p_n)$ represents the vibration response of the FE model determined after the application of a previous deterministic balancing procedure response (following the scheme presented in Figure 3.11 and using Eq. (3.7) as the objective function). Thus, x^* is the vector containing the deterministic correction masses and phase angles and p_n is the nominal values of the considered uncertain parameters.

Therefore, a robustness metric can be defined based on Eq. (3.8) and Eq. (3.9) considering both sets of uncertain scenarios. The robustness metric is illustrated by Eq. (3.10). In this case, the minimization of the Eq. (3.10) leads to a robust balance solution for the considered original rotor system.

$$ro = Pe\left(x,\underline{p}\right) + Op(x,\overline{p}) \tag{3.10}$$

The robustness evaluation procedure as presented was formulated as a nested optimization problem, in the sense that the deterministic model-based response x^* is required for the evalution of the robustness metric, and only the robustness metric (given by Eq.3.10) is accounted in the optimization process. However, the procedure can be easily formulated as a multi-objective optimization problem in which both objectives, related to Eq. (3.7) and Eq. (3.10) are simultaneously assessed.

Figure 3.12 presents a summarized flowchart of the proposed robust balancing method.

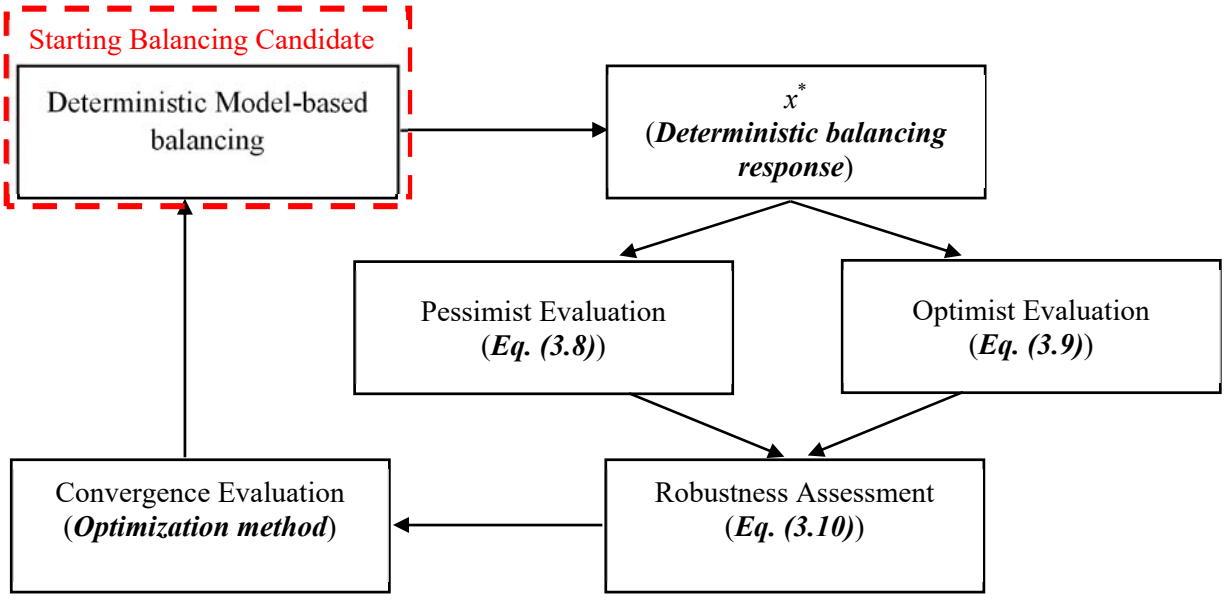

Figure 3.12 - Simplified flowchart of the robust model-based balancing method.

3.3.3 Numerical Evaluation

For the numerical validation of the proposed methodology, the rotor test rig used in the numerical validation of the fuzzy uncertainty analysis (see Section 2.4). As mentioned, the proposed robust balancing methodology is characterized by parametric uncertainties affecting, for instance, the stiffness and damping of the bearings (i.e., due to fixation problem), the dimensions of the discs and shaft (i.e., due to wear), and so on. Therefore, it is expected that a superior balancing performance be obtained when the correction masses and associated phase angles determined by using the robust methodology are used. In this context, the performance of the proposed methodology was evaluated by considering the stiffness along the horizontal and vertical directions of the bearing B_2 (k_X / B_2 and k_Z / B_2, respectively; see Figure 2.4 and Table 2.1) as uncertain information. Table 3.5 shows the uncertainty scenario considered in this section. The stiffness variation was introduced in order to simulate an abrupt screw loss at the fixation support of the bearing.

Table 3.5 Uncertainty scenario considered in the present contribution.

Stiffness	Experimental parameters	Uncertainty intervals
k_X / B_2 (N/m)	5.202×10^7	$5.202 \times 10^3 \leq k_X \leq 5.202 \times 10^7$
k_Z / B_2 (N/m)	7.023×10^8	$7.023 \times 10^3 \leq k_Z \leq 7.023 \times 10^8$

*The experimental parameters are also presented in Table 2.1.

Three different optimization methodologies devoted to the robust balancing were used in this application, namely the deterministic approach (i.e., cost function presented in Eq. (3.7)), a robustness evaluation (i.e., cost function related exclusively to Eq. (3.10)), and a multi-objective optimization associated with both presented pessimist and optimist cost functions (Eq. (3.8) and Eq. (3.9), respectively). Table 3.6 presents the correction masses and phase angles obtained by using the proposed optimization procedures with the rotor operating at 1200 rev/min. In this case, unbalance masses were randomly distributed along the shaft of the rotor (0 ≤ unbalance – g.mm ≤ 300; -π ≤ phase angle – rad ≤ π). Thus, unbalance forces were introduced randomly at each node of the FE model (see Figure 2.4). It is worth mentioning that applying the considered unbalance forces on the deterministic FE model (i.e., using the parameters shown in Table 2.1), the maximum amplitude of the vibration responses (0 to peak amplitude) obtained by the displacement sensors S_{8X}, S_{8Z}, S_{28X}, and S_{28Z}, were 43.6 μm, 38.9 μm, 31.5 μm, and 29.8 μm, respectively.

Figure 3.13 shows the orbits determined in the measurement planes S_8 and S_{28} from the FE model considering the optimist uncertain information, which is the upper limit of the uncertain interval (see Table 3.5). Note that the optimist information is identical to the deterministic case (k_X / B_2 = 5.202 x 10^7 N/m and k_Z / B_2 = 7.023 x 10^8 N/m). The orbits were obtained by using the correction masses and phase angles presented in Table 3.6. As expected, the deterministic solution provided the better balancing performance, presenting maximum vibration amplitudes about 1 μm. Differently, the robust design leads to the worst result with vibration amplitudes around 40 μm. The multi-objective design showed an intermediary result, with vibration amplitudes reaching 6 μm. The orbits obtained from the FE model considering the pessimist uncertain information (lower limit of the uncertain interval; see Table 3.5) are presented in Figure 3.14.

Table 3.6 Balancing responses for each methodology used.

Parameters	Deterministic	Robust	Multi-Objective
unbalance / D_1	669.66 g.mm	55.97 g.mm	861.13 g.mm
phase / D_1	-90.82°	-29.17º	-78.75º
unbalance / D_2	333 g.mm	0 g.mm	462.32 g.mm
phase / D_2	50.22°	0º	89.73º

* The multi-objective solution was found through the compromise programing approach (VANDERPLAATS, 2007).

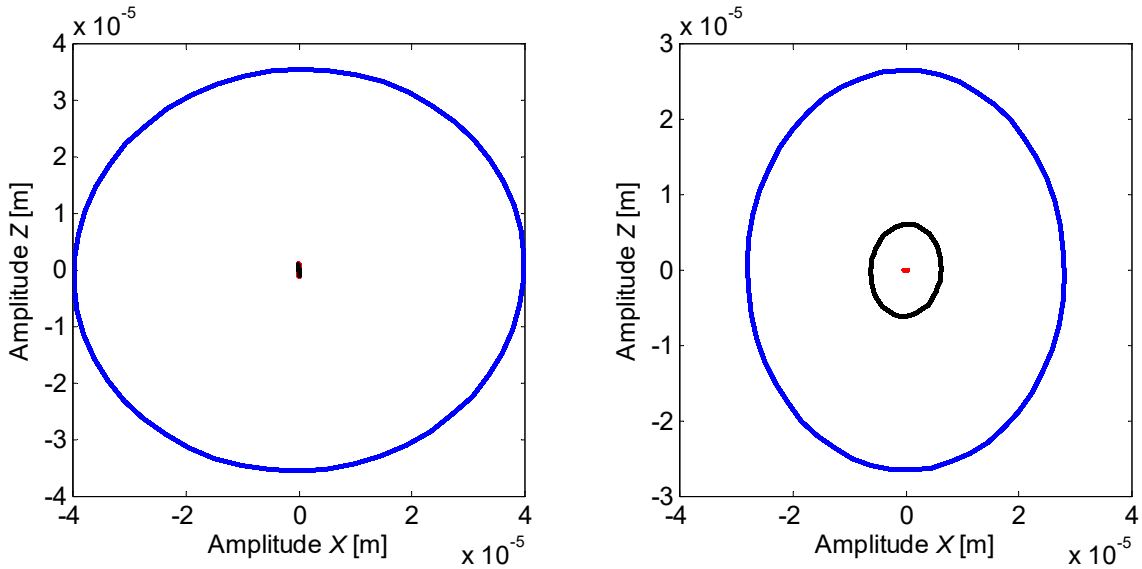

a) Measurement plane S_8. b) Measurement plane S_{28}.

Figure 3.13 - Deterministic (——), robust (——) and multi-objective (——) vibration responses considering the optimist uncertain information.

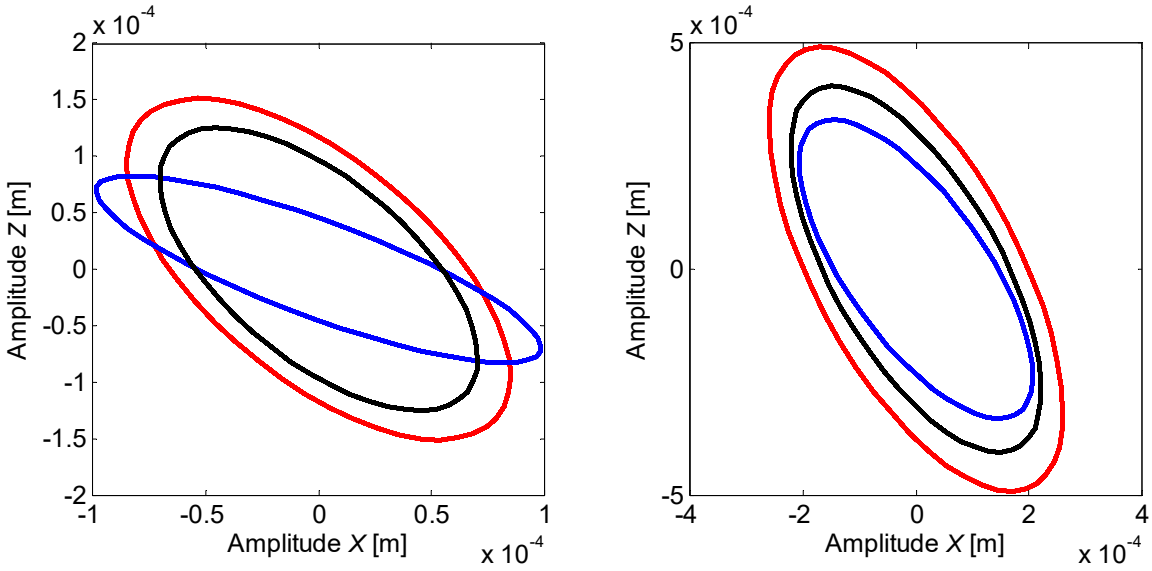

a) Measurement plane S_8. b) Measurement plane S_{28}.

Figure 3.14 - Deterministic (—), robust (—) and multi-objective (—) vibration responses considering the pessimist uncertain information.

Considering the pessimist analysis, Figure 3.14 shows that the performance of the robust and multi-objective balancing processes (see Figure 3.14a and Figure 3.14b, respectively) seems to be better than the one obtained by using the deterministic process. Reminding that the pessimist information is associated with the lower limit of the uncertain interval (simulating an abrupt screw loss at the fixation support of the bearing). In this case, the stiffness of the bearing B_2 along the horizontal and vertical directions were considered as k_X / B_2 = 5.202 x 10^3 N/m and k_Z / B_2 = 7.023 x 10^3 N/m (see Table 3.5). Consequently, it can be observed that the robust and multi-objective solutions present the expected superior balancing performance when compared with the deterministic approach.

Evaluating both pessimist and optimist information, it can be observed that the deterministic design presents a fluctuation of approximately 500 times in amplitude (i.e., difference between the maximum displacement associated with both pessimist and optimist information). The multi-objective design presented a fluctuation of nearly 66 times between the mentioned displacements, while the robust design showed a fluctuation of about 6.5 times among the maximum amplitudes. Figure 3.15 illustrate these results.

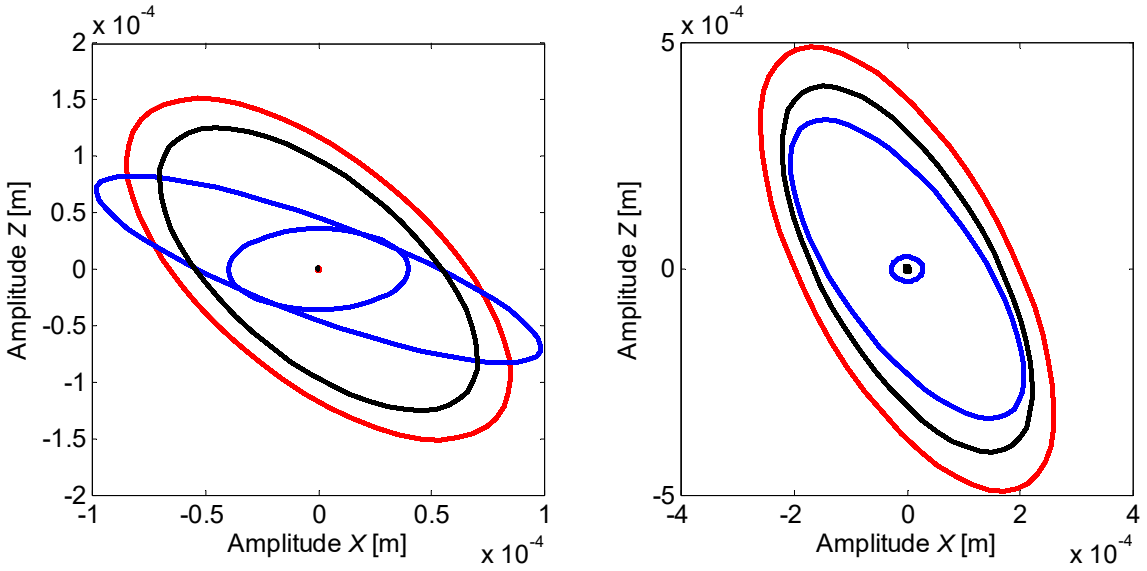

a) Measurement plane S_8. b) Measurement plane S_{28}.

Figure 3.15 - Deterministic (—), robust (—) and multi-objective (—) vibration responses considering the optimist and pessimist uncertain information.

In this section, the deterministic model-based balancing methodology were compared with two different methods based on fuzzy optimization. The uncertainties considered on the application presented were introduced directly on the stiffness coefficients of the self-alignment ball bearings. The numerical application showed that the proposed methodology is able in finding robust solutions, regardless the amplitude of the uncertain information fluctuation. Therefore, a robust balance of a rotating system can be achieved through the fuzzy robust optimization procedure here proposed.

The vibration amplitudes shown in Figure 3.14 and Figure 3.15 clearly represent poor balancing performances with the vibration amplitudes of the balanced system varying from 300 μm to 500 μm. As mentioned, the unbalanced rotating machine presented displacement amplitudes of 43.6 μm, 38.9 μm, 31.5 μm, and 29.8 μm (sensors S_{8X}, S_{8Z}, S_{28X}, and S_{28Z}, respectively). However, this analysis was dedicated to demonstrating the robust balancing concept. Therefore, an experimental investigation should be performed in order to ascertain the results obtained in the numerical application. However, due to the risks associated with the abrupt variation of the bearing stiffness, a different uncertain scenario should be evaluated.

CHAPTER IV

RELIABILITY DESIGN USING FUZZY LOGIC

In this chapter, a novel fuzzy reliability-based design methodology is presented and discussed. This methodology is based on the fuzzy logic approach and considers the possibility concept and fuzzy states assumptions, in which the uncertain parameters are modeled as fuzzy variables. Thus, the associated optimization problems are solved through a nested algorithm. An inner optimization loop is used to obtain the uncertain variables limits and an outer optimization loop evaluates a predefined fuzzy reliability index within the previously obtained bounds. The performance of the proposed approach is evaluated through a benchmark function and two engineering design problems. The reliability fuzzy approach is compared with an existing stochastic strategy.

The chapter begins by revisiting key aspects of reliability-based optimization and fuzzy logic for uncertainty analysis. After, the traditional fuzzy reliability analysis is discussed, followed by the introduction of the proposed fuzzy reliability analysis. Then, the proposed approach is numerically evaluated by means of a benchmark function and two engineering problems. Finally, a brief discussion regarding the obtained results is presented.

4.1 Reliability-based Optimization Review

Safety operating conditions of engineering systems are commonly defined at the design level considering deterministic analyses. The design variables are modeled as deterministic quantities and, consequently, extreme responses due to uncertainties are not taken into account. Thus, the systems performance can be affected by the uncertainties, resulting, in some cases, to unsafety operating conditions and even to catastrophic failures.

The effects of uncertainties should be taken into account for more accurate design processes. For this purpose, robust design (RD) and reliability-based optimization (RBO) approaches have been applied to deal with engineering system design. RD approaches focuses on making the design not sensitive to small variations on the uncertain parameters

(BEYER and SENDHOFF, 2007; GABREL, MURAT and THIELE, 2014). Differently, RBO emphasizes high reliability in design by ensuring the achievement of the constraints at a desired level (LOBATO *et al.*, 2017).

According to LOBATO *et al.* (2017), the RBO approach is based on the probability of system performance failure. Therefore, deterministic analyses around the nominal solution are necessary and the Monte Carlo simulation is commonly used in this sense. The main difficult associated with this approach is the required computational cost. Aiming to overcome this limitation, optimization-based approaches have been proposed to assess the probability of failure without the necessity of sampling techniques. In this sense, the stochastic variables are converted from physical to the standard Hilbert space and an optimization problem is formulated to obtain the largest probability of failure (AGARWAL, 2004; DU and CHEN., 2004; LOBATO *et al.*, 2017).

RBO stochastic approaches are formulated around two strong assumptions (CHENG and MON, 1993), namely *i*) the system behavior can be fully represented by probability measures (probability assumption) and *ii*) the failure states are precise definitions; i.e., at any given time the system is either in safety state or in failure state, with no transient state (binary-state assumption). However, in several applications, due to imprecise information (or lack of information), some uncertain parameters do not satisfy the probability and/or binary-state assumptions, making the probability theory unsuitable to handle the system uncertainties.

In order to provide an alternative, RBO methodology, CHENG and MON (1993) derived the notion of fuzzy states and fuzzy reliability. The fuzzy states were defined based on the binary-state assumption, in which, at any time, a given uncertain parameter may belong to one of two possible fuzzy states, namely fuzzy safety and fuzzy failure states. The authors, in terms of interval confidence, obtained interval ranges of fuzzy reliability by using fuzzy arithmetic operations. In this case, the uncertain parameters were treated as fuzzy triangular numbers. This procedure was later extended by MON and CHENG (1994) to handle different types of fuzzy sets. CREMONA and GAO. (1999) defined a new confidence measure in terms of the distance from the failure surface, similar to the most probable point for failure concept of the probabilistic theory.

In BING, MEILIN and KAI (2000), a fuzzy stress-random strength interference model is proposed. The structural stress and strength are modeled as fuzzy and random variables, respectively. Failure state is defined as a fuzzy event and the failure probability is obtained through fuzzy probability evaluation. LI, LU and XU (2015) proposed a novel fuzzy reliability model to measure the safety condition of structures with fuzzy variables following the probability perspective. This approach was used to treat membership levels of different fuzzy variables as independent standard uniform distributions. In WANG *et al.* (2017), the fuzzy

reliability analysis of heat transfer systems was derived by integral operations. The process is based on interval ranking method and fuzzy reliability indices.

The mentioned contributions focus on revising the binary-state assumption. In most of them, the uncertain information was treated as a random variable, being analyzed by using the probability theory. However, in several applications uncertainties randomness is difficult to be precisely represented. In this work, a novel fuzzy reliability analysis methodology is proposed, in which the uncertain parameters are treated as fuzzy variables (i.e., the probability assumption is modified). In this methodology, a nested optimization algorithm is used to evaluate the problem responses considering uncertainties. An inner optimization loop is used to obtain the bounds of the uncertain variables and an outer optimization loop evaluates a predefined fuzzy reliability index (i.e., the binary-state assumption is modified) within the previously obtained bounds. A Benchmark function and two classical design problems are used to evaluate the effectiveness of the proposed methodology.

4.2 Fuzzy Set Theory Revisited

Uncertainties in engineering systems can either be epistemic or random in nature. ZADEH (1965) proposed the concept of fuzzy sets, in which the so-called membership functions are used to treat epistemic uncertainties. These membership functions are interpreted as a degree of uncertainty, which defines the associated degree of possibility that a parameter u assumes according to a specific element x in the fuzzy set. The membership function μ is a continuous closed interval [0, 1] that weights the pertinence of the element x with respect to the fuzzy set $\tilde{A}$. Values of $\mu_{\tilde{A}}(x)$ close to 1 indicate high compatibility of x to the set $\tilde{A}$. Thus, uncertainties can be computationally modeled as fuzzy numbers by using the fuzzy set theory, in which the parameter value is unknown but limited in an interval weighted by a membership function.

For computational purposes, the fuzzy set $\tilde{A}$ can be represented by subsets namely α-levels. These subsets correspond to real and continuous intervals and are defined by $A_{\alpha k}$, as shown in Eq. (4.1). If the fuzzy set is convex (considering a unidimensional case), each α-level $A_{\alpha k}$ corresponds to the interval $[x_{\alpha kl}, x_{\alpha kr}]$ (see Eq. (4.2)). The α-level α_0 represents the support of the fuzzy set, which is the largest fuzzy set interval containing all considered realizations of the uncertain variable.

$$A_{\alpha k} = \left\{ x \in X, \mu_{\tilde{A}}(x) \geq \alpha_k \right\} \tag{4.1}$$

$$x_{\alpha kl} = \min\left[x \in X \middle| \mu_{\tilde{A}}(x) \geq \alpha_k \right]$$
$$x_{\alpha kr} = \max\left[x \in X \middle| \mu_{\tilde{A}}(x) \geq \alpha_k \right] \tag{4.2}$$

The robustness and/or reliability on the design can be evaluated by mapping the system responses according to the uncertain parameters. In the fuzzy uncertainty analysis, this can be achieved by using a two-stage procedure, known as α-level optimization (see Section 2.3 and Figure 2.3). Firstly, the fuzzy parameters are discretized in α-levels. Thus, for a given α-level α_k, each uncertain parameter x_i (i = 1, …, n; where n is the number of uncertain variables) is considered as an interval $X_{i\alpha k} = [x_{i\alpha kl}, x_{i\alpha kr}]$. Then, two optimization problems are defined aiming to obtain the uncertain parameters configurations that leads to the minimum and maximum system responses, as defined in Eq. (4.3).

$$z_{\alpha kl} = \min_{\mathbf{x} \in \mathbf{X}_{\alpha k}} f(\mathbf{x})$$
$$z_{\alpha kr} = \max_{\mathbf{x} \in \mathbf{X}_{\alpha k}} f(\mathbf{x}) \tag{4.3}$$

in which $z_{\alpha kl}$ and $z_{\alpha kr}$ correspond to the upper and lower bounds of the interval $z_{\alpha k} = [z_{\alpha kl}, z_{\alpha kr}]$ in the α-level α_k, respectively. The vector of fuzzy parameters and the corresponding vector of α-level intervals are given by $\mathbf{x} = (x_1, \ldots, x_n)$ and $\mathbf{X} = (X_1, \ldots, X_n)$, respectively.

Therefore, the effects of uncertain parameters on the system design can be assessed by using an optimization procedure. In this section, the α-level optimization procedure was modified to be performed only for the α-level α_0. Thus, the optimization procedure is applied by considering only the support of the associated fuzzy sets, which corresponds to the inner loop of the proposed reliability analysis.

4.3 Traditional Fuzzy Reliability Analysis

In deterministic design problems, the solution is obtained on a given constraint boundary or at the intersection of constraints boundaries (see Figure 1.1). However, if any perturbation arises in the vector of design variables x_1 and x_2, the violation of some operational/design constraints could emerge resulting in an infeasible condition. Thus, a reliability measure must be assessed to find reliable and feasible solutions considering the effects of uncertainties.

In traditional fuzzy reliability analysis (WANG *et al.*, 2017), the uncertain information is represented as a set of fuzzy parameters. Fuzzy limit state functions (*FLSF*) are defined with respect to the vector of fuzzy parameters, as given by Eq. (4.4).

$$FLSF_j = S_j - R_j = g_j(\mathbf{x}) \tag{4.4}$$

in which R_j and S_j are the so-called structural strengths and stresses, respectively, $g_j(\mathbf{x})$ is defined from the inequality constraints of the problem, and j = 1, …, N (N is the number of constraints).

A critical surface (hypersurface $g_j(\mathbf{x})=0$) is defined, separating the variable space into two parts, namely failure domain ($\{\mathbf{x}|\ g_j(\mathbf{x})>0,\ x_i \in R^n\}$) and safety domain ($\{\mathbf{x}|\ g_j(\mathbf{x})\leq 0,\ x_i \in R^n\}$; feasible domain in Figure 1.1). Therefore, reliability is defined as the difference between structural stress and strength. The limit state functions $FLSF_j$, the structural strengths R_j, and structural stresses S_j are treated as fuzzy variables.

Following the α-level representation, $FLSF_j$ can be rewritten as an interval with respect to the α-level α_k ($FLSF_{j\alpha k} = g_j(\mathbf{x}_{\alpha k})$). Thus, a reliability index $\eta_{j\alpha k}$ is obtained as presented by Eq. (4.5) (index similar to the probabilistic reliability coefficient β).

$$\eta_{j\alpha_k} = \frac{FLSF^C_{j\alpha_k}}{FLSF_{j\alpha_{kr}} - FLSF_{j\alpha_{kl}}} \tag{4.5}$$

in which $FLSF_j{}^C{}_{\alpha k}$ represents the midpoint of $FLSF_j$ along α_k, $FLSF_{j\alpha kr}$ and $FLSF_{j\alpha kl}$ correspond to the lower and upper bounds of the interval $FLSF_{j\alpha k} = [FLSF_{j\alpha kl}, FLSF_{j\alpha kr}]$.

Equation (4.5) indicates that the safety domain is achieved if $\eta_{j\alpha k}\leq 0$ ($g_j(\mathbf{x}_{\alpha k}) \leq 0$ for $\mathbf{x} \in \mathbf{X}_{\alpha k}$ at the α-level α_k). The failure state is obtained if $\eta_{j\alpha k}>0$, since $g_j(\mathbf{x}_{\alpha k}) > 0$ for $\mathbf{x} \in \mathbf{X}_{\alpha k}$. However, a transient state is obtained when $-1 \leq \eta_{j\alpha k} \leq 1$ (both safety or failure states can be achieved), as $g_j(\mathbf{x}_{\alpha k}) \leq 0$ or $g_j(\mathbf{x}_{\alpha k})> 0$ for $\mathbf{x} \in \mathbf{X}_{\alpha k}$. In traditional fuzzy reliability analysis, the binary-state assumption is violated and a clear fuzzy transient state is defined. As mentioned, the safety condition is achieved when $\eta_{j\alpha k} \leq 0$. Consequently, a minimum value of α_k that ensures safety can be obtained. This value corresponding to the intersection point between the structural strength and stress membership functions (WANG *et al.*, 2017) (see Figure 4.1).

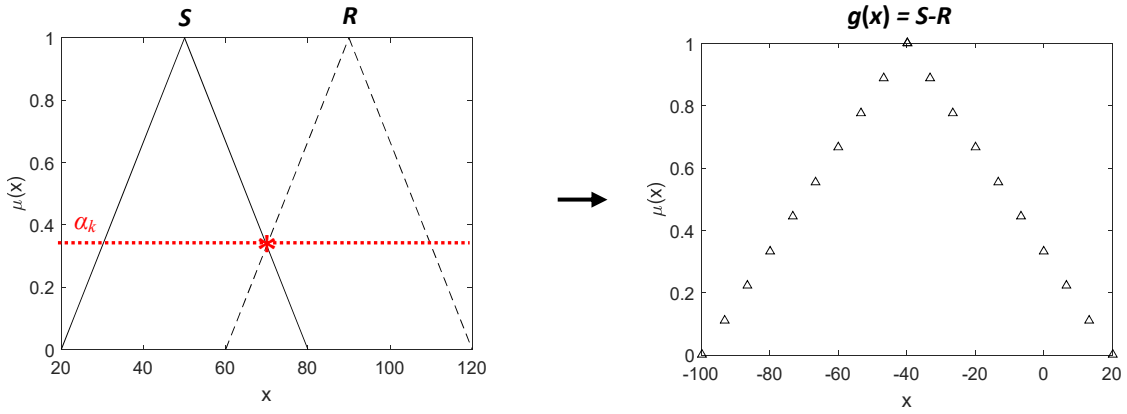

Figure 4.1 – Minimum failure possibility and fuzzy limit state function representations.

4.4 Proposed Fuzzy Reliability Analysis

The traditional fuzzy analysis presents two major drawbacks. Firstly, the minimum failure possibility (minimum value of α_k that ensures safety) is determined based on the structural strength and stress membership functions. Thus, different possibility distributions (shapes of the membership functions) could result in different failure possibility values. Additionally, safety configurations could exist along the transient domain $-1 \leq \eta_{j\,\alpha k} \leq 1$, which can be disregarded in the traditional formulation and in more conservative approaches.

In order to overcome the mentioned limitations, some aspects of the traditional fuzzy analysis were modified in the present contribution. Following the traditional approach, the fuzzy variables are evaluated by using the α-level representation and the failure possibility is assessed through the reliability index presented in Eq. (4.5). However, the traditional approach leads to failure possibilities which are dependent of the α-level intervals. Thus, the reliability index presented in Eq. (4.5) is rewritten as presented by Eq. (4.6) to eliminate the dependence of the possibility distribution (shape of the membership function).

$$\eta_j' = \frac{FLSF_{jL}'}{FLSF_{jR}' - FLSF_{jL}'} \tag{4.6}$$

where η_j' is obtained considering only the support of the fuzzy limit state function $FLSF_j'$. $FLSF_{jR}'$ and $FLSF_{jL}'$ correspond to the upper and lower bounds of fuzzy variable $FLSF_j'$ support, respectively (limits of the interval $FLSF_{j\,\alpha 0}' = [FLSF_{j\,\alpha 0l}', FLSF_{j\,\alpha 0r}']$).

In the proposed methodology, the possibility distribution of a fuzzy set is defined on the support. Thus, the modified fuzzy metric value will be equal even if different possibility distributions are considered (the supports are the same for any shape of membership function).

Regarding Eq. (4.6), the proposed formulation leads to positive values of η_j' when a failure state is achieved since $FLSF_{jL}' > 0$ and $FLSF_{jR}' > FLSF_{jL}'$ (resulting in $g_j(\mathbf{x})>0$). Otherwise, negative values of η_j' could represent either safety or transient states. If $\eta' \leq -1$, the system is definitely in a safety state since $FLSF_{jL}' < 0$ and $FLSF_{jR}' < 0$ (resulting in $g_j(\mathbf{x}) < 0$). The proposed metric must necessarily be lower or equal to -1 as $FLSF_{jL}' < 0$ and $FLSF_{jR}' < 0$. In this case, $|FLSF_{jL}'| > |FLSF_{jR}'|$, thus $FLSF_{jR}' - FLSF_{jL}' > 0$, and $|FLSF_{jL}'| > FLSF_{jR}' - FLSF_{jL}'$. The final possible configuration is $FLSF_{jR}' > 0$ and $FLSF_{jL}' < 0$, in which η_j' would belong to the interval (-1,0] and $g_j(\mathbf{x})$ could either be positive or negative defining then a transient state.

In the traditional reliability fuzzy analysis, the aim is to obtain the system configuration that leads to the minimum possibility of failure. Differently, the proposed approach determines any possible safety configuration, which is evaluated by using an optimization process that assesses the proposed reliability metric. Figure 4.2 presents the flowchart of the proposed methodology. It is worth mentioning that desired reliability indexes can be obtained by rewritten the reliability objective function as an error function.

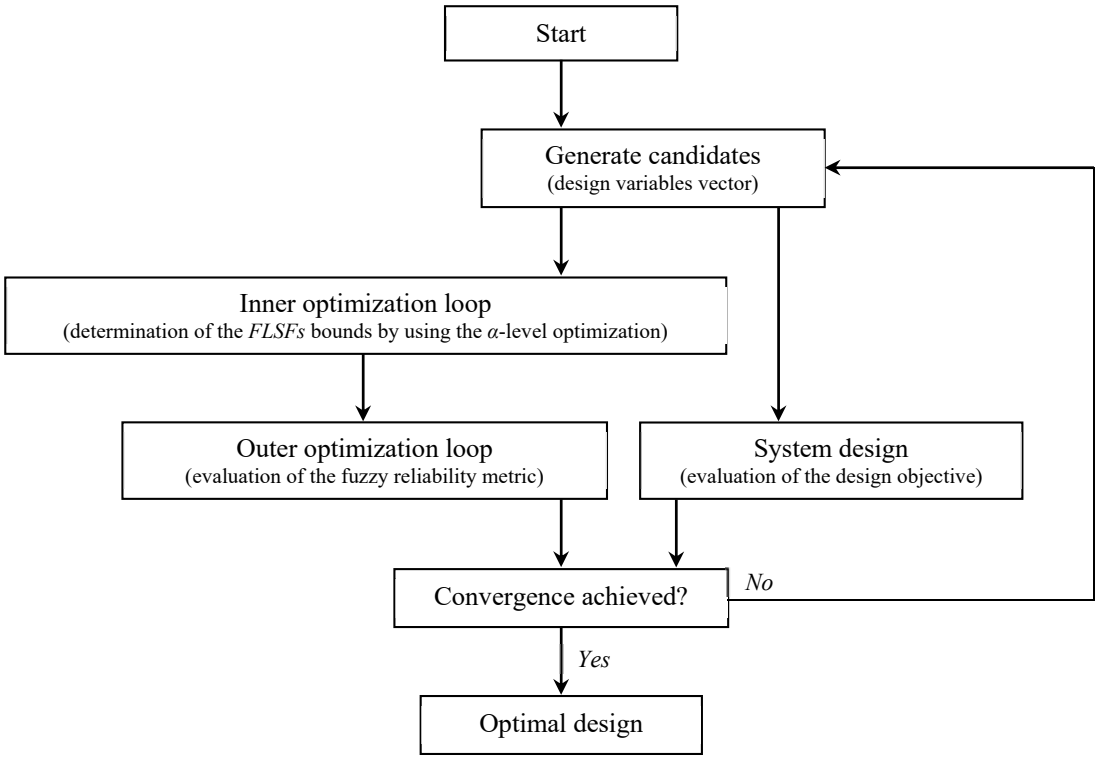

Figure 4.2 – Flowchart of the proposed fuzzy reliability analysis.

In the proposed fuzzy approach, the possibility of failure is defined by considering only the support interval and is associated only to transient states (η_j' belonging to the interval (-1, 0]). In the safety domain, the failure possibility is null. Differently, in the failure domain the failure possibility is assured. Equation (4.7) presents the failure metric f_m that evaluates the possibility of failure along transient states, regarding the width of the support interval (i.e., $FLSF_{jR}'+|FLSF_{jL}'|$) and the width of the failure interval ($FLSF_{jR}'$).

$$f_{jm} = \frac{FLSF_{jR}'}{FLSF_{jR}'+\left|FLSF_{jL}'\right|} \tag{4.7}$$

Note that the proposed approach results in a nested optimization procedure. An inner optimization loop is carried out to determine $FLSF_R'$ and $FLSF_L'$, which corresponds to the maximum and minimum values of $FLSF'$, respectively. Then, an outer optimization loop is performed to minimizes η_j' with respect to predefined uncertain limits (within [$FLSF_L'$, $FLSF_R'$]).

4.5 Numerical Evaluation

In this section, three test cases are presented aiming to evaluate the proposed reliability design optimization methodology, namely i) a nonlinear limit state problem, ii) a cantilever beam problem, and iii) a car-side impact problem. The results obtained by using the probabilistic analysis IRA-DE (LOBATO *et al.*, 2017) is also presented for comparison purposes.

4.5.1 Nonlinear Limit State Function

The original RBO problem was formulated by QU and HAFTKA (2004) and is mathematically represented as shows Eq. (4.8). This problem was originally formulated as containing two design variables (x_{d1} and x_{d2}) and two random variables (x_{r1} and x_{r2}), normally distributed with mean values 5 and 3, respectively, and variation coefficients equal to 0.3 for both variables. Equation (4.9) presents the considered problem rewritten as a reliability fuzzy problem. Following a 5σ model (i.e. $x_r = \mu \pm 5\sigma$) the design test case random variables were converted into fuzzy variables, defined by the support intervals [3.5, 6.5] and [1.5, 4.5] for the variables x_{f1} and x_{f2}, respectively.

$$\begin{cases} \min x_{d_1}^2 + x_{d_2}^2 \\ P\left(0.2 x_{d_1} x_{d_2} x_{r_2}^2 - x_{r_1} \le 0\right) \ge R \\ 0 \le x_{d_i} \le 15,\ i = 1, 2 \end{cases} \tag{4.8}$$

$$\begin{cases} FLSF = x_{f_1} - 0.2 x_{d_1} x_{d_2} x_{f_2}^2 \\ \min x_{d_1}^2 + x_{d_2}^2 \\ \min \eta'\left(FLSF\right) \end{cases} \tag{4.9}$$

Figure 4.3 presents the Pareto's curve obtained by using the proposed reliability approach, in which the safety, transient, and failure domains are indicated. The associated multi-objective optimization problem was solved by using the compromise programming technique allied to the Sequential Quadratic Programming (SQP) algorithm (VANDERPLAATS, 2007). The Pareto's curve was generated considering different weights for the design and reliability cost functions, in which the corresponding mono-objective optimization problems were carried out to obtain the target value for both cost functions. As expected, the value of the cost function increases as the reliability index η' decreases. Figure 4.4 illustrates the variation of the *FLSF*′ support for all obtained designs (according to η'), showing that the design reliability increases as $\eta' \rightarrow -\infty$ ($FLSF_R'$ and $FLSF_L'$ tend to negative values).

Table 4.1 shows the results obtained by using the fuzzy reliability approach and the IRA-DE technique as proposed by LOBATO *et al.* (2017). Considering the minimum safety possibility (design variables values that ensures $\eta' = -1$), it can be observed that the proposed fuzzy approach was able to determine a smaller cost function value ($f = 29.89$) when compared with the IRA-DE technique ($f = 63.09$; target reliability R of 98.9830% corresponding to β=2.32). In this case, IRA-DE was more conservative than the design obtained by using the fuzzy approach, meaning that greater reliability is ensured (in fact IRA-DE response ensures reliability even in a 6σ model) but at the expense of the design cost function value. Note that targeting the same cost function value obtained in LOBATO *et al.* (2017) ($f = 63.09$), a safety configuration with $\eta' = -1.066$ was obtained by the fuzzy approach.

4.5.2 Cantilever Beam Problem

This test case was previously investigated by QU and HAFTKA, (2004); KUO-WEI and GAUTAMA, (2014); and LOBATO *et al.* (2017). The problem consists to find the minimum cross-sectional area of the beam presented in Figure 4.5 following Eq. (4.10).

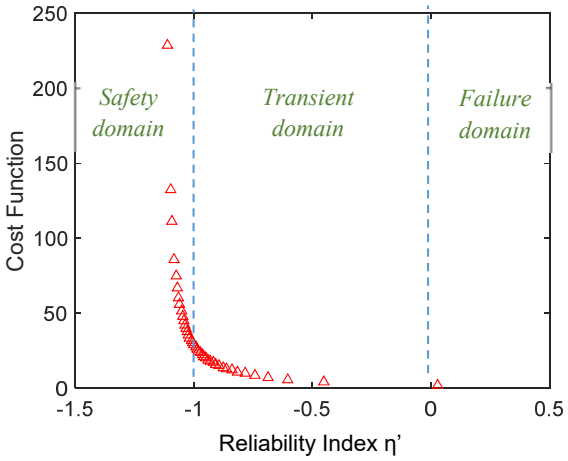

Figure 4.3 – Pareto's curve corresponding to the optimal design solutions of the nonlinear limit state problem.

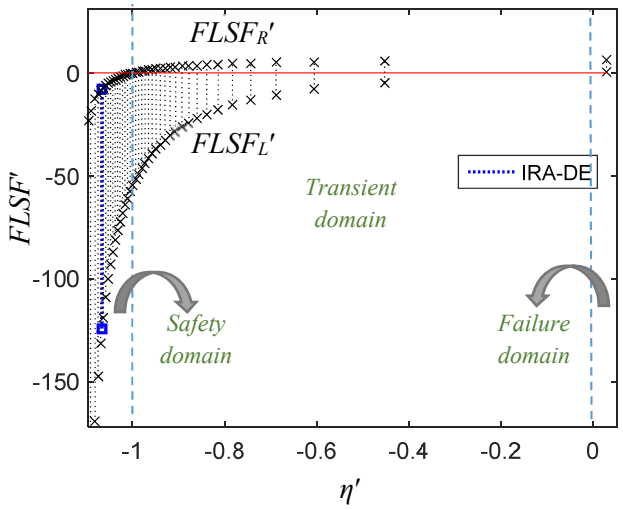

Figure 4.4 – FLSF′ behavior for the nonlinear limit state problem.

Table 4.1 Results associated with the nonlinear limit state problem.

	f	x_{d1}	x_{d2}	$FLSF_L'$	$FLSF_R'$	η'	f_m
IRA-DE	63.09	5.62062	5.61281	-124.267	-7.6964	-1.066	0
Fuzzy	29.89	3.8852	2.52350	-55.0008	-0.0001	-1	0

$$\min_{x_d} \; x_{d1} x_{d2} \tag{4.10}$$

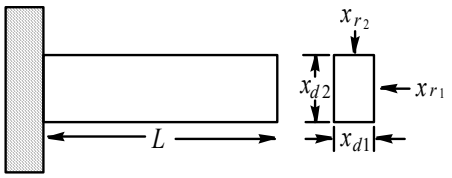

Figure 4.5 - Cantilever beam problem (LOBATO *et al.*, 2017).

where x_{d1} and x_{d2} are the width and height of the beam, respectively, defined as the design variables with lower and upper limits of 0 and 10, respectively.

The two loads x_{r1} and x_{r2} applied at the free end of the beam, the Young's modulus x_{r3}, and the yield strength x_{r4} are random parameters with normal distribution. Similar to the nonlinear limit state problem, the random variables were converted into fuzzy variables, only that in this test case a 2σ model (i.e. $x_r = \mu \pm 2\sigma$) were considered. The stochastic and resulting fuzzy data are presented in Table 4.2.

Table 4.2 Stochastic and fuzzy data used in the cantilever beam problem.

Variable	Mean value	Std	Variable	Nominal	Lower limit	Upper limit
x_{r1} (lb)	500	100	x_{f1} (lb)	500	300	700
x_{r2} (lb)	1000	100	x_{f2} (lb)	1000	800	1200
x_{r3} (psi)	29×10^6	1.45×10^6	x_{f3} (psi)	29×10^6	26.1×10^6	31.9×10^6
x_{r4} (psi)	40000	2000	x_{f4} (psi)	40000	36000	44000

The length L of the cantilever beam is 254 cm and the tip displacement have to be smaller than the allowable displacement d_o = 7.724 cm. The original definition of the first and second failure modes are shown in Eq. (4.11) and the redefined fuzzy problem is given by Eq. (4.12).

$$GS = \frac{600x_{r2}}{x_{d1}x_{d2}^2} + \frac{600x_{r1}}{x_{d1}^2x_{d2}} - x_{r4} \le 0$$

$$GD = \frac{4L^3}{x_{r3}x_{d1}x_{d2}}\sqrt{\left(\frac{x_{r2}}{x_{d2}^2}\right)^2 + \left(\frac{x_{r1}}{x_{d1}^2}\right)^2} - d_o \le 0 \qquad (4.11)$$

$$FLSF_1' = \frac{600x_{f2}}{x_{d1}x_{d2}^2} + \frac{600x_{f1}}{x_{d1}^2 x_{d2}} - x_{f4}$$

$$FLSF_2' = \frac{4L^3}{x_{f3}x_{d1}x_{d2}}\sqrt{\left(\frac{x_{f2}}{x_{d2}^2}\right)^2 + \left(\frac{x_{f1}}{x_{d1}^2}\right)^2} - d_o \qquad (4.12)$$

$$\begin{cases} \min\ x_{d1}x_{d2} \\ \min\max\left[\eta'_{FLSF1}\quad \eta'_{FLSF2}\right] \end{cases}$$

The cantilever beam problem is composed by two distinct failure modes, each one with a corresponding fuzzy limit state function ($FLSF_1'$ and $FLSF_2'$). In the proposed fuzzy procedure, the reliability analysis is performed transforming the reliability constraints in cost functions. Consequently, additional cost functions should be included in the multi-objective problem in cases which more than one limit state function are defined. In order to overcome this limitation, the worst corresponding reliability index (maximum η') is minimized as shown in Eq. (4.12). Thus, values of the reliability index associated with other limit state functions are ensured to be smaller than the currently evaluated η' value in the optimization procedure (safety is pursued in all limit state functions).

Figure 4.6 presents the obtained Pareto's curve for the cantilever beam problem, in which safety and transient configurations were achieved. Figure 4.7 illustrates the behavior of both *FLSF'* functions regarding the obtained designs.

Table 4.3 and Table 4.4 shows the results associated with the minimum safety possibility analysis, obtained by using the proposed fuzzy approach.

Note that the probabilistic response (IRA-DE; target reliability of 99.8651% - β=3) in the proposed methodology standards (fuzzy response considering design cost function value of f = 9.52, see Figure 4.7) consists of a transient response for the first failure mode (η'_{FLSF1} = -0.94), with an associated possibility failure f_m^{FLSF1} = 0.06. Regarding the second failure mode, the response results in an unavoidable failure state (η'_{FLSF2} = 1.02). The fuzzy minimum response ensured a safety state for both failure modes (η'_{FLSF1} = -2.59 and η'_{FLSF2} = -1; see Table 4.4 and Figure 4.7).

Differently of the nonlinear limit state problem, the minimum response safety configuration resulted in a bigger cost function value (f = 18.73; see Table 4.3) when compared with the probabilistic response (f = 9.52; see Table 4.3). This increase in design cost function value is justified with achievement of safety configurations for both failure modes in the fuzzy approach.

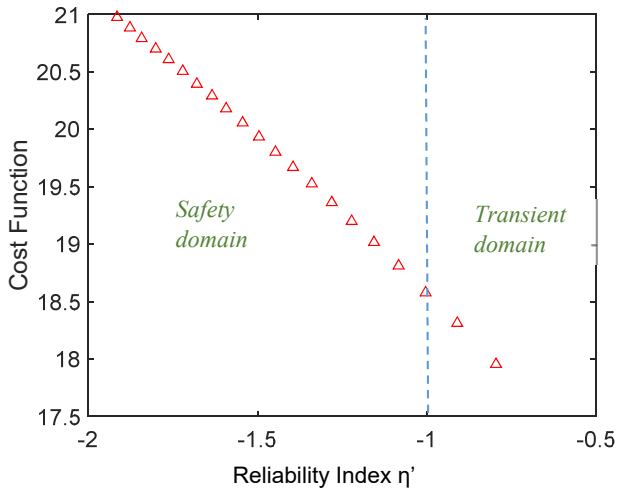

Figure 4.6 - Pareto's curve corresponding to the optimal design solution of the cantilever beam problem.

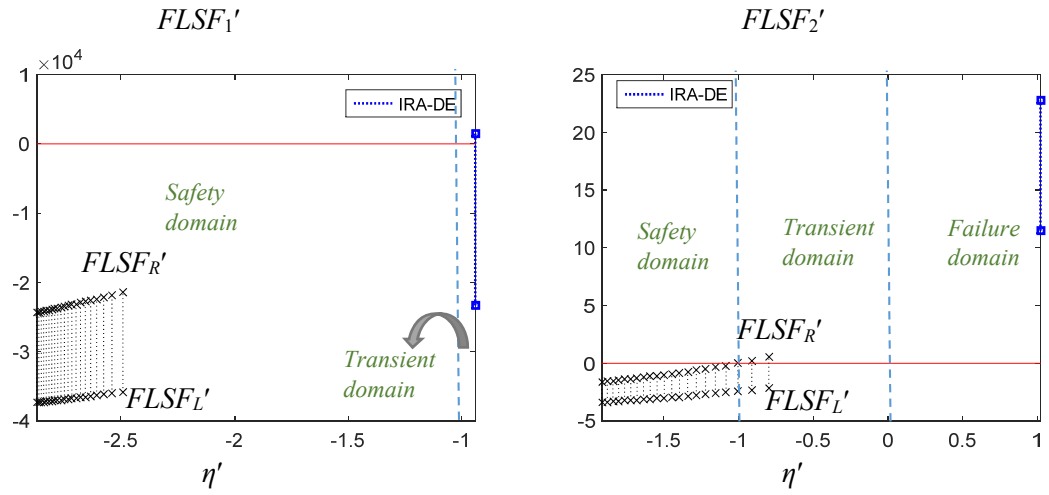

Figure 4.7 - Behavior of FLSF1′ and FLSF2′ according to η′ for the cantilever beam problem.

Table 4.3 Optimization results associated with the cantilever beam problem.

	f (cm^2)	x_{d1} (cm)	x_{d2} (cm)
IRA-DE	9.52	2.4488	3.8877
Fuzzy	18.73	4.0452	4.6314

Table 4.4 Reliability results associated with the cantilever beam problem.

	$FLSF_{1L}'$	$FLSF_{1R}'$	η_1'	f_m^{FLSF1}	$FLSF_{2L}'$	$FLSF_{2R}'$	η_2'	f_m^{FLSF2}	n_{eval}
IRA-DE	-23310	1468	-0.94	0.06	11.48	22.75	1.02	1	20684*
Fuzzy	-36093	-22160	-2.59	0	-2.152	$1.6x10^{-8}$	-1	0	298**

* Mean value. ** Mean after 31 runs considering both inner and outer loops.

4.5.3 Car-side Impact Problem

The car side-impact problem (GU *et al.*, 2001) consists in a car subjected to a side-impact following the standards of the European Enhanced Vehicle-Safety Committee (EEVC). In this test case, there are being considered the effects of the side-impact on a dummy in terms of the head injury, load in abdomen, pubic symphysis force, viscous criterion, rib deflections at the upper, and middle and lower rib locations (DEB *et al.*, 2009). In addition, effects on the car are considered in terms of the B-Pillar velocity at its midpoint and the velocity of the front door at the B-Pillar. The optimization problem consists in minimizing the weight of the car, as defined by Eq. (4.13).

$$\min_{x_d} \; 1.98+4.9x_{d1}+6.67x_{d2}+6.98x_{d3}+4.01x_{d4}+1.78x_{d5}+0.00001x_{d6}+2.73x_{d7} \tag{4.13}$$

in which x_{d1} is the thickness of inner B-Pillar, x_{d2} is the thickness of the B-Pillar reinforcement, x_{d3} is the thickness of inner floor side, x_{d4} is the thickness of the cross members, x_{d5} is the thickness of the door beam, x_{d6} is the thickness of the door beltline reinforcement, and x_{d7} is the thickness of the roof rail. This problem is subject to EEVC restrictions on safety performance, which are given by Eqs. (4.14) to (4.24).

$$g_1 = 1.16 - 0.3717x_{d2}x_{d4} - 0.00931x_{d2}x_{r3} - 0.484x_{d3}x_{r2} + 0.01343x_{d6}x_{r3} \leq 1 \text{ KN} \tag{4.14}$$

$$g_2 = 0.261 - 0.0159x_{d1}x_{d2} - 0.188x_{d1}x_{r1} - 0.019x_{d2}x_{d7} + 0.0144x_{d3} + 0.87570x_{d5}x_{r3} + 0.08045x_{d6}x_{r2} + 0.00139x_{d8}x_{r4} + 0.00001575x_{r3}x_{r4} \leq 0.32 \text{ m/s} \tag{4.15}$$

$$g_3 = 0.214 + 0.00817x_{d5} - 0.131x_{d1}x_{r1} - 0.0704x_{d1}x_{r2} + 0.03099x_{d2}x_{d6} - 0.018x_{d2}x_{d7} + 0.0208x_{d3}x_{r1} + 0.121x_{d3}x_{r2} - 0.00364x_{d5}x_{d6} + 0.0007715x_{d5}x_{r3} - 0.0005354x_{d6}x_{r3} + 0.00121x_{r1}x_{r4} + 0.00184x_{r2}x_{r3} - 0.018x_{d2}^2 \leq 0.32 \text{ m/s} \tag{4.16}$$

$$g_4 = 0.74 - 0.61x_{d2} - 0.163x_{d3}x_{r1} + 0.001232x_{d3}x_{r3} - 0.166x_{d7}x_{r2} + 0.227x_{d2}^2 \leq 0.32 \text{ m/s} \tag{4.17}$$

$$g_5 = 28.98 + 3.818x_{d3} - 4.2x_{d1}x_{d2} + 0.0207x_{d5}x_{r3} + 6.63x_{d6}x_{r2} + 7.77x_{d7}x_{r1} + 0.32x_{r2}x_{r3} \leq 32 \text{ mm} \tag{4.18}$$

$$g_6 = 33.86 + 2.95x_{d3} + 0.1792x_{r3} - 5.057x_{d1}x_{d2} - 11x_{d2}x_{r1} - 0.0215x_{d5}x_{r3} - 9.98x_{d7}x_{r1} + 22x_{r1}x_{r2} \leq 32 \text{ mm} \tag{4.19}$$

$$g_7 = 46.36 - 9.9x_{d2} - 12.9x_{d1}x_{r1} + 0.1107x_{d3}x_{r3} \leq 32 \text{ mm} \tag{4.20}$$

$$g_8 = 4.72 - 0.5x_{d4} - 0.19x_{d2}x_{d3} - 0.0122x_{d4}x_{r3} + 0.009325x_{d6}x_{r3} + 0.000191x_{r4}^2 \leq 4 \text{ KN} \tag{4.21}$$

$$g_9 = 10.58 - 0.674x_{d1}x_{d2} - 1.95x_{d2}x_{r1} + 0.02054x_{d3}x_{r3} - 0.0198x_{d4}x_{r3} + 0.028x_{d6}x_{r3} \leq 9.9 \text{ mm/ms} \tag{4.22}$$

$$g_{10} = 16.45 - 0.489x_{d3}x_{d7} - 0.843x_{d5}x_{d6} + 0.0432x_{r2}x_{r3} - 0.0556x_{r2}x_{r4} \\ -0.000786x_{r4}^2 \le 15.7 \text{ mm/ms} \quad (4.23)$$

$$0.5 \le x_{d1} \le 1.5,\ 0.45 \le x_{d2} \le 1.35,\ 0.5 \le x_{d3} \le 1.5,\ 0.5 \le x_{d4} \le 1.5, \\ 0.875 \le x_{d5} \le 2.625,\ 0.4 \le x_{d6} \le 1.2,\ 0.4 \le x_{d7} \le 1.2 \quad (4.24)$$

where x_{r1} is the material of the inner B-Pillar, x_{r2} is the material of the inner floor side, x_{r3} is the barrier height, and x_{r4} is the barrier hitting position.

Following the strategy proposed by DEB *et al.* (2009), the system variables were separated in two different sets: the uncertain decision variables x_d= (x_{d1}, …, x_{d7}) and the uncertain random variables x_r = (x_{r1}, …, x_{r4}). All variables present normal distribution around their mean values and are assumed as being independent. The uncertain design variables are modeled with unknown mean values, which are determined by using an optimization procedure, with standard deviation of 0.03 mm (except x_{d5} that presents a constant standard deviation of 0.05 mm). Table 4.5 shows the characteristics of remaining random and fuzzy variables, whereas a 3σ model (i.e. $x_r = \mu \pm 3\sigma$) was considered in order to convert random variables into fuzzy variables.

Table 4.5 Stochastic and fuzzy data used in the car side-impact problem.

	Mean value	Standard deviation		Nominal value	Lower limit	Upper limit
x_{r1} (mm)	0.345	0.006	x_{f1} (mm)	0.345	0.3270	0.3630
x_{r2} (mm)	0.192	0.006	x_{f2} (mm)	0.192	0.1740	0.2100
x_{r3} (mm)	0	10	x_{f3} (mm)	0	-30	30
x_{r4} (mm)	0	10	x_{f4} (mm)	0	-30	30

The key aspect of the car side-impact problem is that the design variables are uncertain parameters. Thus, at each iteration of the outer optimization loop, the fuzzy transformation is applied to determine the fuzzy uncertain interval associated with the design variables. The fuzzy reliability analysis of the car side-impact problem results in ten distinct failure modes associated with the multi-objective procedure. In this case, the minimization of the worst reliability index and Eq. (4.13) are the considered cost functions.

Table 4.6 and Table 4.7 illustrates the results obtained by the proposed fuzzy approach, corresponding to the better reliability index response in the multi-objective procedure. In this test case, safety and transient domain responses were determined by the proposed fuzzy approach considering the same cost function value obtained by using IRA-DE (see f = 26.6274 in Table 4.6; target reliability of 99.8651% corresponding to β=3). Note that the safety state is

ensured for the first, third, ninth, and tenth failure modes, while the remaining failure modes leads to transient states with the highest failure possibility of f_m = 0.71 for the fourth failure mode. Similar results were found considering the best configuration achieved by using the proposed fuzzy reliability approach (results associated with f = 36.1915 showed in Table 4.6) with the main difference regarding IRA-DE results being safety state assurance in five of the ten failure modes (first, third, sixth, ninth, and tenth failure modes).

Table 4.6 Optimization results associated with car-side impact problem.

	x_{d1} (mm)	x_{d2} (mm)	x_{d3} (mm)	x_{d4} (mm)	x_{d5} (mm)	x_{d6} (mm)	x_{d7} (mm)	f (Eq. (14))	n_{eval}
IRA-DE	0.500	1.062	0.923	1.500	0.875	1.200	0.400	26.6274	27980*
Fuzzy	1.500	1.164	1.093	1.231	2.222	0.645	0.944	36.1915	5950**

* Mean value. ** Mean after 11 runs considering both inner and outer loops.

Table 4.7 Reliability results associated with the car-side impact problem.

	$FLSF_1'$	$FLSF_2'$	$FLSF_3'$	$FLSF_4'$	$FLSF_5'$	$FLSF_6'$	$FLSF_7'$	$FLSF_8'$	$FLSF_9'$	$FLSF_{10}'$
					IRA-DE					
$FLSF'_L$	-0.82	-26.2	-0.13	-0.03	-2.86	-8.78	-3.10	-0.56	-2.23	-7×10^5
$FLSF'_R$	-0.18	26.1	-0.05	0.06	4.90	4.54	6.17	0.23	-0.10	0.19
η'	**-1.28**	-0.50	**-1.62**	-0.32	-0.37	-0.66	-0.33	-0.71	**-1.05**	**-1**
f_m	0	0.50	0	0.71	0.61	0.34	0.67	0.30	0	0
					Fuzzy					
$FLSF'_L$	-0.70	-61.8	-0.26	-0.06	-7.94	-16.4	-9.28	-0.54	-2.73	-7×10^5
$FLSF'_R$	-0.32	61.5	-0.08	0.05	2.42	-3.47	1.60	0.37	-0.64	-0.39
η'	**-1.84**	-0.50	**-1.49**	-0.57	-0.77	**-1.27**	-0.85	-0.60	**-1.30**	**-1**
f_m	0	0.50	0	0.43	0.23	0	0.15	0.40	0	0

The fuzzy approach was able to reduce the maximum failure possibility, when compared to the IRA-DE method proposed by LOBATO *et al.* (2017) (f_m = 0.71 for the fourth failure mode in IRA-DE, while f_m = 0.50 for the second failure mode in the fuzzy approach). The failure possibility of most failure modes, with the exception of the eighth failure mode, were also reduced by applying the fuzzy approach. It is worth mentioning that the design cost function value increased according to the mentioned failure possibility reduction (see Table 4.6).

In this chapter, a novel fuzzy reliability analysis methodology was proposed. The traditional fuzzy approach was modified in terms of the reliability index, thus eliminating the dependence of the so-called membership functions. In this case, the reliability analysis is performed on the support interval of the associated fuzzy limit state functions. Therefore, the resulting fuzzy reliability design consists of a multi-objective optimization problem wherein a first cost function is associated with design evaluation and an additional cost function is included in the problem to deal with the reliability analysis.

The performance of the proposed algorithm was evaluated by means of three different test cases. The obtained results demonstrated the efficiency and flexibility of the proposed fuzzy methodology, as represented by its capability of obtaining safety, transient, or failure system design configurations. The examples discussed above show that the proposed approach can effectively assess reliability in design problems with uncertain quantities without the the necessity of defining either a probability density function (stochastic approaches) or a possibility distribution (traditional fuzzy approach). In the proposed methodology, only the definition of a support fuzzy interval is required, thus eliminating the probability density function and/or possibility distribution dependency.

CHAPTER V

FINAL REMARKS

This chapter summarizes the present research work discussing its main results and contributions, as well as addressing the prospects for future works.

As previously stated, the main goal of this research work was to evaluate fuzzy logic as a tool for uncertainty, robustness and reliability analyses of mechanical systems. In this sense, Chapter 2 focused on presenting the mathematical basis of fuzzy uncertainty analysis, addressing its fundamental concepts and comparing the proposed fuzzy methodology with existing stochastic approaches. The proposed fuzzy uncertainty analysis technique was then numerically validated by means of the uncertainty assessment of a rotor test rig; the obtained results were compared with those stemming from stochastic approaches responses. At this point, the presented fuzzy logic approach was experimentally validated by means of the assessment of uncertainty effects found in a flexible rotor supported by hydrodynamic bearings. Although the presented fuzzy uncertainty analysis methodology is relatively well known, the numerical and experimental validation presented in this work is novel, resulting an interesting contribution for uncertainty analysis, in general terms. As discussed in Chapter 2 the obtained results demonstrated the suitability of fuzzy logic for the uncertainty analysis of rotating systems, being able to obtain system extreme responses in both frequency and time domains.

In Chapter 3, fuzzy logic was evaluated as a tool for robustness optimization by means of two novel rotor balancing approaches based on fuzzy logic: *i*) a non-parametric approach formulated to enhance the so-called IC method balancing robustness, and *ii*) a parametric methodology formulated to increase the balancing robustness of model-based balancing approach. In the first approach, fuzzy logic tools, particularly fuzzy transformation and defuzzification procedures, were used to define a preprocessing stage in which system vibration responses sets are evaluated in order to obtain a more representative unbalance condition. In the second approach, fuzzy optimization is used to define fuzzy objective functions in which uncertainties effects on the balancing responses are assessed. The non-parametric approach was validated both numerically and experimentally, while the parametric approach was only numerically evaluated. In one hand, obtained results demonstrate that the

non-parametric methodology is sufficiently robust to handle uncertainties effects on the balancing responses, as long as these effects appear in the measured data used in the preprocessing stage. On the other hand, the numerical application of the parametric approach shows that the proposed methodology is able to finding robust solutions, regardless the amplitude fluctuation of the uncertain information. However, an experimental investigation should be performed in the future to validate the numerical results obtained. As confirmed by the results, fuzzy logic can be effectively used for robust optimization of mechanical systems. In this sense, the main contributions of this research work in terms of rotor balancing are the two new robust balancing approaches, as explained above. In terms of robust optimization, the main contribution of this work is related to a methodology that is based on simple mathematical formulations for robust optimization, without the requirement of either probability definitions (i.e., uncertain variables probability density functions) or sampling techniques.

Finally, in Chapter 4, a novel fuzzy logic reliability-based design methodology is discussed. The proposed methodology revises the traditional fuzzy approach in terms of the reliability index, eliminating the dependence of the so-called membership functions. In this sense, the reliability analysis is performed on the support interval of the associated fuzzy logic limit state functions. Therefore, the resulting fuzzy logic reliability design consists of a multi-objective optimization problem wherein a first cost function is related to design evaluation and an additional cost function is included in the problem to deal with the reliability analysis. Thus, the associated reliability-based design optimization problems are solved through a nested algorithm. An inner optimization loop used to obtain the uncertain variables limits and an outer optimization loop that evaluates a predefined fuzzy logic reliability index within the previously obtained bounds. The performance of the proposed algorithm was evaluated by means of three different test cases. The examples presented show that the proposed methodology can effectively assess reliability in design problems with uncertain quantities without the definition of either a probability density function (stochastic approaches) or a possibility distribution (traditional fuzzy logic approach). In this sense the main contribution of the proposed methodology, is the elimation of dependency of probability density function and/or possibility distribution.

Consequently, the main contributions of this doctoral research work can be summarized as follows:

- Numerical and experimental validation of the fuzzy uncertainty analysis α-level optimization procedure for rotating systems.
- Demonstration that fuzzy logic uncertainty analysis can be used to obtain system extreme responses in both frequency and time domains of rotordynamics applications.

- Formulation of two novel robust balancing approaches based on fuzzy logic. A non-parametric approach that was numerically and experimentally validated and a parametric approach based on fuzzy optimization that was numerically investigated.
- Enhancement of overall balancing robustness by means of simple data analysis, as demonstrated in the balancing techniques, where measurements sets are used in the non-parametric approach.
- Definition of a revised fuzzy logic reliability-based design technique in which both probability and possibility distributions dependency were eliminated.
- Demonstration of the competitive results provided by using fuzzy logic approach on uncertainty analysis, robust optimization and reliability-based design, aiming at applications on dynamics of flexible rotors.

To characterize the contributions of this doctorate thesis, journal papers and conference papers are presented in the Appendix A.

For future works, the author suggests the following research efforts:

- The use of fuzzy logic tools, particularly fuzzy logic uncertainty analysis associated with defuzzification procedures to determine robust parameters for design purposes.
- The use of fuzzy logic technique in uncertainty propagation analysis as done in stochastic approaches such as Bayesian networks, as focusing on enhancing system reliability.
- Evaluation of the influence of fuzzy logic transformation parameters on the non-parametric robust balancing method (i.e., decision rule α range, and shape of membership functions) in an attempt to automate the procedure and eliminate users' influence on the results.
- Experimental investigation regarding the parametric robust balancing procedure aiming at validating the simulation results obtained.
- Application of the proposed robust balancing approaches, particularly the non-parametric procedure, to complex rotating machinery for testing on different case studies.
- Application of the new fuzzy logic reliability-based approach in more complex mechanical systems (such as rotating systems) aiming at applications on reliability-based design and structural health monitoring.

- Study of fuzzy logic optimization procedures aiming at simultaneously assessing system robustness and reliability (defining, for instance, a robust and reliable balancing procedure).

REFERENCES

AGARWAL, H. **Reliability Based Design Optimization: Formulations and Methodologies.** PhD thesis, University of Notre Dame. [S.l.]. 2004.

BAO, N.; WANG, C. A Monte Carlo simulation based inverse propagation method for stochastic model updating. **Mechanical Systems and Signal Processing**, v. 60-61, p. 928-944, 2015. https://doi.org/10.1016/j.ymssp.2015.01.011

BENTLY, D. E.; HATCH, C. T. **Fundamentals of Rotating Machinery Diagnostics**. First printing. ed. [S.l.]: Bently Pressurized Bearing Company, 2002. https://doi.org/10.1115/1.801FRM

BEYER, H.-G.; SENDHOFF, B. Robust Optimization—a Comprehensive Survey. **Computer Methods in Applied Mechanics and Engineering**, v. 196, p. 3190–3218, 2007. https://doi.org/10.1016/j.cma.2007.03.003

BINDER, K. **Monte Carlo Methods in Statistical Physics**. [S.l.]: Springer, 1979. https://doi.org/10.1007/978-3-642-96483-1

BING, L.; MEILIN, Z.; KAI, X. A Practical Engineering Method for Fuzzy Reliability Analysis of Mechanical Structures. **Reliability Engineering and System Safety**, v. 67, p. 311-315, 2000. https://doi.org/10.1016/S0951-8320(99)00073-3

BUTKEWITSCH, B. **Projeto Ótimo Robusto Multi-Disciplinar Mediante Experimentos Computacionais: uma Contribuição à Segurança Veicular**. Tese (Doutorado em Engenharia Mecânica) - Universidade Federal de Uberlândia. Uberlândia. 2002.

CADINI, F.; GIOLETTA, A. A Bayesian Monte Carlo-based algorithm for the estimation of small failure probabilities of systems affected by uncertainties. **Reliability Engineering and System Safety** , v. 153, p. 15-27, 2016. https://doi.org/10.1016/j.ress.2016.04.003

CAPONE, G. Orbital Motions of rigid symmetric rotor supported on journal bearings. **La Meccanica Italiana**, v. 199, p. 37-46, 1986.

CARVALHO, V. N. **Balanceamento Robusto de Máquinas Rotativas com Eixos Flexíveis**. Dissertação (Mestrado em Engenharia Mecânica) - Universidade Federal de Uberlândia. Uberlândia. 2017.

CAVALINI JR, A. A.; SANTOS, M.B.; STEFFEN JR, V.; MAHFOUD, J. **Industrial Application of a Model Based Rotor Balancing Technique**. Proceedings of the XVIIIth Symposium on Vibration, Shock, and Noise. Clamart, France: [s.n.]. 2012.

CAVALINI JR, A. A.; LARA-MOLINA, F. A.; SALES, T. P.; KOROISHI, E. H.; STEFFEN JR, V. Uncertainty Analysis of a flexible rotor supported by fluid film bearings. **Latin American Journal of Solids and Structures**, v. 12, p. 1487-1504, 2015. https://doi.org/10.1590/1679-78251582

CAVALINI JR, A. A.; SANCHES, L.; BACHSCHMID, N.; STEFFEN JR, V. Crack identification for rotating machines based on a nonlinear approach. **Mechanical Systems and Signal Processing**, v. 79, p. 72-85, 2016. https://doi.org/10.1016/j.ymssp.2016.02.041

CAVALINI JR., A. A.; SILVA, A.D.G.; LARA-MOLINA, F.A.; STEFFEN JR, V. **Experimental uncertainty analysis of a flexible rotor supported by fluid film bearings**. Proceedings of the DINAME 2015 International Symposium on Dynamic Problems of Mechanics. Natal: [s.n.]. 2015.

CHEN, Y.; SCHUH, C. A. A coupled kinetic Monte Carlo–finite element mesoscale model for thermoelastic martensitic phase transformations in shape memory alloys. **Acta Materialia**, v. 83, p. 431-447, 2015. https://doi.org/10.1016/j.actamat.2014.10.011

CHENG, C. H.; MON, D. L. Fuzzy System Reliability Analysis by Interval of Confidence. **Fuzzy Sets and Systems**, v. 56, p. 29-35, 1993. https://doi.org/10.1016/0165-0114(93)90182-H

CREMONA, C.; GAO., Y. The Possibilistic Reliability Theory: Theoretical Aspects and Applications. **Structural Safety**, v. 19, p. 173-201, 1999. https://doi.org/10.1016/S0167-4730(97)00093-3

DANIEL, G. B.; CAVALCA, K. D. Evaluation of the thermal effects in tilting pad bearing.. **International Journal of Rotating Machinery** , v. 1, p. 1-17, 2013. https://doi.org/10.1155/2013/725268

DE ABREU, G. L. C. M.; MAESTA, M.F.; LOPES, V. JR; DE MARQUI, C. JR; FARIA, C.T.; INMAN, D.J. Active angular control of a sectioned airfoil using shape memory alloys and fuzzy controller. **Journal of the Brazilian Society of Mechanical Sciences and Engineering**, v. 37, p. 1555-1567, 2015. https://doi.org/10.1007/s40430-014-0293-1

DEB, K.; PADMANABHAN, D.; GUPTA, S.; MALL, A. K. Handling Uncertainties Through Reliability-Based Optimization using Evolutionary Algorithms. **IEEE Transactions on Evolutionary Computation**, v. 13, n. 5, p. 1054-1074, 2009. https://doi.org/10.1109/TEVC.2009.2014361

DU, X.; CHEN., W. Sequential Optimization and Reliability Assessment Method for Efficient Probabilistic Design. **Journal of Mechanical Design**, v. 126, p. 225-233, 2004. https://doi.org/10.1115/1.1649968

DUBOIS, D.; PRADE, H. The three semantics of fuzzy sets. **Fuzzy Sets and Systems** , v. 90, p. 141-150, 1997. https://doi.org/10.1016/S0165-0114(97)00080-8

EHRICH, F. F. **Handbook of Rotordynamics**. [S.l.]: McGraw-Hill, 1992.

EISENMANN, R. C.; EISENMANN JR, R. C. **Machinery malfunction, diagnosis and correction**. New Jersey: Prentice Hall, Inc., 1998.

GABREL, V.; MURAT, C.; THIELE, A. Recent Advances in Robust Optimization: an Overview. **European Journal of Operational Research**, v. 235, p. 471–483, 2014. https://doi.org/10.1016/j.ejor.2013.09.036

GHANEM, R. G.; SPANOS, P. D. **Stochastic Finite Elements – A Spectral Approach**. [S.l.]: Spring Verlag., 1991.

GU, L.; YANG, R. J.; THO, C. H.; MAKOWSKI, L.; FARUQUE, O.; LI, Y. Optimization and robustness for crashworthiness of side impact. **International Journal of Vehicle Design**, v. 26, n. 4, 2001. https://doi.org/10.1504/IJVD.2001.005210

HAMROCK, B. J.; SCHMID, S. R.; JACOBSON, B. O. Fundamentals of Fluid Film Lubrication. New York: Marcel Dekker, 2004. https://doi.org/10.1201/9780203021187

HEINRICHSON, N. **On the design of tilting-pad thrust bearings**. PhD Thesis, Technical University of Denmark. [S.l.]. 2006.

HUDSON, A.; TILLEY, D. R. Assessment of uncertainty in emergy evaluations using Monte Carlo Simulations. **Ecological Modelling** , v. 271, p. 52-61, 2014. https://doi.org/10.1016/j.ecolmodel.2013.05.018

ISHIDA, Y.; YAMAMOTO, T. **Linear and Nonlinear Rotordynamics**. [S.l.]: Wiley-VCH, 2012. https://doi.org/10.1002/9783527651894

JENSEN, H. A. . M. F.; PAPADIMITRIOU, C. Reliability sensitivity analysis of stochastic finite element models. **Computer Methods in Applied Mechanics and Engineering**, v. 296, p. 327-351, 2015. https://doi.org/10.1016/j.cma.2015.08.007

KANG, Y.; LIN, T.-W.; CHANG, Y.-J.; CHANG, Y.-P.; WANG, C.-C. Optimal Balancing of Flexible Rotors by Minimizing the Condition Number of Influence Coefficients. **Mechanism and Machine Theory**, v. 43, p. 891-908, 2008. https://doi.org/10.1016/j.mechmachtheory.2007.06.005

KOROISHI, E. H.; CAVALINI JR, A.A.; LIMA, A.M.G.; STEFFEN JR, V. Stochastic Modeling of Flexible Rotors. **Journal of the Brazilian Society of Mechanical Sciences and Engineering** , v. 34, p. 574-583, 2012.

KOSKO, B. Fuzzyness vs. Probability. **International Journal of General Systems** , v. 17, p. 211-240, 1990. https://doi.org/10.1080/03081079008935108

KUNDU, A.; DIAZDELA, F.A.; ADHIKARI, S.; FRISWEL, L.M.I. A hybrid spectral and metamodeling approach for the stochastic finite element analysis of structural dynamic systems. **Computer Methods in Applied Mechanics and Engineering** , v. 270, p. 201-219, 2014. https://doi.org/10.1016/j.cma.2013.11.013

KUO-WEI, L.; GAUTAMA, I. . A Single Loop Reliability-Based Design Optimization Using EPM and MPP-based PSO. **Latin American Journal of Solids and Structures**, p. 826-847, 2014.

LALANNE, M.; FERRARIS, G. **Rotordynamics prediction in engineering**. [S.l.]: John Wiley & Sons, INC, 1998.

LARA-MOLINA, F. A.; KOROISHI, E. H.; STEFFEN JR., V. Uncertainty Analysis of a Flexible Rotors considering fuzzy parameters and fuzzy-random parameters. **Latin American Journal of Solids and Structures**, v. 12, p. 1807-1823, 2015. https://doi.org/10.1590/1679-78251466

LI, G.; LIN, Z.; ALLAIRE, P. E. Robust Optimal Balancing of High-Speed Machinery Using Convex Optimization. **Journal of Vibration and Acoustics**, v. 130, p. 1-11, 2008. https://doi.org/10.1115/1.2890405

LI, G.; LU, Z.; XU, J. A Fuzzy Reliability Approach for Structures Based on the Probability Perspective. **Structural Safety**, v. 54, p. 10-18, 2015. https://doi.org/10.1016/j.strusafe.2014.09.008

LOBATO, F. S.; GONÇALVES, M.S.; JAHN, B.; CAVALINI JR., A.A.; STEFFEN JR., V. Reliability-Based Optimization Using Differential Evolution and Inverse Reliability Analysis for Engineering System Design. **Journal of Optimization Theory and Applications**, 2017. https://doi.org/10.1007/s10957-017-1063-x

LOÈVE, M. **Probability theory I**. [S.l.]: Springer Verlag, 1977.

MEGGIOLARO, M. A.; ALMEIDA, C. A. **On the finite element representation of hydrodynamic bearings**. Proceedings of the DINAME 1997 International Symposium on Dynamic Problems of Mechanics. Angra dos Reis: [s.n.]. 1997.

MÖLLER, B.; BEER, M. **Fuzzy Randomness, Uncertainty in Civil Engineering and Computational Mechanics**. [S.l.]: Springer-Verlag, 2004. https://doi.org/10.1007/978-3-662-07358-2

MÖLLER, B.; GRAF, W.; BEER, M. Fuzzy structural analysis using α-level optimization. **Computational Mechanics**, v. 26, p. 547-565, 2000. https://doi.org/10.1007/s004660000204

MON, D. L.; CHENG, C. H. Fuzzy System Reliability Analysis for Components with Different Membership Functions. **Fuzzy Sets and Systems**, v. 64, p. 145-157, 1994. https://doi.org/10.1016/0165-0114(94)90330-1

MUSZYNSKA, A. **Rotordynamics**. [S.l.]: CRC Press, 2005. https://doi.org/10.1201/9781420027792

NEWMAN, M. E. J.; BARKEMA, G. T. **Monte Carlo Methods in Statistical Physics**. [S.l.]: Oxford University Press, 2001.

OZBEN, T.; HUSEYINOGLU, M.; ARSLAN, N. Fuzzy logic model for the prediction failure analysis of composite plates under various cure temperatures. **Journal of the Brazilian Society of Mechanical Sciences and Engineering**, v. 36, p. 443-448, 2014. https://doi.org/10.1007/s40430-013-0096-9

POTA, M.; ESPOSITO, M.; DE PIETRO, G. Transforming Probability Distributions into Membership Functions of Fuzzy Classes: A Hypothesis Test Approach. **Fuzzy sets and Systems**, v. 233, p. 52-73, 2013. https://doi.org/10.1016/j.fss.2013.03.013

QU, X.; HAFTKA, R. T. Reliability-Based Design Optimization Using Probabilistic Sufficiency Factor. **Structural and Multidisciplinary Optimization**, v. 27, n. 5, p. 314-325, 2004. https://doi.org/10.1007/s00158-004-0390-3

RAO, S. S.; QIU, Y. **A Fuzzy approach for the analysis of rotor-bearing systems with uncertainties**. In: ASME 2011 International Design Engineering Technical Conferences & Computers and Information in Engineering Conference, IDETC/CIE. Washington, DC, USA: [s.n.]. 2011. https://doi.org/10.1115/DETC2011-48528

RÉMOND, D.; FAVERJON, B.; SINOU, J. J. Analysing the dynamic response of a rotor system under uncertain parameters Polynomial Chaos expansion. **Journal of Vibration and Control** , v. 18, p. 712-732, 2011.

RIUL, J. A.; STEFFEN JR, V.; RIBEIRO, C. R. Estudo teórico de mancais hidrodinâmicos cilíndricos.. **Revista Brasileira de Ciências Mecânicas**, v. 14, p. 17-40, 1992.

SALDARRIAGA, M. V.; STEFFEN JR, V.; DER HAGOPIAN, J.; MAHFOUD, J. On the Balancing of Flexible Rotating Machines by Using an Inverse Problem Approach. **Journal of Vibration and Control**, p. 1-13, 2010.

SEGUÍ, B.; FAVERJON, B.; JACQUET-RICHARDET, G. Effects of random stiffness variations in multistage rotors using the Polynomial Chaos expansion. **Journal of Sound and Vibration** , v. 332, p. 4178-4192, 2013. https://doi.org/10.1016/j.jsv.2013.03.005

SEPAHVAND, K. Spectral stochastic finite element vibration analysis of fiber-reinforced composites with random fiber orientation. **Composite Structures** , v. 145, p. 119-128, 2016. https://doi.org/10.1016/j.compstruct.2016.02.069

SEPAHVAND, K.; NABIH, K.; MARBURG, S. Collocation-based stochastic modeling of uncertain geometric mistuning in bladed rotor. **Procedia IUTAM** , v. 13, p. 53-62, 2015. https://doi.org/10.1016/j.piutam.2015.01.015

SINOU, J. J.; DIDIER, J.; FAVERJON, B. Stochastic non-linear response of a flexible rotor with local non-linearities. **International Journal of Non-Linear Mechanics** , v. 74, p. 92-99, 2015. https://doi.org/10.1016/j.ijnonlinmec.2015.03.012

SINOU, J. J.; JACQUELIN, E. Influence of Polynomial Chaos expansion order on an uncertain asymmetric rotor system response. **Mechanical Systems and Signal Processing**, v. 50-51, p. 718-731, 2015. https://doi.org/10.1016/j.ymssp.2014.05.046

STEFFEN JR, V.; LACERDA, H. B. On the Balancing of Flexible Rotors. **The International Journal of Analytical and Experimental Modal Analysis**, v. 11, p. 96-105, 1996.

STORN, R.; PRICE, K. Differential Evolution: A simple and efficient adaptive scheme for global optimization over continuous spaces. **International Computer Science Institute** , v. 12, p. 1-16, 1995.

TAKAGI, T.; SUGENO, M. Fuzzy Identification of Systems and Its Applications to Modeling and Control. **IEEE Transactions on Systems, Man, and Cybernetics**, v. 15, p. 116-132, 1985. https://doi.org/10.1109/TSMC.1985.6313399

UNTAROIU, C. D.; ALLAIRE, P. E.; FOILES, W. C. Balancing of Flexible Rotors Using Convex Optimization Techniques: Optimum Min-Max LMI Influence Coefficient Balancing. **Journal of Vibration and Acoustics**, v. 130, 2008.

VANDERPLAATS, G. N. **Multidiscipline Design Optimization**. [S.l.]: Vanderplaats Research & Development, Inc, 2007.

VIANA, F. A. C.; VENTER, G.; BALABANOV, V.; STEFFEN JR, V. **On how to implement an affordable optimal Latin hypercube**. In: 19th Congress of Mechanical Engineering, COBEM 2007. Brasília: [s.n.]. 2007.

WANG, C.; QIU, Z.; XU, M.; QIU, H. Novel Fuzzy Reliability Analysis for Heat Transfer System Based on Interval Ranking Method. **International Journal of Thermal Sciences**, v. 116, p. 234-241, 2017. https://doi.org/10.1016/j.ijthermalsci.2017.02.016

WOWK, V. **Machinery Vibration:** Balancing. [S.l.]: McGraw-Hill Professional, 1998.

ZADEH, L. Fuzzy sets. **Information and Control**, v. 8, p. 338-353, 1965. https://doi.org/10.1016/S0019-9958(65)90241-X

ZADEH, L. Fuzzy sets as basis for a theory of possibility. **Fuzzy Sets and Systems**, v. 1, p. 3-28, 1968. https://doi.org/10.1016/0165-0114(78)90029-5

ZAPOMEL, J.; FERFECKI, P. A computational investigation of the disk-housing impacts of accelerating rotors supported by hydrodynamic bearings.. **Journal of Applied Mechanics** , v. 78, p. 1-13, 2011. https://doi.org/10.1115/1.4002527

ZHANG, J.; ELLINGWOOD, B. Orthogonal series expansions of random fields in reliability analysis. **J. Eng. Mech.** , v. 120, p. 2660-2667, 1994. https://doi.org/10.1061/(ASCE)0733-9399(1994)120:12(2660)

APPENDIX A: Published and Submitted Papers

DOURADO, A. De P.; LOBATO, F.S.; CAVALINI JR, A.A.; STEFFEN JR, V. Fuzzy reliability based optimization for engineering systems design. **Fuzzy Sets and Systems** (Submitted).

CARVALHO, V.N., RENDE, B.F., DOURADO, A.G.S., CAVALINI JR, A.A., STEFFEN JR, V. Robust balancing approach for rotating machines based on fuzzy logic. **Journal of Vibration and Acoustics** (Submitted).

CAVALINI, A.A.; DOURADO A.G.S.; LARA-MOLINA, F.A.; STEFFEN JR, V. Dynamic analysis of a flexible rotor supported by hydrodynamic bearings with uncertain parameters. **Meccanica** (Milano. Print), 2017.

DOURADO, A.G.S.; CAVALINI, A.A.; STEFFEN JR, V . Uncertainty quantification techniques applied to rotating systems: A comparative study. **Journal of Vibration and Control**, DOI: 107754631769855, 2017.

CAVALINI, A.A.; DOURADO, A.G.S.; LARA-MOLINA, F.A.; STEFFEN JR, V. uncertainty analysis of a tilting-pad journal bearing using fuzzy logic techniques. **Journal of Vibration and Acoustics**,2016.

SILVA, A. D. G.; CAVALINI JR, A. A. ; STEFFEN Jr, V. . Fuzzy Robust Design of Dynamic Vibration Absorbers. **Shock and Vibration**, 2016.

DOURADO, A.G.S. CAVALINI JR, A.A.; STEFFEN JR, V. Model Based Robust Balancing Approach for Rotating Machines. **Conference Proceedings of the Society for Experimental Mechanics Series. 1ed.: Springer International Publishing**, 2016, v. 3, p. 243-251.

CARVALHO, V.N.; DOURADO, A.G.S.; RENDE, B.R.F.; CAVALINI JR, A.A.; STEFFEN JR, V. Robust model based balancing approach for flexible rotors. **Proceedings of IceDyn 2017**, 2017.

CARVALHO, V.N.; DOURADO, A.G.S.; CAVALINI JR, A.A.; STEFFEN JR, V. Experimental validation of robust model based balancing approach. **Proceedings of XXIV ABCM International Congress of Mechanical Engineering, COBEM 2017, Curitiba, Brazil**, 2017.

BARBOSA, J.S.; DOURADO, A.G.S.; SICCHIERI, L.C.; CAVALINI JR, A.A.; STEFFEN JR, V. Theoretical and experimental analysis of hydrodynamic and thermohydrodynamic models of cylindrical bearings. **Proceedings of XXIV ABCM International Congress of Mechanical Engineering, COBEM 2017, Curitiba, Brazil**, 2017.

DOURADO, A.G.S.; LOBATO, F.S.; CAVALINI JR, A.A.; STEFFEN JR, V. Reliability based design optimization using fuzzy logic. **Proceedings of XXIV ABCM International Congress of Mechanical Engineering, COBEM 2017, Curitiba, Brazil**, 2017.

CAVALINI JR, A.A.; BORGES, A.S.; DOURADO, A.G.S.; STEFFEN JR, V. Fuzzy analysis of the unbalance response of a vertical rotor. **Proceedings of UNCERTAINTIES 2016, Maresias, São Paulo, Brazil**, 2016.

STEFFEN JR, V.; CAVALINI JR, A.A.; DOURADO, A.G.S. Uncertainty analysis of rotating machines using fuzzy logic approach. **Proceedings of XXIV ICTAM, Montreal, Canada**, 2016.

CAVALINI JR., A.A.; LARA-MOLINA, F.A.; DOURADO, A.G.S.; STEFFEN JR., V. Experimental Uncertainty Analysis of a Flexible Rotor Supported by Fluid Film Bearings. **Proceedings of the XVII International Symposium on Dynamic Problems of Mechanics**, **DINAME 2015, Natal,** 2015.

CAVALINI JR., A. A. ; LARA-MOLINA, F. A. ; DOURADO, A.G.S.; STEFFEN JR., V. Fuzzy uncertainty analysis of a tilting-pad journal bearing. **In: ASME 2015, 2015, Boston. ASME 2015 International Design Engineering Technical Conferences & Computers and Information in Engineering Conference IDETC/CIE 2015**, 2015.

DOURADO, A.G.S.; CAVALINI JR., A. A.; STEFFEN JR., V. Optimization under Uncertainty in Mechanical Systems. **In: Cilamce, 2015, Rio de Janeiro. CILAMCE 2015**, 2015.

PINTO, W. J. G. S. ; DOURADO, A.G.S.; CAVALINI JR., A. A. ; STEFFEN JR., V. Uncertainty analysis in a rotor system by using the fuzzy logic approach. **In: Cilamce, 2015, Rio de Janeiro. CILAMCE 2015**, 2015.

DOURADO, A.G.S.; CAVALINI JR., A. A. ; STEFFEN JR., V. A Comparison Study of Uncertainty Analysis Approaches for Rotor Dynamics Applications. **In: ABCM International Congress of Mechanical Engineering COBEM 2015, 2015, Rio de Janeiro. Proc. of the 23rd ABCM International Congress of Mechanical Engineering COBEM 2015**, 2015.

RESUMO EXPANDIDO EM PORTUGUÊS

DOURADO, A. De P. **Lógica Fuzzy como uma Ferramenta para Análise de Incerteza, Robustez e Confiabilidade de Sistemas Mecânicos.** 2018. 89 páginas. Tese de Doutorado, Universidade Federal de Uberlândia, Uberlândia.

Resumo Expandido em Português

O principal objetivo deste trabalho foi avaliar o uso da *Lógica Fuzzy* como uma ferramenta para análises de incertezas, robustez e confiabilidade. Neste sentido, no Capítulo 2 a base matemática da anaálise de incertezas via lógica *fuzzy* é discutida, abordando seus conceitos fundamentais e comparando a metodologia *fuzzy* utilizada com abordagens estocásticas existentes. A metodologia *fuzzy* proposta foi numérica validada por meio da análise de incertezas em um rotor flexível e os resultados obtidos foram comparados com respostas das abordagens estocásticas clássicas. Posteriormente a metodologia proposta foi experimentalmente validada através da análise dos efeitos das incertezas em um rotor flexível suportado por mancais hidrodinâmicos. Os resultados obtidos demonstraram que a lógica *fuzzy* é uma ferramenta adequada para a análise de incertezas em sistemas rotativos, sendo capaz de obter as respostas extremas do sistema tanto no domínio da frequência como no domínio do tempo. No Capítulo 3 o uso da lógica *fuzzy* como uma ferramenta para otimização robusta foi avaliada por meio de duas novas abordagens fuzzy para balanceamento, uma abordagem não-paramétrica formulada para aumentar a robustez do método de balanceamento conhecido como Coeficientes de Influência, e uma metodologia paramétrica desenvolvida para aumentar a robustez da metodologia de balanceamento baseada em modelos representativos. Na primeira abordagem ferramentas da lógica *fuzzy,* em especial os procedimentos de transformação *fuzzy* e de desfuzificação, são utilizados para definir uma etapa de pré-processamento na qual conjuntos de respostas de vibração do sistema são avaliadas objetivando obter uma condição de desbalanceamento representativa do sistema. Na segunda abordagem, teoria de otimização *fuzzy* é utilizada para definer funções objetivo *fuzzy* nas quais os efeitos das incertezas na resposta ao balanceamento do sistema são avaliados. A abordagem não-paramétrica foi numérica e experimentalmente validada, enquanto a abordagem paramétrica foi avaliada por meio de uma aplicação numérica. Por

fim, no Capítulo 4, uma nova metodologia *fuzzy* para projetos baseados em confiabilidade é discutida. A metolodogia proposta revisa a abordagem *fuzzy* tradicional em termos da métrica de confiabilidade, eliminando a dependência das funções de pertinência. Desta forma, a metodologia proposta consiste de um problema de otimização multi-objetivo no qual uma função objetivo está relacionada com a avaliação do projeto e uma função objetiva adicional é formulada para avaliar a confiabilidade do projeto. A avaliação da confiabilidade do projeto é feita por meio de um algoritmo aninhado, no qual um *loop* interno é utilizado para definir os limites das variáveis incertas, e um *loop* externo avaliada uma métrica de confiabilidade *fuzzy* predefinida considerando os limites obtidos no *loop* interno. Os exemplos apresentados demonstram como a abordagem proposta pode avaliar de forma eficaz a confiabilidade de um projeto com parâmetros incertos sem a definição de funções de densidade de probabilidade ou distribuições de possibilidade.

Palavras-Chave: Lógica Nebulosa, Análise de Incertezas, Robustez e Confiabilidade.